Charles University

Faculty of Science

Study programme: Genetics, Molecular Biology, and Virology

Branch of study: Genetics and Molecular Biology of Eukaryotes

Bc. Linda Stokičová

Glucose effect on lipid metabolism homeostasis in pancreatic β-cells

Vliv glukózy na rovnováhu lipidového metabolismu v β-buňkách slinivky břišní

Diploma thesis

Supervisor: Mgr. Blanka Holendová, Ph.D.

Prague, 2024

Prohlášení

Prohlašuji, že jsem tuto diplomovou práci vypracovala samostatně a že jsem uvedla všechny použité informační zdroje a literaturu. Tato práce ani její podstatná část nebyla předložena k získání jiného nebo stejného akademického titulu.

V Praze, 23.4.2024

……………………..

Bc. Linda Stokičová

Poděkování

Děkuji své školitelce Mgr. Blance Holendové, Ph.D. za vedení při tvorbě této diplomové práce a souvisejících experimentech, za cenné rady, obohacující podněty, trpělivost, a za čas, který věnovala konzultacím a opravám práce.

Dále bych chtěla poděkovat také RNDr. Lydii Plecité, Ph.D., vedoucí laboratoře, ve které jsem tuto práci vypracovávala, za ochotu, cenné připomínky vedoucí k zamyšlení a za vedení nově vzniklé laboratoře.

Děkuji také Mgr. Monice Křivonoskové za seznámení s laboratorními metodami a pomoc s jejich osvojením.

Všem členům laboratoře pro Výzkum pankreatických ostrůvků děkuji za skvělou přátelskou atmosféru, pracovní nasazení a podporu jak ve vědě, tak mimo ni.

Abstract

Lipids create an essential part of pancreatic β-cells. Not only they are the principal structural components and energy source, but they also play an indispensable role in β-cell physiology. Their metabolism is tightly interconnected with the metabolism of glucose, the fundamental β-cell molecule. The presence of lipids is critical for glucose-stimulated insulin secretion and their turnover is inevitable for correct β-cell function. Lipids in the form of triacylglycerols, retinyl esters and cholesterol esters are stored in lipid droplets. These dynamic cellular structures are important for lipid metabolism and the protection of the cells against various types of stress. However, chronic exposure of β-cells to glucose and lipids can lead to disrupted glycerol/non-esterified fatty acid (GL/NEFA) cycle function, glucolipotoxicity and further dysfunction of β-cells, their dedifferentiation, insulin resistance, and finally type 2 diabetes. The experimental part focused on lipid metabolism in pancreatic β-cells in connection with glucose metabolism and redox environment. Glucose-induced expression of proteins involved in lipid metabolism (fatty acid activation, lipolysis, lipogenesis, etc.) and the effect of modulated redox environment was investigated in β-cell line INS1E and isolated mouse pancreatic islets. The lipid droplet content was dependent on the amount of glucose and reactive oxygen species content and was increased in the presence of oleate and orlistat (lipolysis inhibitor). Glucose and reactive oxygen species production also affected the content of free fatty acids in INS1E cells and the release of glycerol. Based on the experiments, it is evident that in the short term, glucose activates lipid metabolism in pancreatic β-cells, allowing the creation of metabolic coupling factors for insulin secretion and fine-tuning the cellular metabolism to maintain the proper function of β-cells.

Keywords: pancreas, glucose, lipids, redox environment, metabolism

Abstrakt

Lipidy jsou důležitou součástí β-buněk. Nejenomže jsou nezbytnou strukturní složkou buněčných membrán a zdrojem energie, ale hrají nepostradatelnou roli ve fyziologii β-buněk. Jejich metabolismus je těsně propojen s metabolismem glukózy, zásadní molekulou pro β-buňky. Přítomnost lipidů je důležitá pro glukózou stimulovanou sekreci inzulinu a jejich metabolismus je nezbytný pro správnou funkci β-buněk. Lipidy jsou skladovány v tukových kapénkách ve formě triacylglycerolů, retinol esterů a cholesterol esterů. Tyto dynamické buněčné struktury jsou důležité pro metabolismus lipidů a ochranu buňky před různými typy stresu. Chronické vystavování β-buněk glukóze a lipidům vede ale k narušení GL/NEFA cyklu (cyklus glycerolu a volných mastných kyselin), glukolipotoxicitě a dále k dysfunkci β-buněk, jejich dediferenciaci, insulinové rezistenci a diabetu 2. typu. Experimentální část je zaměřena na charakteristiku lipidového metabolismu v β-buňkách ve spojení s metabolismem glukózy a redoxním prostředím. Glukózou indukovaná exprese proteinů účastnících se lipidového metabolismu (aktivace mastných kyselin, lipolýza, lipogeneze, atd.) a efekt pozměněného redoxního prostředí byly analyzovány v INS1E buněčné linii β-buněk a izolovaných myších pankreatických ostrůvcích. Množství tukových kapének bylo závislé na množství glukózy a obsahu reaktivních forem kyslíku a bylo zvýšené v přítomnosti oleátu a orlistatu (inhibitor lipolýzy). Glukóza měla také vliv na obsah volných mastných kyselin v INS1E buňkách a měla za následek sekreci glycerolu. Na základě provedených experimentů je patrné, že z krátkodobého hlediska glukóza aktivuje lipidový metabolismus v β-buňkách, čímž umožňuje vznik regulačních a výkonných metabolických faktorů pro sekreci inzulinu, a upravuje buněčný metabolismus pro zachování správné funkce β-buněk.

Klíčová slova: slinivka břišní, glukóza, lipidy, redoxní prostředí, metabolismus

Table of contents

List of abbreviations

AACS	Acetoacetyl-CoA synthetase
ABHD6	Ab-hydrolase domain-containing protein 6
ACAT1	Acetyl-CoA acyltransferase 1
ACAA2	Acetyl-CoA acyltransferase 2
ACC	Acetyl-CoA carboxylase
ACLY	ATP citrate lyase
ACOT7	Acyl-CoA thioesterase 7
ACP	Acyl carrier protein
ACSL	Long-chain acyl-CoA synthetase
AGPAT	1-acylglycerol-3-phosphate acyltransferase
APT	Acyl-protein thioesterase
ATB	Antibiotics
ATGL	Adipose triglyceride lipase
BCA	Bicinchoninic acid
BSA	Bovine serum albumin
B2M	β-2-microglobulin
CACT	Carnitine-acylcarnitine translocase
cAMP	Cyclic adenosine monophosphate
CD36	Cluster of differentiation 36
CGI-58	Comparative gene identification-58
CoA	Coenzyme A
CPT	Carnitine palmitoyl transferase
DAG	Diacylglycerol
DGAT	Diacylglycerol O-acyltransferase
DGK	Diacylglycerol kinase
DHAP	Dihydroxyacetone phosphate
ER	Endoplasmic reticulum
ETC	Electron transporting chain
FA	Fatty acid

FA-CoA	Fatty acyl-coenzyme A
FAS	Fatty acid synthase
Fasn	Gene coding fatty acid synthase
FBS	Fetal bovine serum
FFAR	Free fatty acid receptor
GK	Glycerol kinase
glc	Glucose
GPAT	Glycerol-3-phosphate acyltransferase
GL/NEFA cycle	Glycerol/non-esterified fatty acid cycle
GPR	G protein-coupled receptor
GSIS	Glucose-stimulated insulin secretion
G3P	Glycerol-3-phosphate
G3PP	Glycerol-3-phosphate phosphatase
HFD	High-fat diet
HMG-CoA	Hydroxymethylglutaryl-CoA
HPRT	Hypoxanthine phosphoribosyltransferase
HSL	Hormone-sensitive lipase
IL	Interleukin
INS1E	Insulinoma 1E
IP3	Inositol-1,4,5-triphosphate
IS	Insulin secretion
JNK	c-Jun N-terminal kinase
KO	Knock-out
LD	Lipid droplet
LDH	Lactate dehydrogenase
Lipe	Lipase E
LPA	Lysophosphatidic acid
MUT	Mutant
MafA	Musculoaponeurotic fibrosarcoma oncogene homolog A
MAGL	Monoacylglycerol lipase
MCF	Metabolic coupling factor

NEFA	Non-esterified free fatty acids
NF-κB	Nuclear factor-kappa B
Nkx-6.1	Homeobox Protein NK-6 Homolog A
PA	Phosphatidic acid
PBS	Phosphate buffered saline
PC	Pyruvate carboxylase
PDH	Pyruvate dehydrogenase
Pdx1	Pancreatic and duodenal homeobox 1
PKA, PKC, PKD	Protein kinase A, C, D
PLC	Phospholipase C
PLIN	Perilipin
PRDX	Peroxiredoxin
PUFA	Polyunsaturated fatty acid
ROS	Reactive oxygen species
RT	Room temperature
SC-CoAs	Short-chain acyl-CoA
SCOT	Succinyl-CoA:3-ketoacid-CoA transferase
SFM	Serum-free medium
SOD	Superoxide dismutase
SSO	Sulfosuccinimidyl-oleate
TAG	Triacylglycerol
TNF-α	Tumor necrosis factor-alpha
TXN	Thioredoxin
T2D	Type 2 diabetes
WT	Wild type
YWHAZ	Tyrosine 3-monooxygenase/tryptophan 5-monooxygenase activation protein zeta
1-MAG	1-monoacylglycerol
4-HNE	4-hydroxy-2E-nonenal

1. Introduction

Pancreatic β-cells are endocrine cells located in the islets of Langerhans within the pancreas. Characterized by their unique ability to sense and respond to glucose, β-cells are essential for maintaining glucose homeostasis through the secretion of insulin. Insulin secretion leads to a decrease in blood glucose levels, promotes glycogen synthesis in the liver, stimulates triacylglycerol synthesis in adipocytes, and inhibits glucagon secretion from α-cells. Lipid metabolism is inevitable for proper insulin secretion and β-cell function. Acute exposure to lipids enhances glucose-stimulated insulin secretion. By lowering the level of plasma-free fatty acids, the acute insulin response to elevated glucose is significantly diminished (Stein *et al.,* 1996). Chronic exposure to elevated levels of lipids can lead to lipotoxicity, cellular stress, disrupted metabolic homeostasis, β-cell dedifferentiation, insulin resistance and type 2 diabetes (Cinti *et al.,* 2016; Ji *et al.,* 2019). Lipid metabolism is regulated by glucose. In β-cells, most of the carbon from glucose enters mitochondria as pyruvate (Schuit *et al.,* 1997), leading to the formation of citrate, which can be redirected from mitochondria to enter anaplerotic pathways. From citrate, malonyl-CoA is synthesized, inhibiting the import of fatty acids to mitochondria, and thus blocking the β-oxidation of fatty acids. The central molecule linking glucose and lipid metabolism is glycerol-3-phosphate, which serves as an electron donor for the mitochondrial electron transport chain, or it can be esterified with fatty acyl-CoA to enter lipogenesis or dephosphorylated to glycerol. Due to the low expression of glycerol kinase in β-cells (Noel *et al.,* 1997), free glycerol cannot re-enter lipogenesis but is instead released from the cell by aquaglyceroporin, which serves as a detoxification mechanism. Triacylglycerol synthesis and hydrolysis are parts of the glycerol/non-esterified fatty acid cycle (GL/NEFA). Some intermediates of this cycle also act as metabolic coupling factors that augment glucose-stimulated insulin secretion. Additionally, the GL/NEFA cycle plays a role in the protection of the cells against glucolipotoxicity by generating triacylglycerols, which are stored in lipid droplets. Lipid droplets are dynamic cellular structures storing neutral lipids (triacylglycerols, cholesterol esters and retinol esters) in the core, which is wrapped in a phospholipid monolayer. Lipid droplets contribute to energy homeostasis, prevent lipotoxicity and protect the cells against endoplasmic reticulum and oxidative stress (Welte *et al.,* 2017).

Redox environment also plays an important role in β-cells. Owing to the relatively low expression of the classical enzymes of the antioxidative defence (Tiedge *et al.,* 1997), β-cells can react to minor fluctuations in the redox environment and maintain redox signalling mediated by thioredoxins and peroxiredoxins (Stancill *et al.,* 2019). H_2O_2 is one of the mediators of the redox signalling and in the cytoplasm, it is produced by NADPH oxidases (NOX) upon glucose stimulation. Among the NOX isoforms, only NOX4 is constitutively active and assembled in β-cells. NOX4-derived H_2O_2 is indispensable for proper redox signalling and insulin secretion (Plecitá-Hlavatá *et al.,* 2020). Mice with *Nox4* β-cell-specific knockout show dysregulated lipid metabolism and significantly increased lipid accumulation (Holendová *et al.,* 2024).

In the experimental part, the glucose and *Nox4* silencing/knockout impact on the lipid metabolism and turnover in pancreatic β-cells was analysed. The expression of genes involved in lipid generation and flux and lipid droplet accumulation under different nutritional conditions were analysed. Also, the content of non-esterified fatty acids and glycerol release were quantified. All these findings create the basis for understanding the interconnection between glucose metabolism, redox environment, and lipid handling in pancreatic β-cells which is crucial for the explanation of T2D development.

2. Literature review

2.1. Pancreas

The human pancreas is a lobulated multifunctional organ with an elongated J-shape with a length of 12–15 cm. It lies on the posterior abdominal wall behind the stomach. During the ontogenesis, it is formed from the endoderm.

2.1.1. Anatomy

The average pancreas of an adult has a volume of 72 cm^3 (Saisho *et al.,* 2007) and a weight of 50-100g (Rahier *et al.,* 1981; Rahier *et al.,* 1983). It consists of a head (caput), neck (isthmus), body (corpus) and tail (cauda). The head is aligned with the upper curvature of the duodenum. The pancreas is enclosed by a fibrous capsule. The mouse pancreas consists of 3 parts: the duodenal, the splenic and the gastric lobe. The lobes of the mouse pancreas are usually separated by adipose and connective tissues.

2.1.2. Histology

Pancreas consists of the endocrine (pars endocrina) and exocrine parts (pars exocrina). The exocrine part comprises about 80% of the pancreas and consists of acini that produce digestive enzymes in the duodenum (Fig. 1). These include trypsin, lipase, amylase, elastase, and chymotrypsin. Each acinus is formed from a cluster of pyramidal acinar cells. The pancreatic duct vents into the duodenum adjacent to the common bile duct (Dolenšek *et al.,* 2015). The endocrine part of the pancreas is formed by islets of Langerhans. One islet is composed of a few to several thousand endocrine cells. There are several types of endocrine cells (Fig. 2). β-cells create 50-70% of the islet cells in humans (60-80% in mice), and α-cells make up 20-40% of cells in humans (10-20% in mice) (Dolenšek *et al.,* 2015). Other cell types are PP-cells also known as F-cells (or formerly γ-cells) producing pancreatic polypeptide, δ-cells, which release somatostatin and ε-cells secreting ghrelin. Rodent pancreatic islets have β-cells clustered in the centre of an islet with a mantle of α- and δ-cells. In contrast, humans have a more heterogeneous centre of islets containing a larger percentage of α-cells in the central position compared to rodents. However, smaller human islets resemble those in rodents (Levetan & Pierce, 2013). Differences between human and rodent pancreas are also in innervation and vasculature (Dolenšek *et al.,* 2015).
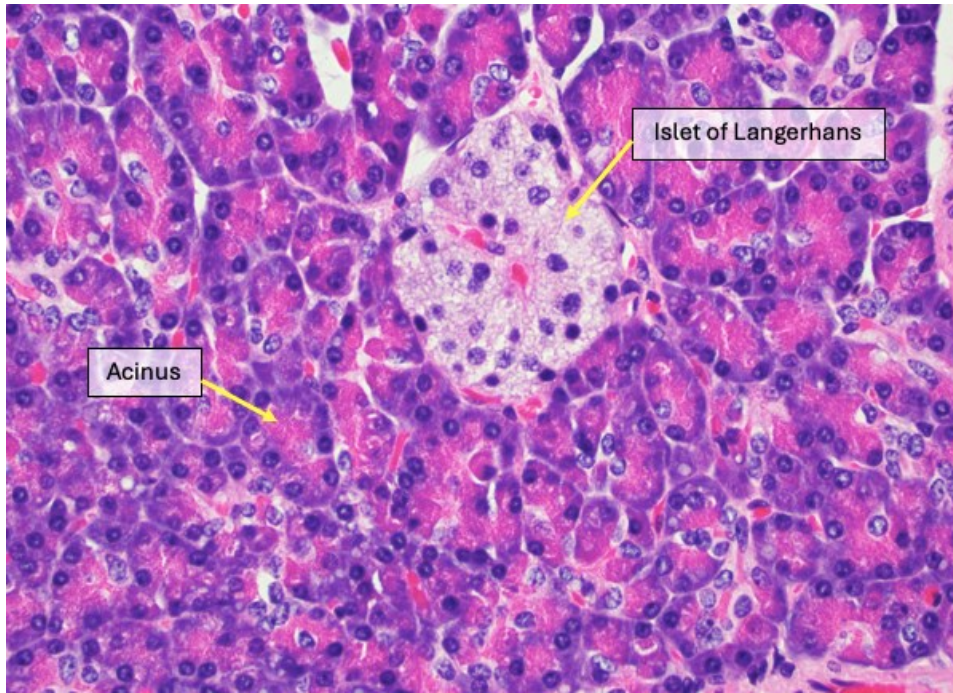
Figure 1: **Pancreas histology.** The exocrine part of pancreas is formed by acini. The endocrine part is composed of the islets of Langerhans. Medicine.nus.edu.sg. (n.d.).
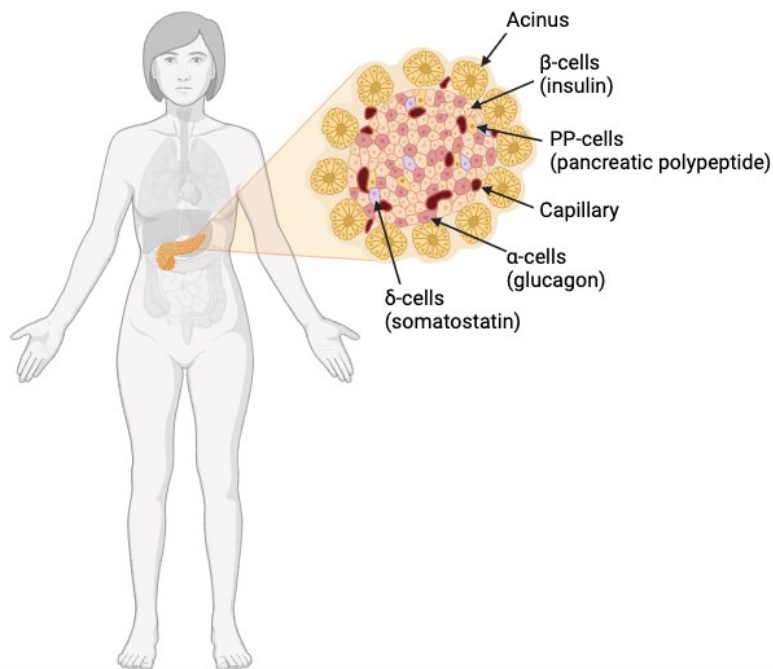
Figure 2: **Histology of human pancreas.** The human pancreas is located on the posterior abdominal wall behind the stomach. The exocrine part consists of acini producing digestive enzymes in the duodenum. The endocrine part of the pancreas is the Langerhans islets encompassing β-cells producing insulin, α-cells producing glucagon, δ-cells producing somatostatin and PP-cells producing pancreatic polypeptide. (Created with Biorender.com)

2.1.2.1. β-cells

Pancreatic β-cells are sensors of glucose. Their key ability is to maintain normoglycemia. Depending on the blood glucose concentration β-cells secrete insulin, which impacts other cells. Secretion of insulin causes a decrease in blood glucose, glycogen synthesis in the liver, synthesis of triacylglycerols in adipocytes and inhibition of secretion of glucagon from α-cells. β-cells are formed by duplication of existing differentiated β-cells or by neogenesis (differentiation from pancreatic duct cells) (El-Gohary *et al.,* 2016; Dor *et al.,* 2004). Terminal differentiation of β-cells does not automatically mean their functional maturity, as β-cell maturation in mammals occurs postnatally (Bliss & Sharp, 1992). The stimulating postnatal factor for β-cell maturation in mice is the change in the diet of newborns from a high-fat milk diet to carbohydrate-based diet (Helman *et al.,* 2020). During maturation of β-cells, glucose-induced insulin secretion is enhanced and the rate of proliferation declines (Bonner-Weir *et al.,* 2016). The maturity level of β-cell derived by duplication likely depends on the maturity level of the parent cell. The population of β-cells is not homogenous as it is composed of β-cell subpopulations of different origin and different ages.

2.2. Glucose uptake

Glucose enters cells through glucose transporters (GLUT) in the plasma membrane by facilitated diffusion. GLUTs are tissue-specific with different transport characteristics (Berger & Zdzieblo, 2020). Rodent β-cells express GLUT1 with Km = 1-2 mM and GLUT2 with Km = 15-20 mM (Thorens *et al.,* 1988; Gorovits & Charron, 2003). GLUT1 is expressed in most mammalian tissues (Gorovits & Charron, 2003). GLUT2 has a low affinity and the highest capacity for glucose (Efrat 1997). Expression of GLUT2 in human β-cells is much smaller in comparison to rodents (McCulloch *et al.,* 2011). The most prevalent GLUTs in humans are GLUT1 and GLUT3 (McCulloch *et al.,* 2011). It is not clear whether GLUT2 is part of the glucose transport in human pancreatic β-cells. However, human islets are resistant to streptozotocin, a glucose analog transported by GLUT2, which suggests GLUT2 does not play a key role in glucose transport in humans (Wang & Gleichmann, 1998; Eizirik *et al.,* 1994). In addition, homozygous mutations in GLUT2 demonstrate themselves more mildly than in the mouse model *Slc2a2$^{-/-}$*, which suffers severe β-cell failure (Berger & Zdzieblo, 2020).

2.3. Glucose-stimulated insulin secretion

Glucose-stimulated insulin secretion (GSIS) happens in two phases (Henquin, 2000). The first phase begins when glucose enters the cell through glucose transporters by facilitated diffusion and is phosphorylated to glucose-6-phosphate by hexokinase (glucokinase in β-cells), so it can be further metabolized. Thanks to the phosphorylation it remains in the cell. Glucose-6-phosphate then enters glycolysis producing pyruvate. Pyruvate is transformed into acetyl-CoA entering the Krebs cycle localized in the mitochondrial matrix. Krebs cycle produces reduced coenzymes NADH and FADH$_2$, which are oxidized in the following respiratory chain. It results in ATP production, meaning glucose

elevation causes an increase in ATP/ADP ratio. Then ATP-sensitive potassium channels on the cytoplasmatic membrane are inhibited and the membrane is depolarized. As a result, the voltage-gated calcium channels are activated allowing entry of Ca^{2+} into the cell and thus increasing cytosolic Ca^{2+}. This activates the fusion of insulin granules with the cytoplasmatic membrane and their exocytosis. These events are currently considered as the canonical pathway of insulin secretion (IS).

Glucose metabolism, fatty acid (FA) metabolism and metabolism of some amino acids are sources of so-called metabolic coupling factors (MCFs), which amplify the second phase of the GSIS. However, MCFs cannot stimulate GSIS at physiological concentrations in the absence of glucose (Henquin *et al.,* 2006). They can be divided into regulatory and effectory MCFs. Regulatory MCFs modulate metabolic pathways, which affect the GSIS. Effectory MCFs are directly involved in the final steps of the signalization cascade, e.g. insulin granule exocytosis (Prentki *et al.,* 2020).

The main MCFs are NADPH, reactive oxygen species (ROS), ATP, fatty acyl-CoA, citrate, malonyl-CoA, glutamate, cAMP, monoacylglycerol (MAG) and diacylglycerol (DAG). Apart from MCFs for example incretins can also amplify GSIS (Gheni *et al.,* 2014).

2.4. Pentose phosphate pathway

The pentose phosphate pathway consists of several anabolic reactions and provides pentoses, which are formed from glucose. It has oxidative (irreversible) and non-oxidative (reversible) phases. Besides other molecules, ribose which is needed for nucleotide synthesis is created here. Reduced coenzyme NADPH is created in this pathway. It is a substrate for example for NOX enzymes and is used in fatty acid synthesis. Other molecules created in the cycle are xylulose-5-phosphate, sedoheptulose-7-phosphate, glyceraldehyde-3-phosphate, erythrose-4-phosphate fructose-6-phosphate and glyceraldehyde-3-phosphate. Fructose-6-phosphate and glyceraldehyde-3-phosphate are further metabolised in glycolysis. In the context of β-cells, the generation of glycerol-3-phosphate is important because this molecule interconnects glucose and lipid metabolism.

In β-cells, the pentose phosphate pathway has a low contribution to total glucose utilisation, and it decreases with rising glucose concentration (Schuit *et al.,* 1997). After an elevation of glucose from 2.8 mM to 16.7 mM, the NADPH/NADP$^+$ ratio increases significantly. When glucose-6-phosphate dehydrogenase is inhibited (also NADPH formation is inhibited), GSIS is decreased by 41% in INS1 cells and by 57% in rat pancreatic islets. In contrast, GSIS is not affected by an inhibition of 6-phosphogluconic acid dehydrogenase, which inhibits the formation of NADPH only partially (Spégel *et al.,* 2013). These findings show the importance of the pentose phosphate pathway even during GSIS. Furthermore, glucose induces the production of ribose-5-phosphate, which was confirmed by the incorporation of [U-^{13}C]-glucose experiment (Spégel *et al.,* 2013).

2.5. Lipid metabolism in β-cells

Lipids are a heterogenous class of structurally and functionally diverse non-polar compounds insoluble in polar solvents such as water, but they are soluble in non-polar or weakly polar organic solvents (ether, chloroform, benzene, acetone). The supply of FAs to β-cells is exogenous (plasma FAs) and endogenous (triacylglycerols and phospholipids) (Nolan *et al.,* 2006). In plasma, mostly FAs are esterified in triacylglycerols, cholesteryl esters and phospholipids, which are bound to albumin and lipoproteins. Pancreatic islets express and secrete lipoprotein lipases, so the non-esterified fatty acid (NEFA) concentration around the islet can be higher than in plasma (Pappan *et al.,* 2005). Fatty acids that can be uptaken by β-cells include short-chain FAs (C < 6), such as propionate and butyrate produced by gut microbiota (Koh *et al.,* 2016); medium-chain FAs (6 – 12 C), like capric acid and lauric acid absorbed from dietary plant oils and milk; long-chain FAs (12 - 18 C), with palmitic and linoleic acid being the most abundant in plasma; and very long-chain (for example, arachidonic acid) (Risé *et al.,* 2007). Lipids are important for all types of cells including β-cells. They provide energy for the cell, are components of the cytoplasmatic membrane, and can function in signalling.

Lipid metabolism involves the synthesis of storage lipids in the form of triacylglycerols, which are the source of energy when catabolized. The synthesis also provides structural and functional lipids, for example, components of cellular membranes. Lipid catabolism is carried out through β-oxidation localized in mitochondria and peroxisomes.

2.5.1. Fatty acid uptake and signalling

Fatty acids are hydrophobic molecules and can enter the cell via passive diffusion or by fatty acid transport proteins. The most studied are FA translocase cluster of differentiation 36 (CD36), FA transporter protein family (FATP1) and FA binding protein 1 (FABPpm), which is membrane-bound, and fatty acid binding receptors. In the cell, there are cytosolic FA binding proteins (FABPc), which transport FAs to the specific organelles. CD36 increases the uptake of FAs by β-cells. It was confirmed that CD36 is directly involved in FA uptake by the experiment with sulfosuccinimidyl-oleate (SSO), a CD36 inhibitor. Treatment of mouse β-cell line MIN6 with 0,5 mmol/l SSO caused inhibition of palmitate uptake by $46 \pm 9,7\%$ in comparison to cells treated only with palmitate. In human pancreatic islets, CD36 is localized in the cytoplasmatic membrane and the insulin secretory granules. In the hyperglycemic state, the expression of CD36 is increased, which supports the FA uptake even more. Long-term exposure to FAs inhibits GSIS, elevates the intracellular content of lipids and leads to the reduction of glucose oxidation and utilization by human pancreatic islets (Noushmehr *et al.,* 2005).

Fatty acid binding receptors of the family of G protein-coupled receptors bind several ligands including hormones, neurotransmitters, proteins, and FAs translating the signal into an intracellular response through heterotrimeric G proteins. G protein-coupled receptor 40 (GPR40), also known as free fatty acid receptor 1 (FFAR1), is mainly expressed in the pancreas (β-cells) and brain (Briscoe *et al.,*

2003). The receiver is activated by medium- and long-chain fatty acids, mostly those with 15 and 16 carbon chain length (Briscoe et $al.,$ 2003). GPR40 activates phospholipase C (PLC), which cleaves phosphatidyl-4,5-bisphosphate to inositol-1,4,5-triphosphate (IP3) and 1,2-DAG, the second messengers. DAG activates protein kinase D1 resulting in F-actin remodelling and insulin secretion. IP3 induces [Ca^{2+}] release from ER through the IP_3 receptor, thus increasing cytosolic [Ca^{2+}], whose flux is primarily mediated by voltage-dependent calcium channels on the cytoplasmic membrane from the extracellular space. As a result of the downregulation of GPR40, FA augmentation of IS is impaired. (Itoh et $al.,$ 2003). Overexpression of GPR40 leads to an increase in GSIS (Nagasumi et $al.,$ 2009). GPR120 (FFAR4) is activated by long-chain unsaturated non-esterified fatty acids (NEFAs), with α-linoleic acid being the most potent (Hirasawa et $al.,$ 2005). Both receptors, GPR40 and GPR120 mediate palmitic and oleic acid potentiation of GSIS (Gehrmann et $al.,$ 2010). Another G protein-coupled receptor expressed in β-cells is GPR119. The ligand, which binds to this receptor and activates it, is lysophosphatidylcholine (Soga et $al.,$ 2005). It is still not known whether the FAs, which modulate the function of the FFARs, are coming from endogenous (inside the cells e.g. from lipolysis) or exogenous sources (Nolan et $al.,$ 2006).

2.5.2. Fatty acid transport into mitochondria

Short-chain fatty acids and medium-chain fatty acids pass through the mitochondrial membranes in a transporter-independent manner. Fatty acids with long-chain (12 - 18 C) enter the mitochondria using carnitine. Fatty acids with chains longer than 18 carbons (very long-chain fatty acids) cannot pass and enter peroxisomes instead (Oberhauser & Maechler, 2021). L-carnitine (β-hydroxy-γ-trimethylaminobutyrate) is the physiologically active enantiomer. D-carnitine on the other hand has a toxic effect on the metabolism. L-carnitine is synthesized from lysine and methionine mostly in the liver, kidneys and brain (Ferreira & McKenna, 2017). During stress or physical exertion, the endogenous production of L-carnitine might not be sufficient, so it must be part of the diet (meat, dairy products). L-carnitine also transports some toxic compounds out of the mitochondria. (Pekala et $al.,$ 2011). During the transport into mitochondria, a fatty acid connects with CoA (coenzyme A) to form FA-CoA in order to enter mitochondria via the L-carnitine shuttle. This reaction requires one molecule of ATP. CPT1 (carnitine palmitoyl transferase) transfers fatty acyl to L-carnitine so acylcarnitine is formed in the intermembrane space of mitochondria. CACT (carnitine-acylcarnitine translocase) on the inner mitochondrial membrane exchanges acylcarnitine for free L-carnitine from the mitochondria. CPT2 transfers acyl from acylcarnitine to mitochondrial CoA and fatty acyl-CoA is formed again. It then enters β-oxidation in the mitochondrial matrix. At the same time, free L-carnitine is released, and it returns to the outer mitochondrial membrane (Fig. 3). Inhibitors of CPT1 are 2-bromostearate (Tamarit-Rodriguez et $al.,$ 1984), 2-bromopalmitate (Chen et $al.,$ 1994) and etomoxir (Zhou et $al.,$ 1996). By the inhibition of CPT1 by etomoxir or by providing NEFA, reduced GSIS can

be restored in the cells overexpressing CPT1 (Rubí *et al.,* 2002). After the inhibition of CACT by miRNA, the level of fatty acylcarnitine was increased and so was GSIS (Soni *et al.,* 2014).
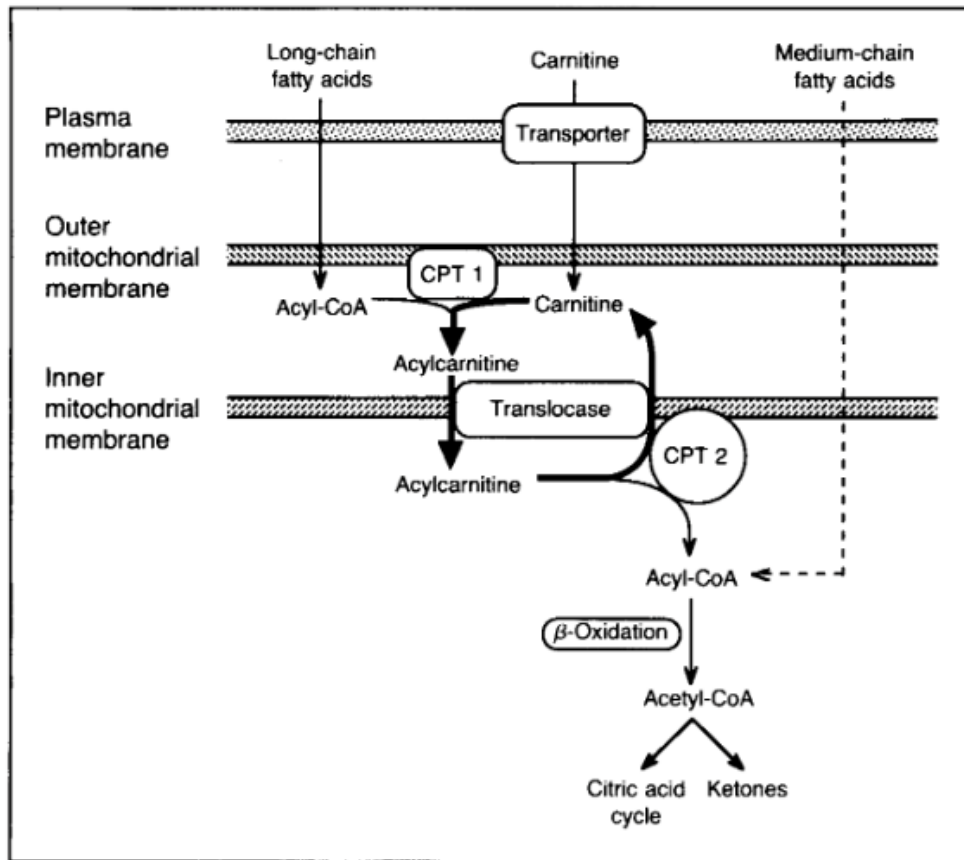

Figure 3: **Fatty acid transport into mitochondria.** Short-chain and medium-chain fatty acids pass the mitochondrial membranes in a transporter-independent manner. Long-chain fatty acids are transported to the mitochondria by L-carnitine shuttle. Fatty acids have to be in an activated form of acyl-CoA. Carnitine palmitoyl transferase 1 (CPT1) on the outer mitochondrial membrane transfers acyl from acyl-CoA to L-carnitine so acylcarnitine is formed. Acylcarnitine is exchanged for free L-carnitine from mitochondria by carnitine-acylcarnitine translocase (CACT) on the inner mitochondrial membrane. Carnitine palmitoyltransferase 2 tranfers acyl from acylcarnitine to mitochondrial CoA and free L-carnitine is released returning to the outer mitochondrial membrane. Formed acyl-CoA enters β-oxidation in the mitochondrial matrix. (Stanley *et al.*, 1992)

2.5.3. β-oxidation

β-oxidation is a catabolic process of utilizing fatty acids in mitochondrial matrix. During β-oxidation, long-chain FAs are broken down into acetyl-CoA, which continues to the Krebs cycle. Apart from acetyl-CoA, reduced coenzymes (NADH and $FADH_2$) are formed going to the respiratory chain producing ATP. FAs are a rich source of energy for the cell. Based on equation (1) it can be count how many molecules of ATP a FA provides.

$$ATP = 8{,}5n - 7 \tag{1}$$

where $n = number\ of\ carbons\ in\ the\ fatty\ acid$

Medium-chain and long-chain fatty acids are oxidized mostly in mitochondria and small amounts in peroxisomes. However, very long-chain fatty acids are catabolized solely in the peroxisomal

β-oxidation. In mitochondrial β-oxidation, FAs are shortened by two carbons and the cycle repeats until a fatty acid is shortened to acetyl-CoA. In the first step, acyl-CoA is oxidized to trans-enoyl-CoA by acyl-CoA dehydrogenase. Followingly, trans-enoyl-CoA is hydrated to hydroxyacyl-CoA with a double bond between Cα and Cβ. This reaction is done by enoyl-CoA hydratase. Hydroxyacyl-CoA is then dehydrogenated by hydroxyacyl-CoA dehydrogenase to ketoacyl-CoA. The last step is a thiolytic cleavage of ketoacyl-CoA by ketoacyl-CoA thiolase. This reaction requires one molecule of CoA since the products of this reaction are acetyl-CoA and acyl-CoA shorter by two carbons. Acyl-CoA enters another round of β-oxidation.

In β-cells, almost all glucose entering the cell is oxidized through glycolysis to pyruvate and further by oxidative phosphorylation to ATP. A small amount of glucose is metabolized to lactate since lactate dehydrogenase in β-cells has very low activity (Sekine *et al.,* 1994). Alos β-cells have only small storage of glycogen (< 10% of glucose uptake) (Ashcroft *et al.,* 2017). During fasting conditions, the main endogenous energy source for basal cell functions is fatty acids (Malaisse *et al.,* 1983). In the form of acyl-CoA they enter mitochondria for β-oxidation. After an increase in glucose (most often postprandially), a higher amount of citrate is produced in the Krebs cycle and the citrate leaves the mitochondria. Followingly ATP citrate lyase (ACLY) transforms citrate to acetyl-CoA. Acetyl-CoA is then carboxylated by acetyl-CoA carboxylase 1 (ACC1) to malonyl-CoA, which inhibits CPT1 and prevents fatty acids from entering mitochondria. Through this mechanism, fatty acid synthesis blocks β-oxidation. When β-oxidation is blocked fatty acids can enter the lipogenic arm of the GL/NEFA cycle. Overexpression of malonyl-CoA carboxylase led to a decreased level of malonyl-CoA after the addition of NEFA. The result is a higher rate of β-oxidation and reduced GSIS (Roduit *et al.,* 2004). These data indicate the importance of lipids during GSIS.

2.5.4. Anaplerotic pathways preceding lipid synthesis in β-cells

Carbon from pyruvate (originating from glucose) is incorporated into metabolites stimulating or supporting GSIS in mitochondria. These metabolites include short-chain acyl-CoA (SC-CoAs), for example, acetyl-CoA, malonyl-CoA, acetoacetyl-CoA, and hydroxymethylglutaryl-CoA (HMG-CoA). SC-CoAs cannot pass the inner mitochondrial membrane, so they are converted to other metabolites, which can be exported out of mitochondria. In the cytosol, they are converted back to SC-CoAs (El Azzouny *et al.,* 2016). 60% of glucose enters mitochondria via pyruvate dehydrogenase and the remaining 40% by pyruvate carboxylase when both enzymes metabolize pyruvate (Khan *et al.,* 1996; Cantley *et al.,* 2019). There are two redundant pathways of anaplerosis of SC-CoAs for lipid synthesis beginning in mitochondria, one involving citrate, the other one acetoacetate.

In the classical pathway, pyruvate is carboxylated by pyruvate carboxylase to oxaloacetate. Pyruvate dehydrogenase converts pyruvate to acetyl-CoA. Oxaloacetate and acetyl-CoA are metabolized by citrate synthase to citrate, which is then transported out of mitochondria and converted back to acetyl-CoA and oxaloacetate by ACLY in the cytosol. ACC mediates the carboxylation

of acetyl-CoA to malonyl-CoA. This reaction requires one molecule of ATP and is rate-limiting. ACLY showed high expression on the mRNA level in human and rat pancreatic islets (MacDonald *et al.,* 2013b). In rat islets, the activity of ACLY was 17-fold higher than in rat kidney and 12-fold higher than in rat liver. In human pancreatic islets, the activity was 25% of the activity in rat islets and INS1 cells (MacDonald *et al.,* 2013b).

ACC is active in its dephosphorylated form. It is positively regulated by citrate and insulin and negatively by palmitate. ACC is substantially activated during the first 5 minutes of glucose stimulation (Brun *et al.,* 1996). β-cells possess a fair amount of ACC mRNA corresponding with the enzymatic activity (Brun *et al.,* 1996). There are two isoforms of the ACC enzyme – ACC1 and ACC2. In human and rat pancreatic islets and INS1 cells, isoform ACC1 is the only isoform present. This isoform is also expressed in lipogenic tissues (MacDonald *et al.,* 2008). Islets from mice with knockdown of *Acc1* in β-cells have defective GSIS, showing the necessity of ACC1 for their function. *Acc1* β-specific knockdown also leads to a reduction of β-cell mass by 46% and smaller cell size, which are accompanied by a decrease in insulin content (Cantley *et al.,* 2019). Glucose-induced ACC1 mRNA can be inhibited by long-chain fatty acyl-CoAs, both saturated and unsaturated (palmitate and linoleate) (Brun *et al.,* 1997). Constitutively active ACC1 supports GSIS. In contrast, when ACC1 is inhibited, less malonyl-CoA is created and the inhibition of CPT1 is less effective. Thanks to this, fatty acids enter β-oxidation and GSIS is decreased (Prentki *et al.,* 2020; Zhang & Kim, 1998).

The acetoacetate pathway is formed by the following reactions. Acetyl-CoA in mitochondria is converted to acetoacetyl-CoA by acetyl-CoA acyltransferase 1 or 2 (ACAT1 or ACAA2). Then acetoacetyl-CoA is converted to acetoacetate by succinyl-CoA:3-ketoacid-CoA transferase (SCOT). Acetoacetate is transported out of mitochondria to cytosol, where acetoacetyl-CoA synthetase (AACS) converts it back to acetoacetyl-CoA and further to acetyl-CoA by cytosolic ACAT2 and ACAA1. Acetyl-CoA then proceeds to fatty acid synthase (Fig. 4).

Evidence for the two pathways are studies, where *Acly* knockdown was performed (MacDonald *et al.,* 2007; El Azzouny *et al.,* 2016). Neither *Acly* knockdown nor inhibition by hydroxycitrate inhibited GSIS or affected the flux of glucose into lipids (El Azzouny *et al.,* 2016; Chen *et al.,* 1994). These data were supported with other studies showing inhibition of ACLY by radicicol, that partly inhibited GSIS in rat β-cells (Flamez *et al.,* 2002; Guay *et al.,* 2007). These findings suggest that there is a redundant pathway that creates acetyl-CoA in the cytosol without the involvement of ACLY. The only known pathway is the acetoacetate pathway. Knockdown of the genes coding the acetoacetate pathway enzymes SCOT and AACS leads to inhibition of GSIS in INS1 cells (Hasan *et al.,* 2010; MacDonald *et al.,* 2007). Overall, these findings suggest that ACLY maintains malonyl-CoA levels in resting β-cells, while the acetoacetate pathway produces malonyl-CoA after glucose stimulation (El Azzouny *et al.,* 2016).
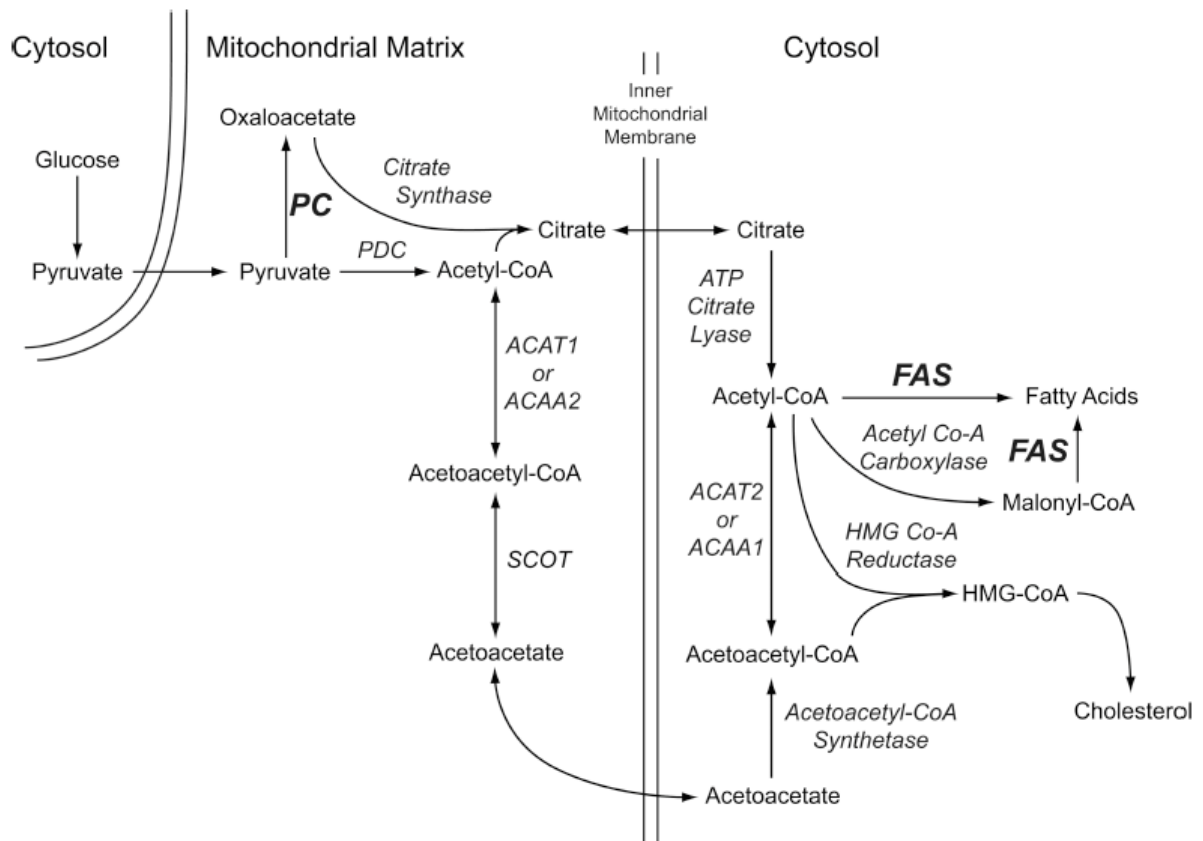
Figure 4: **Anaplerotic pathways preceding lipid synthesis.** Glucose is metabolized to pyruvate in glycolysis, which takes place in the cytosol. Pyruvate enters mitochondria where it can be carboxylated by pyruvate carboxylase (PC) to oxaloacetate or converted to acetyl-CoA by pyruvate dehydrogenase (PDH). Oxaloacetate is condensed with acetyl-CoA by citrate synthase and citrate is formed. There are two ways of processing citrate. The classical one is when citrate is transported out of mitochondria and ATP citrate lyase (ACLY) converts it back to acetyl-CoA. Followingly, acetyl-CoA carboxylase generates malonyl-CoA from citrate, which together with acetyl-CoA enters fatty acid synthesis by fatty acid synthase (FAS). Another way is the acetoacetate pathway. Acetyl-CoA in mitochondria is converted to acetoacetyl-CoA by acetyl-CoA acyltransferase 1 or 2 (ACAT1 or ACAA2. Succinyl-CoA:3-ketoacid-CoA transferase (SCOT) mediates the conversion of acetoacetyl-CoA to acetoacetate, which leaves mitochondria. In the cytosol, acetoacetate is transformed back to acetoacetyl-CoA by acetoacetyl-CoA synthetase (AACS) and acetoacetyl-CoA to acetyl-CoA by ACAT2 or ACAA1. Acetyl-CoA also serves as a precursor for cholesterol synthesis with its intermediate hydroxymethylglutaryl-CoA (HMG-CoA), which is formed from acetyl-CoA by HMG-CoA reductase (MacDonald *et al.*, 2013a)

2.5.5. Fatty acid synthesis

The process of fatty acid synthesis takes place in the cytoplasm of a cell. Fatty acid synthase (FAS) is a complex multi-domain enzyme. Type I is present in all eukaryotes except plants. It is encoded by the gene *Fasn*. During the reactions of fatty acid synthesis, the acyl is transferred by acyl carrier protein (ACP) from an enzyme to another enzyme. The synthesis begins with the binding of acetyl-CoA to ACP. Next, malonyl-CoA binds to ACP and it is condensed with acetyl-CoA forming acetoacetyl-ACP, which is then reduced by NADPH to 3-hydroxybutyryl-ACP. Water is eliminated forming enoyl-ACP. Enoyl-ACP is then reduced by NADPH to butyryl-ACP. Butyryl enters another round of the synthesis, and the acyl is extended until the palmitate is created. In ER, palmitate can be further modified to other fatty acids. Elongases create longer fatty acids than palmitate (16C) and desaturases make double bonds.

11

It was shown that INS1 cells have about 50% of the concentration of FAS as liver and rat pancreatic islets about 25% of the liver level. However, the enzyme activity in INS1 is 46% and in islets 65% of the liver FAS activity (MacDonald *et al.*, 2008). The expression level of FAS in human pancreatic islets and INS1 cells is quite high (MacDonald *et al.*, 2011), compared to low expression in rat pancreatic islets (Brun *et al.*, 1996). β-cells seem to be a lipogenic tissue that synthesizes lipids rather than catabolizing them as fuel. Rapid *de novo* synthesis of lipids correlates with insulin secretion (MacDonald *et al.*, 2008).[14]C-glucose (glc) labelling experiment revealed rapid incorporation of labelled carbon into lipids in β-cells. The levels of lipids were increased 15 times at 10 mM glucose in comparison to 1 mM glucose in INS1 cells. *Fasn* knockdown causes lowered incorporation of glucose carbon into lipids by 20-30% (MacDonald *et al.*, 2013a).

Cerulenin, an antifungal antibiotic isolated from *Cephalosporium caerulens*, is an inhibitor of sterol and fatty acid synthesis by preventing palmitoylation of FAS and hydroxymethylglutaryl-CoA synthase (Vance *et al.*, 1972; Ohno *et al.*, 1974). When used in experiments with INS1 cells and rat pancreatic islets it decreases GSIS (MacDonald *et al.*, 2008). Overall, these data indicate that lipid synthesis is important for normal GSIS (MacDonald *et al.*, 2013a).

2.5.6. GL/NEFA cycle

GL/NEFA cycle is the central pathway of lipid metabolism in β-cells. Not only it generates intermediates for complex lipid synthesis, but some of its intermediates increase GSIS. It also has an indispensable role in the protection of cells against glucolipotoxicity and metabolic stress. The cycle consists of TAG hydrolysis and TAG synthesis, the lipolytic and lipogenic arms, respectively (Fig. 5).
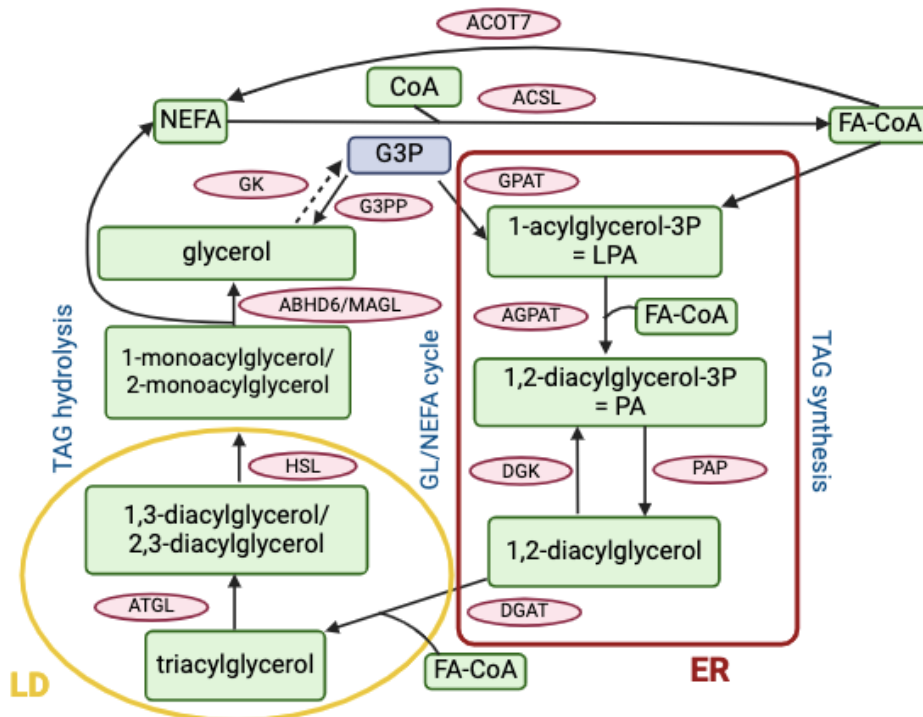
Figure 5: **Glycerol/non-esterified fatty acid cycle (GL/NEFA cycle)**. GL/NEFA cycle has lipolytic and lipogenic arms. The lipolytic arm is the triacylglycerol (TAG) hydrolysis beginning in the lipid droplets. TAGs are cleaved by adipose triglyceride lipase (ATGL) so 1,3- or 2,3-diacyglycerol (DAG) is formed. Hormone sensitive lipase catalyses the hydrolysis of DAG to 1- or 2-monoacylglycerol (MAG). MAG is hydrolyzed to glycerol and free fatty acid by ab-hydrolase domain-containing protein 6 (ABHD6). Glycerol is phosphorylated to glycerol-3-phosphate (G3P) by glycerol kinase however, this enzyme is negligibly expressed in β-cells. G3P is dephosphorylated by glycerol-3-phosphate phosphatase. Fatty acids must be activated for the metabolism by addition of CoA. This reaction is catalyzed by long-chain acyl-CoA synthetase (ACSL). The reverse reaction is provided by acyl-CoA thioesterase 7. In the lipogenic arm of the cycle, triacylglycerols are synthesized in the endoplasmic reticulum. From G3P and fatty-acyl-CoA 1-acylglycerol-3-phosphate (lysophosphatidic acid, LPA) is formed by glycerol-3-phosphate acyltransferase (GPAT). 1-acylglycerol-3-phosphate acyltransferase (AGPAT) catalyzes binding of another fatty acyl-CoA and 1,2-diacylglycerol (phosphatidic acid, PA) is formed. PA is then dephosphorylated to 1,2-diacylglycerol by phosphatidic acid phosphatase (PAP). The reverse reaction is mediated by diacylglycerol kinase (DGK). In the last step, diacylglycerol acyltransferase (DGAT) connects diacylglycerol with third fatty acyl-CoA forming triacylglycerol stored in lipid droplets. (Created with Biorender.com)

In the lipolytic arm triacylglycerols (TAGs) are hydrolyzed. The first step of hydrolysis is rate-limiting and is catalyzed by adipose triglyceride lipase (ATGL) (Eichmann *et al.,* 2012). ATGL initiates the lipolysis in lipid droplets where triacylglycerols are stored (Zimmermann *et al.,* 2004). It removes FA from the sn-1 or sn-2 position when co-activated by its co-activator called comparative gene identification-58 (CGI-58) (also known as α/β-hydrolase domain-containing 5) thus 2,3-DAG or 1,3-DAG is formed, respectively. Products of ATGL reaction cannot directly go to glycerophospholipid synthesis because the substrate for the synthesis is 1,2-DAG and ATGL does not produce a detectable volume of this stereoisomer (Eichmann *et al.,* 2012). ATGL has the highest activity for tripalmitolein

(1,2,3-tripalmitoleoylglycerol). In general, the activity of the enzyme decreases with the increasing length of the FA a its desaturation (Eichmann *et al.*, 2012). Another FA is removed from the sn-3 position by hormone-sensitive lipase (HSL), encoded by the gene lipase E (*Lipe*), forming 1-MAG or 2-MAG (Mulder *et al.*, 1999; Rodriguez *et al.*, 2010). 1-MAG can serve as a metabolic coupling factor for insulin secretion as it binds to protein Munc13-1 facilitating insulin granules exocytosis through SNARE complex formation (Sheu *et al.*, 2003). HSL located in the cytoplasm is phosphorylated by protein kinase A (PKA) to translocate to a lipid droplet's surface (Sztalryd *et al.*, 2003). HSL is also capable of hydrolysing cholesterol or retinyl ester bonds, unlike ATGL. As for substrates, HSL can cleave both TAGs and DAGs, so it is partially redundant with ATGL. The specific activity of HSL for DAGs is ten times greater than for TAGs. On the other hand, DAG-hydrolase activity of ATGL is low (Zimmermann *et al.*, 2004). Hydrolysis of MAG is mediated by the ab-hydrolase domain-containing protein 6 (ABHD6) or monoacylglycerol lipase (MAGL) (Tornqvist and Belfrage, 1976; Blankman *et al.*, 2007). ABHD6 is cytoplasmic membrane lipase and is prevailing over MAGL in β-cells (Zhao *et al.*, 2014). MAGL is typical for other tissues and has both cytosolic and membrane forms (Labar *et al.*, 2010).

Fatty acids must be activated so they can enter metabolic pathways. For the connection of the long-chain fatty acids with Co-A an enzyme called long-chain acyl-CoA synthetase (ACSL) is required. Newly formed fatty acyl-CoA ester can be incorporated into triacylglycerols, phospholipids or cholesterol, or it can be oxidized in mitochondria. There are five isoforms of ACSL known in mammalian cells (ACSL1, ACSL3, ACSL4, ACSL5 and ACSL6). ACSLs can convert saturated and unsaturated fatty acids with 8-22 carbons to fatty acyl-CoA. Each family of ACSL has different intracellular localization and substrate specificity (Quan *et al.*, 2021). The family of ACSL is divided into two sub-families. The first one contains ACSL1, ACSL5 and ACSL6. This sub-family prefers saturated fatty acids as a substrate. The other sub-family consists of ACSL3 and ACSL4, which prefers highly unsaturated fatty acids. The difference between ACSL3 and ACSL4 isoforms is, that ACSL3 can metabolize a wider range of substrates than ACSL4. ACSL3, ACSL4 and ACSL5 were detected in INS1 cells and ACSL3 and ACSL4 are present in rat and human pancreatic islets. ACSL1 was found in the human and rat liver and rat heart. ACSL6 was reported in human and rat liver. ACSL3 and ACSL4 are concentrated in the mitochondria and even more in insulin secretory granules. Both isoforms prefer arachidonate over palmitate as a substrate. Knockdown of *Acsl3* and *Acsl4* leads to lower GSIS by about 50% in INS1-derived cells and human pancreatic islets (Ansari *et al.*, 2017). No inhibition of GSIS was observed when *Acsl1*, *Acsl5* and *Acsl6* knockdown was performed in INS1-derived cells (Ansari *et al.*, 2017). Knockdown of *Acsl4* changes the composition of fatty acids in phospholipids in β-cells (Ansari *et al.*, 2017).

Acyl-CoA thioesterase 7 (ACOT7) is an enzyme, which catalyzes the hydrolysis of fatty acyl-CoA. However, this enzyme is selectively repressed in mouse pancreatic islets and purified β-cells maintaining hydrolysis of fatty acyl-CoA to minimum. Overexpression of ACOT7 in MIN6 and INS1 cells

with the addition of 20 mmol/l glucose and 0,5 mmol/l oleate:palmitic acid (2:1) leads to decreased insulin secretion, reduced level of Ca^{2+} and lowered ATP/ADP ratio (Martinez-Sanchez *et al.,* 2016). These findings indicate that an adequate amount of FAs and low ACOT7 levels are required for normal GSIS and proper β-cell function.

In the lipogenic arm of the GL/NEFA cycle, TAGs are generated from activated glycerol in the form of G3P and activated fatty acid (FA-CoA). The reactions of the lipid biosynthesis take place in the ER. In the first step, G3P and FA-CoA are connected by GPAT (glycerol-3-phosphate acyltransferase) forming 1-acylglycerol-3P (lysophosphatidic acid, LPA). LPA is then connected with another FA-CoA by the action of AGPAT (1-acylglycerol-3-phosphate acyltransferase) resulting in 1,2-diacylglycerol-3P (phosphatidic acid, PA). PA is then dephosphorylated by phosphatidic acid phosphatase (PAP), creating 1,2-diacylglycerol (1,2-DAG). DAG can be reversibly phosphorylated by diacylglycerol kinase (DGK). This enzyme terminates DAG signalling and initiates PA signalling. DGKα and DGKγ isoforms are highly expressed in mouse pancreatic islets and MIN6 cells (Kurohane Kaneko *et al.,* 2013). Inhibition of DGK leads to the accumulation of DAG. When the accumulation is mild, DAG amplifies GSIS in a protein kinase C (PKC)-dependent manner. During excessive accumulation of DAG, GSIS is inhibited via inhibition of voltage-dependent calcium channels (Kurohane Kaneko *et al.,* 2013; Sawatani *et al.,* 2019). There are three DAG pools in the cell. The first pool includes 1,2-DAG from the *de novo* lipogenesis in the ER. This pool of DAG provides substrates for lipogenesis and the DGAT (diacylglycerol O-acyltransferase) enzyme or can be metabolized by CDP-choline:1,2-diacylglycerol choline phosphotransferase. The second pool is created by 1,3-DAG and 2,3-DAG, which are generated in lipid hydrolysis by ATGL. The third pool is 1,2-DAG, which is cleaved from the cytoplasmatic or ER membrane by PLC (Eichmann *et al.,* 2012). Only 1,2-DAG has a signalling role by activation of PKC regulating many physiological and pathological processes (Rando & Young, 1984), including insulin secretion and apoptosis (Eitel *et al.,* 2003). 1,2-DAG also regulates insulin secretion through the regulation of Munc13-1, which is a PKC-independent process (Rhee *et al.,* 2002). In the last step of triacylglycerol synthesis, 1,2-DAG is connected with FA-CoA by the enzyme DGAT, and triacylglycerol is generated (Eichmann *et al.,* 2012). There are two isoforms of DGAT in β-cells, DGAT1 and DGAT2. Both isoforms process all stereoisomers but with different efficiencies. This may be caused by structural differences in DGAT isoforms (Eichmann *et al.,* 2012). Another difference between these isoforms is their localization. DGAT1 mostly resides in the ER and DGAT2 in the phospholipid monolayer of LDs (Gluchowski *et al.,* 2017). Newly synthesized TAGs are stored in lipid droplets (LDs).

This pathway is highly energy-requiring and its function is enhanced during fuel oxidation, thus reducing the fuel load (Prentki & Madiraju, 2012). The disrupted function of the cycle can lead to pathogenesis such as insulin resistance or type 2 diabetes (T2D) (Prentki & Madiraju, 2008). Flux through the GL/NEFA cycle depends on the availability of G3P and fatty acyl-CoA (Mugabo *et al.,* 2016). High levels of fatty acids are toxic, so when they are incorporated into TAGs in the GL/NEFA

cycle and stored in LDs, their toxicity is alleviated. GL/NEFA cycle plays a role in detoxification also through another mechanism. Glucodetoxification is mediated by directing glucose carbons to glycerol, which leaves the cell. Because β-cells express glycerol kinase on a very low level, free glycerol cannot enter the cycle (see below) (Noel *et al.,* 1997). Another role of the GL/NEFA cycle is during lipodetoxification. NEFAs released from LDs during lipolysis can be transported out of the cell or oxidized in mitochondria through β-oxidation (Martins *et al.,* 2004). NEFAs released from the cell can probably target FFAR receptors in an autocrine or paracrine manner (Nolan *et al.,* 2006). The lipogenic arm of the GL/NEFA cycle also provides signalling molecules for β-cell growth (PA, LPA). When the lipolytic arm is reduced, the cell growth is favoured. On the other hand, when lipolysis prevails insulin secretion is supported (Prentki & Madiraju, 2012). In animals, the prediabetic state relates to an increased GL/NEFA cycling. This is a possible compensatory mechanism that enhances insulin secretion during nutrient-rich conditions. The accumulation of TAGs caused by FAs is dependent on glucose because it provides the glycerol-3-phosphate backbone originating from glycolysis (Prentki & Madiraju, 2012).

2.5.7. Glycerol-3-phosphate - a central metabolite at the crossroad of metabolism

Glycerol-3-phosphate (G3P) can be derived from lipid hydrolysis (GL/NEFA cycle) or glycolysis (Fig. 6). Dihydroxyacetone phosphate (DHAP) formed in glycolysis is partially transformed into G3P. It is a central metabolite standing at the crossroads of glycolysis, lipid metabolism, energy metabolism and gluconeogenesis (in the liver and kidney) (Possik *et al.,* 2021). Most of the carbon from glucose enters mitochondria as pyruvate in β-cells (Schuit *et al.,* 1997). Expression of lactate dehydrogenase (LDH) mediating reversible conversion of pyruvate to lactate is very low in β-cells, so efflux of lactate is minimal (Sekine *et al.,* 1994). G3P is part of the glycerol phosphate shuttle, which transports reducing equivalents from the cytosol to mitochondria, where the electron transport chain followed by ATP production happens. During the glycerol phosphate shuttle, DHAP and $NADH + H^+$ are transformed into G3P and oxidized NAD^+ by cytosolic glycerol-3-phosphate dehydrogenase. G3P accepts two reducing equivalents and passes them to FAD forming $FADH_2$ and again DHAP. This reaction is catalysed by mitochondrial glycerol-3-phosphate dehydrogenase with simultaneous transfers of electrons to coenzyme Q, which passes them on the complex III of the respiratory chain. This enzyme is bound to the outer face of the inner mitochondrial membrane (Mráček *et al.,* 2013). There is evidence that lipolysis is not the only source of free glycerol in β-cells. Pancreatic islets from whole-body *Atgl*-KO (knock-out) and β-specific *Atgl*-KO mice showed glycerol production in significant amounts at high glucose concentrations (Peyot *et al.,* 2009; Attané *et al.,* 2016). Another proof is that GSIS and lipolysis are inhibited by pan-lipase inhibitor orlistat, measured as NEFA release. However, glycerol release remains the same. (Mugabo *et al.,* 2016). Previously described phosphoglycolate phosphatase (Rose, 1981) acts as a glycerol-3-phosphate phosphatase (G3PP) in mammalian cells. G3PP dephosphorylates

G3P to glycerol controlling glucose and lipid metabolism (Mugabo *et al.,* 2016). This pathway was proposed to be named "glycerol shunt" (Al-Mass *et al.,* 2022). The free glycerol can then leave the cell through aquaglyceroporin. Aquaglyceroporin 7 (AQP7) is the only isoform expressed in mouse β-cells (Matsumura *et al.,* 2007) and rat β-cells (Best *et al.,* 2009). It is permeable to water, glycerol, and urea (Virreira *et al.,* 2011). Increased glycerol content and insulin secretion were observed in pancreatic islets isolated from $Aqp^{-/-}$ mice. Increased insulin production, secretion and glucose uptake were observed in the pancreatic islets of $Aqp7^{-/-}$ mice (Matsumura *et al.,* 2007). Because β-cells express glycerol kinase on a negligible level, glycerol is not metabolized (Noel *et al.,* 1997). It is believed that the release of glycerol by β-cells functions as glucolipodetoxification and defence against nutritional stress (Prentki & Madiraju, 2012; Possik *et al.,* 2021). When G3P is not dephosphorylated, it can either enter the GL/NEFA cycle or transfer electrons into mitochondria through the glycerol phosphate shuttle. These effects were observed in β-cells at elevated glucose concentrations (10-16 mM). (Mugabo *et al.,* 2016). RNAi knockdown of *G3pp* in INS832/13 cells caused increased synthesis of 1,2-DAG and 2,3-DAG followed by increased GSIS. The amount of TAGs, phospholipids, lysophosphatidylinositol, lysophosphatidate and lysophosphatidylcholine was also higher. As expected, overexpression of G3PP decreased their synthesis and NEFA release was enhanced. Similar findings were observed in pancreatic rat islets. G3PP also controls signalling through the production of lipid signalling mediators (Mugabo *et al.,* 2016). Islets from β-cell-specific *G3pp*-KO mice incubated on high glucose showed enhanced GSIS and mild hyperinsulinemia. These effects were caused by the increased availability of G3P, resulting in an augmented flux through the GL/NEFA cycle (lipogenic part) and the production of MCFs. Increased GSIS can be also caused by accelerated malonyl-CoA production supporting the ACC/malonyl-CoA/CPT1 signalling network. Mitochondrial oxidative phosphorylation was also enhanced under hyperglycemic conditions and in the presence of NEFAs because of the G3P shuttle. β-cell-specific *G3pp*-KO islets exposed to elevated glucose for 7 days (glucotoxicity) showed a significant decrease in insulin content and increased apoptosis (Al-Mass *et al.,* 2022).
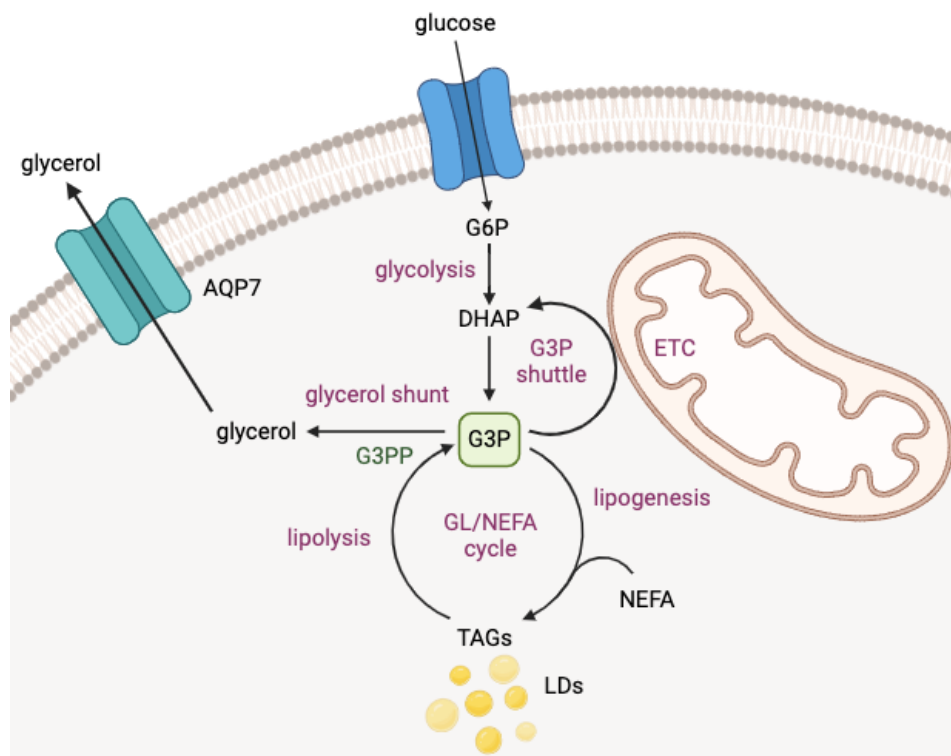
Figure 6: **The role of glycerol-3-phosphate**. Dihydroxyacetone phosphate (DHAP) formed in glycolysis is partially converted to glycerol-3-phosphate (G3P), which is on the crossroad of glucose, lipid and energy metabolism. It can be part of the glycerol phosphate shuttle transporting reducing equivalents from cytosol to mitochondria with the use of NAD^+ and FAD to the electron transporting chain (ETC). G3P can enter lipogenic arm of the GL/NEFA cycle to form triacylglycerols (TAGs), which are stored in LDs (lipid droplets), or it can be dephosphorylated by glycerol-3-phosphate phosphatase (G3PP) to glycerol, which leaves the cell through aquaglyceroporin 7 (AQP7). (Created with Biorender.com)

2.5.8. Lipid droplets

Lipid droplets (LDs) are cellular structures occurring in animals, plants, fungi, and bacteria (Murphy *et al.,* 2012). They consist of a core containing neutral triacylglycerols and sterol esters (cholesterol, retinol esters), which is wrapped in a polar phospholipid monolayer including many proteins with distinct functions. Proteins of lipid metabolism are involved in FA transport, TAG metabolism and maintenance of LDs. Some of the proteins are involved in interactions with other organelles (e.g. mitochondria, nucleus, endoplasmic reticulum, lysosomes and autophagosomes) (Welte *et al.,* 2017).

The structural/resident proteins of LDs are perilipins (PLINs), which are important for LD stabilization, lipolysis and interactions with other organelles, which is ensured thanks to their mobility. Perilipins exist in five isoforms PLIN1-PLIN5. Each of them is important for the determination of the function of the LD. In mammals, only PLIN1 and PLIN2 are considered as LD proteins. PLIN3, 4 and 5 can be cytosolic or located in the ER (Skinner *et al.,* 2009; Bartholomew *et al.,* 2012). Expression of each PLIN differs between β-cells and pancreatic islets as well as between humans and rodents. Nevertheless, PLIN2 is the most abundant PLIN in mice β-cells (MIN6), rat β-cells (INS1) and human and rodent pancreatic islets (Faleck *et al.,* 2010; Trevino *et al.,* 2015) It is considered to be a marker

of LDs. The expression of PLIN2 strongly correlates with the amount of triacylglycerols because the incorporation of PLIN2 into LDs prevents its ubiquitination and further degradation (Trevino *et al.,* 2015). Knockdown of *Plin2* significantly decreases LD accumulation in human β-cells, whereas PLIN2 overexpression supports it (Tong & Stein, 2021). PLIN3 is expressed in mouse and human pancreatic islets; however, it was not detected in INS1 or MIN6 cells (Trevino *et al.,* 2015). The specific function of PLIN3 in β-cells is unknown (Imai *et al.,* 2020). In adipose tissue, it prevents lipolysis (Lee *et al.,* 2018). PLIN5 is highly expressed in tissues that oxidize FAs as a fuel (heart, skeletal muscle, brown adipose tissue). Its expression is increased in fasted pancreatic islets. PLIN5 can increase lipolysis via PKA-mediated phosphorylation when it interacts with ATGL and its co-activator CGI-58. It also interacts with mitochondria to facilitate the transport of FAs from LDs to mitochondria (Trevino *et al.,* 2015). PLIN1 prevents lipolysis upon non-stimulated conditions in adipocytes (Xu *et al.,* 2018). The expression of PLIN1 is low in β-cells compared to PLIN2, 3 and 5. The expression of PLIN4 is very low in β-cells and pancreatic islets and it is the least studied PLIN in β-cells (Imai *et al.,* 2020).

LD growth can be mediated by the relocalization of TAG synthetic enzymes from ER to LD (Wilfling *et al.,* 2013). This applies to GPAT4, which initiates the LD lipid formation by lipid-loading (Xu *et al.,* 2018). Lipid catabolic enzymes (lipases) are also located on the surface of LDs. When HSL is phosphorylated, it translocates to LD (Sztalryd *et al.,* 2003). ATGL is also present on LDs, where it is regulated by PLIN5 (Wang *et al.,* 2011). There are also proteins involved in membrane trafficking (Ras-associated binding proteins, SNARE proteins) on LDs (Bartz *et al.,* 2007; Liu *et al.,* 2004) and signalling proteins (MAP kinases, PKC, and phosphatidylinositol-3-kinase) (Yu *et al.,* 1998; Chen *et al.,* 2002; Yu *et al.,* 2000).

LDs are very important particles in cells as they contribute to energy homeostasis by keeping the balance between the storage of lipids in the form of TAGs and their lipolysis. During overnutrition, triacylglycerol synthesis in the endoplasmic reticulum (ER) is enhanced and so is the formation of LDs. LD formation has a protective role in lowering ER stress and oxidative stress in the cell. LDs also serve as storage of fat-soluble vitamins (vitamins A, D, E and K). For example, retinol (vitamin A) in LDs is esterified with FAs forming retinol esters (Welte *et al.,* 2017). In addition, LDs play an important role in insulin secretion by generation of MCFs (Imai *et al.,* 2020).

2.6.   Glucolipotoxicity in β-cells

Glucolipotoxicity is a concept referring to a chronic fuel excess, namely glucose and lipids. The effects of glucotoxicity and lipotoxicity are synergistic, therefore the term glucolipotoxicity is used (El-Assaad *et al.,* 2003). Some lipotoxic effects can be observed only in the presence of elevated glucose conditions (Jacqueminet *et al.,* 2000).

Acute exposure of β-cells to glucose stimulates GSIS; however, long-term superabundant glucose leads to increased metabolite flux through glycolysis, lipid synthesis and electron transfer. These cause fat accumulation and higher ROS production in mitochondria (Possik *et al.,* 2021). Nutritional excess

triggers the development of T2D. Long-term hyperglycemia and increased ROS production inhibit the first phase of GSIS through inhibition of glyceraldehyde-3-phosphate dehydrogenase, a glycolytic enzyme (Sakai *et al.,* 2003). Furthermore, the expression and activity of glucose-6-phosphate dehydrogenase (rate-limiting enzyme of pentose phosphate pathway) is decreased resulting in lower production of NADPH, which is required by antioxidative enzymes. There are other sources of NADPH in the cell; however, glucose-6-phosphate dehydrogenase was shown to be the most important one (Pandolfi *et al.,* 1995). Due to the lack of NADPH, there is low activity of antioxidant enzymes and increased cell apoptosis (Zhang *et al.,* 2010). Due to chronic exposure to glucose, GSIS is impaired (Fu *et al.,* 2017) and the expression of β-cell-specific transcription factors, for example, *Pdx1/Ipf1*, *MafA* and *Nkx-6.1*, is decreased. This results in the dedifferentiation of β-cells to progenitor-like cells or trans-differentiation to α-cells (Ahlgren *et al.,* 1998; Cinti *et al.,* 2016). Another consequence of chronic exposure to glucose or high-fat diet (HFD) is chronic activity of NOX4, leading to local inflammation (Holendová *et al.,* 2024)

Acute exposure of β-cells to lipids (mainly those rich in saturated FAs) (Imai *et al.,* 2020) potentiates GSIS, an effect coupled with glucose (Fu *et al.,* 2017). However, in the long-term, exposure to fatty acids induces oxidative stress, ER stress, mitochondrial dysfunction, ceramide generation, inflammation, and β-cell dysfunction (Oberhauser & Maechler 2021; Busch *et al.,* 2002). An overload of saturated fatty acids alters the membrane composition and causes the production of proinflammatory metabolites (Moffitt *et al.,* 2005; Salvadó *et al.,* 2013). Lipotoxicity is considered the main triggering factor of T2D by promoting insulin resistance and inflammation. The inflammation is caused by the activated c-Jun N-terminal kinase (JNK)/nuclear factor-kappa B (NF-κB) pathway, which increases the expression of inflammatory cytokines including tumor necrosis factor-alpha (TNF-α), interleukins IL-1β, IL-6 and IL-8 (Igoillo-Esteve *et al.,* 2010). The toxic effect of NEFA increases with the increasing chain length (Elsner *et al.,* 2011). Chronic exposure (10 weeks) of INS-1 cells to glucose resulted in the impairment of GSIS. This effect is even stronger with glucose in combination with palmitate (Fu *et al.,* 2017). High glucose with oleate causes a massive accumulation of LDs in β-cells. This effect is augmented by orlistat inhibiting lipolysis to its maximal capacity (Oberhauser *et al.,* 2022). There are different effects of saturated and unsaturated fatty acids in lipotoxic conditions. Palmitate promotes ER stress and ceramide formation resulting in β-cell death. Cytotoxicity and apoptosis by palmitate were described also by Moffitt *et al.,* 2005. Palmitate induces two pathways of ceramide formation: *de novo* synthesis and acylation of sphinganine. The beginning of the *de novo* synthesis is mediated by serine palmitoyltransferase, which catalyzes the condensation of L-serine and palmitate. This step is rate-limiting. The product is reduced by 3-ketodehydrosphinganine reductase. Exposure to palmitate causes 30% increase in the expression of one of the two isoforms of serine palmitoyltransferase in MIN6 cells. 3-ketodehydrosphinganine reductase expression is increased by 70% after exposure to palmitate. The total ceramide levels increased 2-fold after MIN6 cells were cultured in the presence of palmitate for 48 hours. When the cells were incubated with oleate no harmful

effect was observed. The expression of genes involved in ceramide biosynthesis was the same in control cells and for the combination of both palmitate and oleate. The total ceramide level was the same in cells treated with oleate alone, with both fatty acids and in control cells. These data show oleate has a protective effect on β-cell properties and prevents deleterious effects caused by palmitate (Manukyan *et al.,* 2015). Palmitate-induced reduction of the expression of proteins regulating calcium homeostasis (secretagogin and sarcoplasmic/endoplasmic reticulum calcium ATPase 2) by 45-50% in MIN6 cells. This effect was not alleviated by oleate (Sargsyan *et al.,* 2016). ER stress promoted by palmitate can be reversed by oleate, which activates pro-survival pathways of the ER stress response, such as the upregulation of chaperones (Sargsyan *et al.,* 2016). It has been reported that FFAR1 signalling has a protective effect on β-cells against palmitate (Panse *et al.,* 2015). FAs also impact the antioxidant defence system. Palmitate suppressed the expression of peroxiredoxins in MIN6 cells, whereas oleate preserved it (Sargsyan *et al.,* 2016). Another mechanism by which palmitate promotes β-cell death is decreasing the expression of proteins involved in autophagy. When oleate was also present the reduction was milder (Sargsyan *et al.,* 2016). The protective effect of free fatty acids on cells was described as lipohormesis, the mechanism of which is probably mild lipid peroxidation (Haeiwa *et al.,* 2014).

2.7.　　 **Reactive oxygen species**

Reactive oxygen species (ROS) are oxygen-containing molecules, that are capable of independent existence. They exist in the form of a radical with one or more unpaired electrons: superoxide radical ($\bullet O_2^-$), hydroxyl radical (HO•), alkoxy radical (RO•), peroxy radical (ROO•); or non-radical form (H_2O_2). Because the radicals have an unpaired electron, they can initiate chain reactions by abstracting the H atom from another molecule creating another radical and so the reaction is propagated further (Lenzen, 2017). ROS in the form of a radical are therefore more reactive than non-radicals. H_2O_2 is a small non-charged molecule, which shares many physicochemical properties with H_2O (Lenzen, 2017). Under physiological conditions, H_2O_2 is relatively stable and less reactive compared to other ROS (Bienert *et al.,* 2006). At the same time, it is the only molecule among ROS, which can pass through cellular and subcellular membranes. The permeation is limited by the permeability coefficient of the membrane. However, it can be accelerated by certain isoforms of aquaporins (Bienert *et al.,* 2006).

One of the sources of ROS production is mitochondria. In mitochondria, ROS are generated in the respiratory chain mostly on complex I and complex III and mitochondrial glycerol-3-phosphate dehydrogenase (Mráček *et al.,* 2013). Mitochondrial β-oxidation also contributes to ROS generation, however to a small extent (Elsner *et al.,* 2011). Significant amounts of ROS are generated in the initial step of peroxisomal β-oxidation by acyl-CoA oxidases. During lipotoxicity, H_2O_2 production is increased leading to peroxisomal stress. H_2O_2 is also generated in the ER, where disulfide bonds in proteins are created by protein disulfide isomerase, which also induces disulfide isomerisation of misfolded proteins. During the reaction, protein disulfide isomerase is reduced. To be reoxidized it requires oxidoreductase 1, which reduces O_2 to H_2O_2 in this process. The unfolded protein response is activated

when the demand for protein folding is high. If this compensatory mechanism fails it results in ER stress, thus leading to greater risk of apoptosis (Lenzen, 2017). In cytosol, ROS are generated by xanthine oxidases and NOX enzymes. These membrane-bound enzymes are formed of multiple subunits that reduce $NADP^+$ (mostly supplied from the pentose phosphate pathway) to NADPH. In β-cells, NOX1, NOX2 and NOX4 are expressed (Oliveira *et al.,* 2003; Uchizono *et al.,* 2006). During oxidation of NADPH, NOX1 and NOX2 produce $\bullet O_2^-$ unlike NOX4, which produces H_2O_2. NOX4 is the only isoform that is constitutively active and assembled in β-cells. Its activity is induced by glucose metabolism (Plecitá-Hlavatá *et al.,* 2020).

β-cells have low expression levels of classical antioxidant enzymes (superoxide dismutase – SOD, catalase, and glutathione peroxidase) compared to other cell types (Tiedge *et al.,* 1997). SOD catalyzes the dismutation of superoxide radicals into oxygen and H_2O_2. In β-cells, there are 2 isoforms expressed. SOD1 is expressed in the cytosol, the mitochondrial intermembrane space, the peroxisomes, and the nucleus, whereas SOD2 is expressed in the mitochondrial matrix (Lenzen *et al.,* 1996). H_2O_2 can be converted to H_2O and O_2 mainly by catalase, glutathione peroxidase and peroxiredoxin 4 in the ER (Mehmeti *et al.,* 2014). Catalase even belongs to the disallowed genes, which are repressed in β-cells (Schuit *et al.,* 2012). Low expression of the enzymes of antioxidant defence is the key factor that enables β-cells to sense ROS as signals (Pi *et al.,* 2007). Defence against H_2O_2 in β-cells is provided by thioredoxins (TXNs) and peroxiredoxins (PRDXs), which are important for the redox signalling by redox relays (Stancill *et al.,* 2019). TXN and PRDX are predisposed to partly interact with H_2O_2 and to its detoxification. H_2O_2 can be degraded by glutathione or PRDX to H_2O. Oxidized PRDX is reduced by TXN, which is subsequently reduced by TXN reductase with the use of NADPH. The redox reactions happen on the thiol groups of cysteines of these enzymes. Apart from the detoxification of H_2O_2, the oxidation signal from TXN can finally be passed further to the target proteins (Stöcker *et al.,* 2018). The oxidation of a thiol group leads to the formation of sulfenic acid, which can be irreversibly oxidized to sulfinic or sulfonic acid (Holendová & Plecitá-Hlavatá, 2023).

H_2O_2 is one of the metabolic coupling factors for insulin secretion. The significant production of H_2O_2 was observed at 20 mM glucose and accompanied 10-fold increased insulin secretion. In addition, stimulation of INS1 cells with H_2O_2 at 3 mM glucose led to significantly increased insulin secretion (Pi *et al.,* 2007). After an exposition of INS1 cells to oxidative stressors for 6 hours, the expression of antioxidant enzymes was dramatically increased. At the same time, H_2O_2 accumulation and GSIS were suppressed (Pi *et al.,* 2007). It was shown that increasing the ATP/ADP ratio alone is not sufficient for GSIS and that redox signalling is required (including NOX4-derived H_2O_2) (Plecitá-Hlavatá *et al.,* 2020). β-cell-specific *Nox4*KO (β*Nox4*KO) mice on HFD showed suppressed insulin secretion and hyperinsulinemia in comparison with WT mice. In addition, β*Nox4*KO mice accumulated epidydimal and ectopic fat (in pancreatic islets) showed by increased triglyceride content. Increased expression of *Acsl3* in the islets could enhance *de novo* lipogenesis. Sustained NOX4 activity

led to long-term secretion of IL-1β resulting in local inflammation during chronic overnutrition (Holendová *et al.,* 2024).

ROS induce lipid peroxidation, which is a process that continues autocatalytically once initiated. During this process, lipid hydroxyperoxides and secondary products are formed from polyunsaturated fatty acids (PUFAs). These advanced lipoxidation end products have cytotoxic effects and are associated with β-cell dysfunction and insulin resistance during T2D (Maulucci *et al.,* 2016; Toyokuni *et al.,* 2000). Inhibition of GSIS by lipid peroxidation products was reported (Miwa *et al.,* 2000). Under hyperglycemic conditions, lipid peroxidation is enhanced and causes inflammation and organelle damage in β-cells (Imai *et al.,* 2020; Lenzen, 2017). The reaction is initialized by the abstraction of a bis-allylic hydrogen in PUFA. 4-hydroxyalkenals are the products of the reaction. Depending on the type of PUFA different products are generated. n-3 PUFA produces 4-hydroxyl-2E-hexenal and n-6 PUFA generate 4-hydroxy-2E-nonenal (4-HNE), which has a signalling function (Sasson, 2017). Its converse effect may be dose-dependent (Sasson, 2017). In low concentrations, 4-HNE induces the transcription of antioxidant enzymes. In contrast, a high concentration of 4-HNE activates proinflammatory response (Sasson, 2017).

3. Aims of the thesis

1) Examine the impact of glucose on the expression of genes involved in lipid metabolism, fatty acid activation, lipolysis, and lipogenesis reflecting the redox state in INS1E cells and isolated mouse pancreatic islets

   o Hypothesis: stimulating glucose concentration augments the expression of the genes involved in lipid synthesis and storage serving as a protective mechanism from glucotoxicity to maintain β-cell function

   o Hypothesis: a reduced redox environment mediated by a decrease in *Nox4* expression affects the expression of genes involved in lipid metabolism

2) Estimate the effect of glucose and reduced redox environment on LD deposition in pancreatic β-cells

   o Hypothesis: *Nox4* silencing causes altered lipid droplet accumulation in INS1E cells

3) Examine the effect of glucose and a more reduced redox environment on the non-esterified fatty acid homeostasis

4) Quantify lipolysis by measuring the secreted glycerol in conditions of non-/stimulating glucose and oleate for the assessment of the detoxification pathway mediated by glycerol release

4. Material and methods

4.1.   Chemicals and solutions

Chemicals	Manufacturer
Fetal Bovine Serum (FBS) Qualified (FB-1090/500)	Biosera
BODIPY 493/503	Invitrogen™
Sodium oleate*	Sigma-Aldrich®
RNeasy Mini Kit	Qiagen
Reverse transcriptase with buffer: GrandScript cDNA synthesis kit (A103b)	TATAA Biocenter
Forget-Me-Not 40X Template Buffer (cat. 99802)	Biotium
EvaGreen® Dye, 10X in water (31000)	Biotium
Pierce™ BCA Protein Assay Reagent A	Thermo Scientific™
Fatty acid-free bovine serum albumin (BSA)	Sigma-Aldrich®
GenMute™ Reagent	SignaGen® Laboratories
GenMute™ Transfection Buffer	SignaGen® Laboratories
Trypan Blue	Invitrogen™
BD Cytofix	BD Biosciences
Saponin	Sigma-Aldrich®
Non-esterified Free Fatty Acids (NEFA) Colorimetric Assay Kit, E-BC-K014	Elabscience®
High Sensitivity Free Glycerol Assay Kit, MAK270	Sigma-Aldrich®
2-mercaptoethanol	Sigma-Aldrich®
Hoechst 33258, 33342	Invitrogen™

* For the experiments, 15 µM oleate conjugated with BSA was used

INS medium			
	Stock solution concentration	Final concentration	1000 ml
Cell culture grade water	-	-	638 ml
RPMI 5x glucose-free	5x	1x	200 ml
Glutamin	200 mM/3%	2 mM/0.03%	10 ml
Sodium pyruvate	100 mM	1 mM	10 ml
$NaHCO_3$	7.5%	0.2%	27 ml
HEPES (pH 6.8)	1M	10 mM	10 ml

Mercaptoethanol	100%	0.35%	3.5 μl
Phenol red	0.4%	0.0005%	1250 μl
Glucose	250 mM	11 mM	44 ml
ATB (penicilin/streptomycin)	100x	1x	10 ml
FBS	100%	5%	50 ml

CMRL medium	100 ml
CMRL	83 ml
FBS	10 ml
HEPES pH 6,8	5 ml
Glutamin 3%	1 ml
ATB (penicilin/streptomycin)	1 ml
Adjust the pH to 7,3	

PBS 10x was supplied by the Institute of Molecular Genetics of the Czech Academy of Sciences. In our laboratory, it was diluted with sterile water to 1x concentrated.

PBS 10x	g/l
NaCl	80
KCl	2
KH_2PO_4	2
NA_2HPO_4	11.5

	5'-3' sequence of SiRNAs for *Nox4* silencing	
	Sense	**Antisense**
si*Nox4*A	GUUAUACAUUGAUGGCCCA[dT][dT]	UGGGCCAUCAAUGUAUAAC[dT][dT]
si*Nox4*B	CAAGAAGAUUGUUGGACAA[dT][dT]	UUGUCCAACAAUCUUCUUG[dT][dT]

Antibodies		
Name	Manufacturer	Used concentration
ADFP Recombinant Rabbit Monoclonal Antibody (PLIN2)	Invitrogen™	1:100
Alexa Fluor 555 Donkey Anti-rabbit	Invitrogen™	1:1000

Primers			
Rattus norvegicus			
Gene	**Forward sequence**	**Reverse sequence**	**Manufacturer**
Acsl3	TGTATGCGACTCTGGGAGGT	GGTGTGTACAATGACGCCCT	Metabion

Acsl4	AAGCCAAACCCCAGAGGTGA	TCAGTGCGGCTTCGACTTTC	Metabion
Acly	TGGATGGGTTCATCGGCGTT	ATACAGCCCTTGCTTCAGCC	Metabion
Lipe	CCAAAGGGAGGTGCCATCAT	TCCTGGGTAGTCTGTGAGGG	Metabion
Fasn	GAGCCGCCGACCAGTATAAA	TGTAATCGGCACCCAAGTCC	Metabion
B2m	TGACCGTGATCTTTCTGGTG	GTGGGTGGAACTGAGACACG	Metabion
Ywhaz	AGCCCGTAGGTCATCTTGGA	TGCGAAGCATTGGGGATCAA	Metabion

Mus musculus			
Gene	**Forward sequence**	**Reverse sequence**	**Manufacturer**
Acsl3	GCAGCTTTGAAGAACCTCCC	TGTCACCAGACCAGTTTCGG	Metabion
Acsl4	AGCACCTTCGACTCAGATCAC	TGGAAGCAGCAGTAAGAGTAGC	Metabion
Acly	CTCCTTAATGCCAGCGGGAG	CCTTGCAGGGATCTTGGACT	Metabion
Acc	GACCTGGAGCAGCACTTGAC	GRAGACTGCCCGTGTGAAGC	Metabion
Plin2	GTGGAAGAGAAGCATCGGCT	AGCATTGCGGAATACGGAGT	Metabion
Plin5	ATGCCTGTGTGGATGAGTTCC	CAGCTCTGGCATCATTGTGTG	Metabion
Gpat4	TCAGTTTGGTGACGCCTTCT	TTCAATCCACCGTCCCACAG	Metabion
Lipe	GAAGTGAGACCCATGGACGG	GCCATGCGGCAGATCTTCTA	Metabion
Fasn	CACTGCCTTCGGTTCAGTCTC	ATGCTATTCTCTACCGCTGGG	Metabion
Hprt	CAGTCCCAGCGTCGTGATTAG	TGATGGCCTCCCATCTCCTT	Metabion

Inhibitors		
Name	**Manufacturer**	**Used concentration**
Cerulenin	Sigma-Aldrich®	100 µM
Orlistat	Sigma-Aldrich®	200 µM

4.2. Laboratory equipment

Instrument	**Manufacturer**
LUNA-II™ Automated Cell Counter	Logos biosystems
BioPhotometer	Eppendorf
Centrifuge 5427 R	Eppendorf
Centrifuge Z 306	Hermle
SW22 Shaking water bath	Julabo
CPX40 Ultrasonic Homogenizer	Cole-Parmer
C1000 Touch Thermal Cycler	Bio-rad
CFX Connect Real-time system	Bio-rad
LSRII Flow Cytometer	BD
Electronic pipette Xplorer	Eppendorf
DNA/RNA UV-cleaner UVC/T-AR	Biosan

AG204 Analytical balance	Mettler Toledo
NanoDrop^{TM} One	Thermo Fisher Scientific
Confocal microscope Leica SPE (DM 2500 CSQ V-VIS)	Leica
BioTek Cytation 3 Cell Imaging Multi-Mode Reader	BioTek$^{®}$

4.3. Methods

4.3.1. Cell culture cultivation

Rat insulinoma INS1E (C0018009, AddexBio, San Diego, CA) is a cell line isolated from the parental INS1 cell line. The INS1 cell line was originally isolated from an x-ray-induced transplantable insulinoma from *Rattus Norvegicus* (Asfari *et al.,* 1992). Both cell lines are adherent and dependent on the reducing agent 2-mercaptoethanol.

In our laboratory, INS1E cells are cultivated on cell culture flasks with different areas of surface (25 cm^2, 75 cm^2, 175 cm^2). Cell cultures are kept in the incubator with a temperature of 37°C and 5% CO_2. Culture flasks contain INS culture medium (11 mM glucose). The composition of the INS medium can be seen above in the chemicals and solutions. For the treatment in experiments 3 mM glucose (starving condition) and 25 mM glucose (stimulating condition) was used. The threshold of glucose concentration for the stimulation of insulin secretion in INS1E is 16,7 mM. During the culture at 3 mM INS1E are starving and 25 mM glucose is used to stimulate insulin secretion. Every three or four days the cells are passaged as they reach approximately 85-90% confluency. The medium is aspirated. Cells are then washed with PBS (phosphate buffered saline) and 0.1% trypsin is added for approximately 5 minutes, so the cells become detached from the culture flask. The reaction is stopped by adding 1 volume of the culture medium. The cells are counted with a cell counter, and they are seeded on corresponding size and number of flasks. For counting, 10 µl of Trypan Blue and 10 µl of cells suspended in the medium were mixed by pipetting and 10 µl of this mixture was injected in the cell counting chamber slide and measured with LUNA-II^{TM} Automated Cell Counter. Cells with passage numbers between 2 and 12 were used in the experiments.

4.3.2. *Nox4* silencing

For silencing of *Nox4* in INS1E cells were transfected with siRNA. Scrambled sequence (SCR) was used as control in all experiments. Mixtures were prepared according to this table (the volume is per one well of a six-well plate):

SCR	si*Nox4*
80 µl H_2O	80 µl H_2O
20 µl GenMute™ Transfection Buffer	20 µl GenMute™ Transfection Buffer

2.2 μl SCR RNA	2.2 μl si*Nox4*A; 2.2 μl si*Nox4*B
4 μl GenMute™ Reagent	4 μl GenMute™ Reagent

The mixture was mixed by pipetting and incubated for 15 mins at RT. The cells were provided with a fresh medium and the mixture of SCR or si*Nox4* were distributed to the wells. The cells were always silenced one day after seeding.

4.3.3. Preparation of bovine serum albumin-oleate conjugate

Because fatty acids have low solubility in aqueous solutions oleate was conjugated with BSA so it can be absorbed and utilized by cells. For the preparation of 1 mM sodium oleate/0,17 mM bovine serum albumin (BSA) (6:1), fatty acid-free BSA was mixed with 150 mM NaCl and dissolved in 37°C. The solution was filtered. 30,6 mg of sodium oleate was added to 44 ml of 150 mM NaCl and heated to 70°C. 40 ml of hot oleate was transferred to the 50 ml of BSA solution already stirring at 37°C and it was further stirred for 1 hour. The final volume was adjusted to 100 ml with 150 mM NaCl. The pH was adjusted to 7,4. Aliquots were prepared and stored at -20°C.

4.3.4. Mice models

The β-cell-specific *Nox4*KO (β*Nox4*KO) mouse was generated by crossing *Nox4*$^{Flox/Flox}$ mouse (from Prof. Brandes from J. W. Goethe University, Frankfurt, Germany) with B6(Cg)-Ins2tm1.1(*cre*)Thor/J mouse (bought from the Jackson Laboratory, Bar Harbor, Maine, USA). Thus obtained β*Nox4*KO mouse was named B6.Cg-Nox4<tm1Ams>Tg(Ins2-*Cre*)25Mgn. Control mice (WT) were acquired by intercrossing β*Nox4*KO mice with C57BL6/J mice for 10 generations. Pancreatic islets isolated from WT mice and β*Nox4*KO mice (MUT = mutant) were used in the experiments. The mice were bred under welfare principles and the EU directive on the protection of laboratory animals used for scientific purposes at the Institute of Molecular Genetics of the Czech Academy of Sciences.

4.3.5. Pancreatic islets isolation

Mice were anaesthetized with the Zoletil/Rometar mixture. The pancreases were digested with collagenase and the pancreatic islets were isolated on a Ficoll gradient. The yield of the islets was 100-200 per mouse. The islets were incubated in 5 mM glucose (non-stimulating) or 25 mM glucose (stimulating glucose) for 48 hours. The threshold of glucose concentration for the stimulation of insulin secretion in the islets is 8 mM.

4.3.6. Gene expression analysis

Gene expression of genes of lipid metabolism was quantified on mRNA level in INS1E and mouse pancreatic islets.

4.3.6.1. RNA isolation

RNA was isolated from the INS1E cells seeded on a six-well plate (500,000 cells per well) or from isolated pancreatic islets (islets from 3 mice were pooled for generation of one sample). From

the six-well plate with INS cells, the medium was aspirated. Then 350 μl of RLT, the lysis buffer from RNeasy Mini Kit (Qiagen), was added. The wells were thoroughly washed, and the volume was transferred to a microtube. One volume of 70% was added and the mixture was mixed by pipetting and displaced into a spin column with a collection tube.

For the isolation of total RNA, the RNeasy Mini Kit (Qiagen) was used. The procedure followed the manufacturer's protocol. The concentration of isolated RNA was measured immediately after the isolation on NanoDrop. The RNA then proceeded to reverse transcription or was stored at -80°C.

4.3.6.2. Reverse transcription

During reverse transcription, the mRNA is transcribed into cDNA, which is used in qPCR. Each sample of RNA was diluted to 100 ng/μl with RNase-free water. The reaction contained:

- 2,5 μl RT buffer
- 5 μl diluted RNA (500 ng)
- 2 μl RNase-free water
- 0.5 μl reverse transcriptase

The reaction had a total volume of 10 μl and always contained 500 ng of RNA. The reaction was performed in a thermal cycler with this protocol: 22°C/5 min, 42°C/45 min, 85°C/5 min, 6°C/∞.

4.3.6.3. Real-time qPCR

Real-time qPCR (RT-qPCR) was used for validating designed primers and for quantification of gene expression in INS1E and mouse pancreatic islets. The lyophilised primers were diluted with H_2O according to the manufacturer. Aliquots were prepared using 10 μl of diluted primers and 90 μl of H_2O. cDNA from the reverse transcription was diluted using 10 μl of cDNA + 25 μl H_2O + 5 μl Forget-Me-Not 40X Template Buffer. The reaction contained:

- 5 μl EvaGreen
- 2 μl H_2O
- 0.5 μl FW primer
- 0.5 μl RV primer

2 μl of cDNA were added. The reaction had a total volume of 10 μl. Each sample was measured in a duplicate on 94-well plate. After pipetting the mixture on the well, it was sealed with a plate sealer and centrifuged for 1 min, 800g. The plate was put in a thermal cycler with the following protocol: preincubation (95°C/3 min); 50 cycles of amplification: 95°C/5 sec, 59°C/10 sec, 72°C/15 sec; melting 95°C/10 sec, 65°C followed by a gradual increase of temperature by 0.5°C during 4 seconds until 95°C. The data from RT-qPCR were analysed using the ΔΔCt method with *B2m* (β-2-microglobulin) as a reference gene for the gene expression in INS1E and *Hprt* in mouse pancreatic islets.

4.3.7. Lipid droplet analysis

4.3.7.1. Flow cytometry

For the flow cytometry, INS1E cells were seeded on six-well plates with 500,000 cells per well. The next day, *Nox4* silencing was performed. The cells were treated with 3 mM glucose (starvation), 25 mM glucose (stimulating glucose) or 25 mM glucose with 15 µM oleate for 24 or 72 hours. Some samples were provided with serum-free medium (SFM) for 24 hours. To some samples, orlistat at 200 µM and cerulenin at 100 µM were added for 3 hours. Orlistat (tetrahydrolipstatin), a pan-lipase inhibitor, irreversibly binds to the catalytic site of many lipases and blocks their activity (Borgström, 1988). It also blocks the activity of fatty acid synthase (Kridel *et al.,* 2004). Cerulenin is an antifungal antibiotic isolated from *Cephalosporium caerulens*, which inhibits sterol and fatty acid synthesis by preventing palmitoylation of FAS and hydroxymethylglutaryl-CoA synthase (Vance *et al.,* 1972; Ohno *et al.,* 1974). On the day of the analysis, live or fixed cells were stained and the measurement on the cytometer LSRII was performed.

Live cells: the medium was aspirated from all the wells. The cells were washed with 1 ml of PBS, 500 µl of trypsin was added and the cells were kept in the incubator for approximately 5 minutes. The reaction was stopped with 500 µl of 10% FBS/PBS. Samples were transferred to microtubes and centrifugated at 350g, 5 min, RT. The supernatant was aspirated, and the pellet was resuspended in 200 µl of PBS with 0.5 mM EDTA and the corresponding amount of glucose. BODIPY (4,4-Difluoro-1,3,5,7,8-Pentamethyl-4-Bora-3a,4a-Diaza-s-Indacene), a fluorescent dye staining neutral lipids in the cell, was added to all samples except unstained controls at 0.5 µM concentration. The samples were incubated for 10 minutes in the dark. Then the samples were centrifuged at 350g, 5 min, RT, the supernatant was aspirated, and the cells were resuspended in 200 µl of PBS with 0.5 mM EDTA and the corresponding amount of glucose, oleate, orlistat and cerulenin. Before the measurement, 5 µM Hoechst 33258 was added.

Fixed cells: The cells were washed with PBS and trypsinized. The trypsinization was stopped by 10% FBS/PBS. Then, 20 min fixation with 80 µl of Cytofix (RT, dark) followed. 150 µl of FC buffer (PBS + 0.5% BSA + 0.2 mM EDTA) was added. The cells were then centrifuged at 700g, RT, for 5 minutes and the supernatant was aspirated. The cell membrane was then permeabilised by saponin (PBS + 1% BSA + 0.1% saponin). First, the cells were washed with saponin followed by centrifugation and then they were incubated with saponin for 10 minutes. BODIPY (0.5 µM), Hoechst 33258 (5 µM) and rabbit anti-rat primary antibody PLIN2 (1:100) were added. The cells were incubated for 30 minutes at dark. Next, the saponin wash followed, the cells were centrifuged again and resuspended in 200 µl of saponin. Alexa Fluor 555, a donkey anti-rabbit secondary antibody, was added (1:1000). The cells were incubated for 30 minutes at dark, centrifuged as previously, and resuspended in 200 µl of PBS + 0.5 mM EDTA.

4.3.7.2. Confocal imaging

INS1E cells were seeded on 22 mm polylysinated glasses (250,000 cells per glass). Treatment included 3 mM/25 mM glucose, 25 mM glucose + 15 μM oleate for 48 or 72 hours + 200 μM orlistat and 100 μM cerulenin for 3 hours. The fixation and staining of cells followed the protocol used for flow cytometry with these exceptions:

- Cells were not trypsinized but were adherent to the glass
- Incubation with the primary antibody lasted 1 hour
- Hoechst 33342 was used (3 μM)
- FC buffer did not contain EDTA

Samples with live cells were also prepared for confocal imaging. These cells were stained with 0.5 μM BODIPY and Hoechst 33342 (3 μM) for 10 minutes before the imaging, for both live and fixed cells water immersion was used with ACS APO 63x objective.

4.3.8. Free fatty acid quantification

Free fatty acids were quantified from INS1E cells. Five million of the cells were seeded, next day *Nox4* was silenced and the cells were treated with 3 or 25 mM glucose or 25 mM glucose + 15 μM oleate for 72 hours. First, the culture medium was aspirated then the cells were washed with PBS and trypsinized. The trypsinisation was stopped with PBS. The cell suspension was transferred to a microtube. Centrifugation for 5 min, 1000g followed. The supernatant was aspirated. The pellet was resuspended in 1 ml of PBS and the sample was centrifuged again for 5 min, 1000 g. The supernatant was aspirated, and the pellet was resuspended in 50 μl of PBS. Samples were sonicated two times for 20 seconds with an amplitude of 33%. The lysates were stored at -80°C.

The free fatty acid content in the lysates was quantified using the Non-esterified Free Fatty Acids (NEFA) Colorimetric Assay Kit from Elabscience. The manufacturer's protocol was followed.

4.3.9. Total protein quantification in INS1E

Total protein volume was quantified using BCA (bicinchoninic acid) assay. 10 μl of the sample was mixed with 90 μl of distilled water. BSA was used as a standard for the calibration curve:

- 100 μl H_2O = blank
- 95 μl H_2O + 5 μl BSA
- 90 μl H_2O + 10 μl BSA
- 80 μl H_2O + 20 μl BSA
- 70 μl H_2O + 30 μl BSA
- 60 μl H_2O + 40 μl BSA
- 50 μl H_2O + 50 μl BSA

BCA solution (reagent A) was mixed with 4% $CuSO_4 \times 5H_2O$ (reagent B) resulting in solution A: B. For one sample 20 μl of 4% $CuSO_4$ and 880 μl of BCA solution were needed. 900 μl of solution A: B

was added to the standards, the blank and the samples. Incubation at 37°C for 30 minutes followed. The absorbance was measured at 562 nm on a BioPhotometer.

4.3.10. Quantification of glycerol release

For the quantification of glycerol release, half a million of the INS1E cells were seeded. Next day *Nox4* was silenced and the cells were treated with 3 or 25 mM glucose or 25 mM glucose + 15 μM oleate for 24 hours. Glycerol released from the cells into the medium, which did not contain phenol red and FBS because of their autofluorescence, was measured with the use of the fluorometric High Sensitivity Free Glycerol Assay Kit from Sigma-Aldrich®. The procedure followed the manufacturer's protocol. The fluorescence intensity was measured at λ_{ex} = 535 nm, λ_{em} = 587.

4.3.11. Result analysis and statistics

The graphs were created in GraphPad Prism version 10.1.2. for Windows, GraphPad Software, Boston, Massachusetts USA, www.graphpad.com. The results were statistically processed in the same software using two-way ANOVA followed by Tukey's multiple comparisons test or paired t-test (α = 0.05). Images from the confocal microscopy were analysed in Fiji software (Schindelin *et al.,* 2012). The flow cytometry results were analysed using FlowJo™ v10.8.2 Software (BD Life Sciences). Microsoft Excel 365 was used for other calculations.

5. Results

5.1. Glucose impact on the transcripts of lipid metabolism in INS1E cells

Lipids are important for the proper β-cell function and their metabolism is tightly connected with the metabolism of glucose. Therefore, the expression of enzymes involved in lipid metabolism was evaluated depending on the glucose concentration and the length of exposure. Enzymes representing different pathways of lipid metabolism were estimated, including ACLY for the anaplerotic pathway, FASN for the fatty acid synthesis, ACSL3 and ACSL4 for activating fatty acids and HSL for lipolysis. The gene expression was quantified after 2 hours and 24 hours of exposure of INS1E cells to low glucose (3 mM – starving condition) and high glucose (25 mM – stimulating condition) concentrations. The condition with 3 mM glucose after 2 hours was established as 100%. The expression was normalised to the expression of the *B2m* (β-2-microglobulin) gene. ACLY is an enzyme of the anaplerotic pathway preceding fatty acid synthesis, which converts citrate to acetyl-CoA. Its expression increases both with time and exposure to glucose (Fig. 7A). The increase after 24 hours at high glucose was significant ($p = 0.0122$) compared to low glucose (by 96% ± 16%). *Fasn* (fatty acid synthase) had slightly higher expression at 25 mM glucose in comparison to 3 mM glucose both after 2 hours (by 19% ± 9%) and 24 hours (by 19% ± 7%) (Fig. 7B). In addition, at both glucose concentrations, there was a decrease in the expression after 24 hours compared to the expression after 2 hours (by 21% ± 8% at 3 mM glucose, $p = 0.0376$ and by 21% ± 3% at 25 mM glucose, $p = 0.0346$).

ACSL3, which activates fatty acids with CoA so they can be further metabolized, showed an increase (by 31% ± 11%) in the expression after 24h compared to 2 hours at 3 mM glucose (Fig. 7C). However, the expression at 25 mM was decreased (by 23% ± 2%) after 24 hours compared to the expression after 2 hours. Overall, the expression of *Acsl3* was higher (by 60% ± 22%) at 25 mM after 2 hours than on 3 mM glucose. This increase was not significant; however, it can be caused by the augmented fatty acid synthesis under acute high glucose exposure. After 24 hours the effect is no longer present. The expression of *Acsl4*, which is another isoform of ligase connecting fatty acids with CoA, was increased (by 59% ± 36%) after 24 hours at 3 mM glucose in comparison to the expression at 3 mM glucose after 2 hours (Fig. 7D). At 25 mM glucose, both the expression of *Acsl4* after 2 hours and 24 hours on average did not differ from the expression at 3 mM glucose after 2 hours.

A significant decrease ($p < 0.0001$) in *Lipe* (gene coding a lipase involved in the lipolytic arm of the GL/NEFA cycle) both at low (by 64% ± 5%) and high glucose (by 70% ± 14%) after 24 hours compared to the expression after 2 hours was observed (Fig. 7E). Overall, these data show that glucose significantly impacts the expression of certain genes involved in lipid metabolism, suggesting enhanced pathways for fatty acid activation, anaplerotic pathways, and fatty acid synthesis.
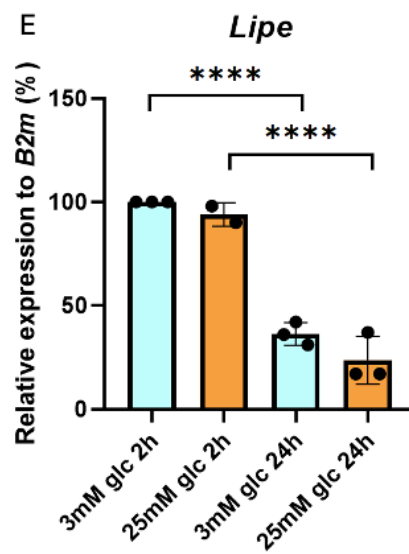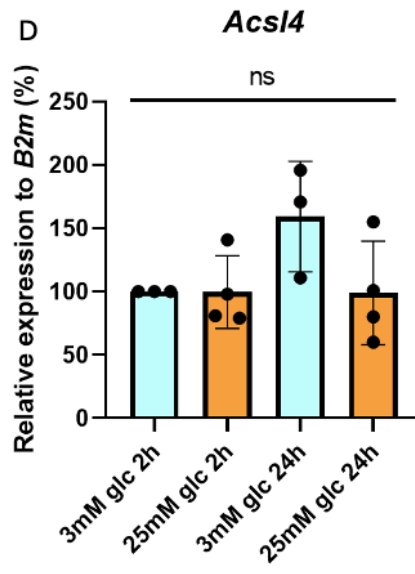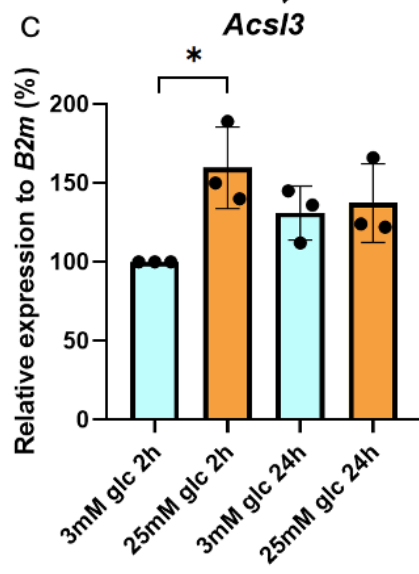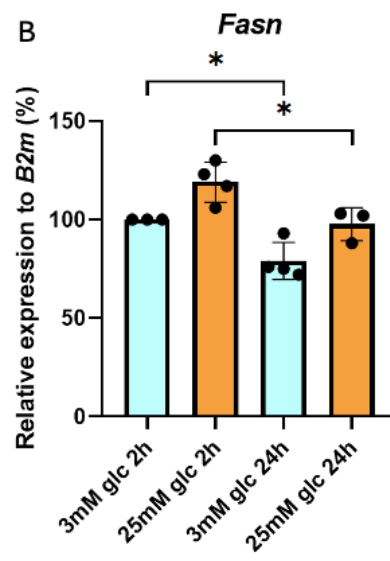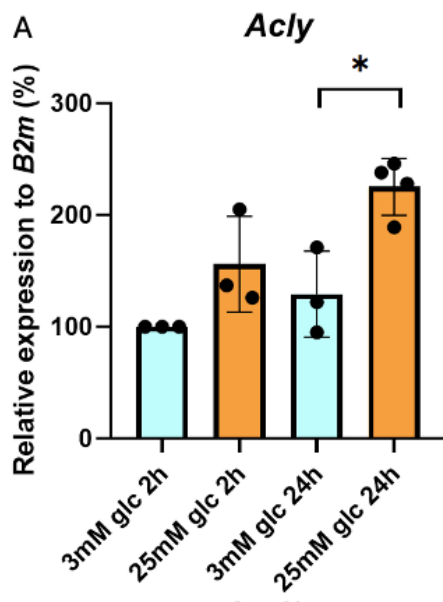
Figure 7: **Expression of genes of lipid metabolism in INS1E cells.** Gene expression of A: *Acsl3* (long-chain acyl-CoA synthetase 3), SD for 3 mM glc 2h = 3%; B: *Acsl4* (long-chain acyl-CoA synthetase 4), SD for 3 mM glc 2h = 26%; C: *Acly* (ATP citrate lyase), SD for 3 mM glc 2h = 2%; D: *Lipe* (hormone sensitive lipase), SD for 3 mM glc 2h = 1%; E: *Fasn* (fatty acid synthase), SD for 3 mM glc 2h = 16%. The cells were exposed to 3 or 25 mM glucose for 2 or 24 hours. The gene expression was normalized to the reference gene *B2m* (β-2-microglobulin) expression. The expression at 3 mM glucose after 2 hours was established as 100%. N = 3-4; * $p < 0.05$; ** $p < 0.01$; *** $p < 0.0001$; **** $p < 0.0001$. Other compared values were not significant.

5.2. *Nox4* silencing impact on the gene expression in INS1E cells

Due to the *Nox4* silencing using a pair of siRNA oligonucleotides, the *Nox4* expression was decreased at the mRNA level by 79% ± 5%, $p < 0.0001$ after 24-hour exposure to 3 mM glucose and by 56% ± 5%, $p = 0.0005$ after exposure to 25 mM glucose (Fig. 8) resulting in the creation of a more reductive redox environment in the cytoplasm. Scramble siRNA oligonucleotide (SCR) was used as a control. The impact of the *Nox4* silencing on the expression of genes of lipid metabolism after the exposure to 3 mM and 25 mM glucose for 24 hours was studied. The condition SCR 3 mM glucose was established as 100%. The expression was normalised to the expression of the *B2m* (β-2-microglobulin) gene. *Acly* expression decreased with *Nox4* silencing both at 3 mM glucose (16% ± 9%) and 25 mM glucose (by 45% ± 7%; $p = 0.0075$) (Fig. 9A). At 25 mM glucose, the expression was increased compared to 3 mM glucose both in SCR (by 53% ± 11%, $p = 0.0033$) and si*Nox4* (by 24% ± 4%, $p = 0.0183$) samples. The expression of SCR vs. si*Nox4* at 25 mM was similar. The silencing of *Nox4* also decreased the expression of *Fasn* both at 3 mM glucose (by 28% ± 9%) and 25 mM glucose (by 59% ± 31%) (Fig. 9B). *Acsl3* showed a decrease in the expression when *Nox4* was silenced at 3 mM glucose (by 28% ± 9%) and 25 mM glucose (by 10% ± 1%) (Fig. 9C). There was a decrease (25% ± 8%) in *Acsl4* with *Nox4* silencing at low glucose (Fig. 9D). The expression at high glucose was on average the same as the si*Nox4* at 3 mM. However, there was no difference between SCR and si*Nox4*. *Lipe* showed a significant ($p = 0.0229$) decrease by 40% ± 16% after the silencing of *Nox4* at 3 mM glucose (Fig. 9E). The data indicate that the more reduced environment affects the expression of enzymes involved in lipid metabolism and turnover.
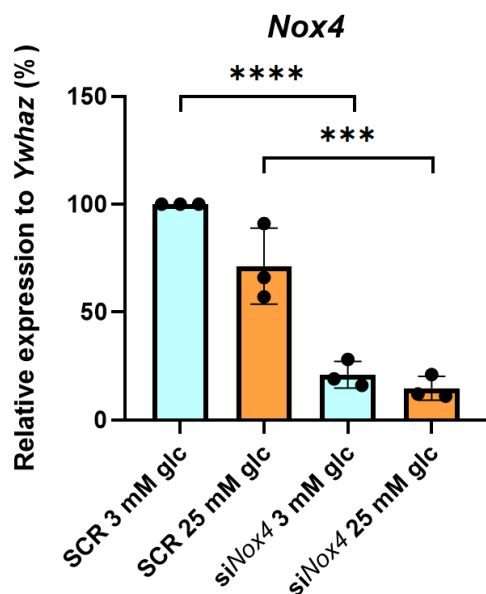

Figure 8: **Expression of *Nox4* after silencing.** Nox4 was silenced in INS1E, then the cells were treated with 3 mM or 25 mM glucose for 24 hours. The gene expression was normalized to the reference gene *Ywhaz* (tyrosine 3-monooxygenase/tryptophan 5-monooxygenase activation protein zeta) expression. The expression of SCR at 3 mM glucose was established as 100%. N = 3. * $p < 0.05$; ** $p < 0.01$; *** $p < 0.0001$; **** $p < 0.0001$. Other compared values were not significant.
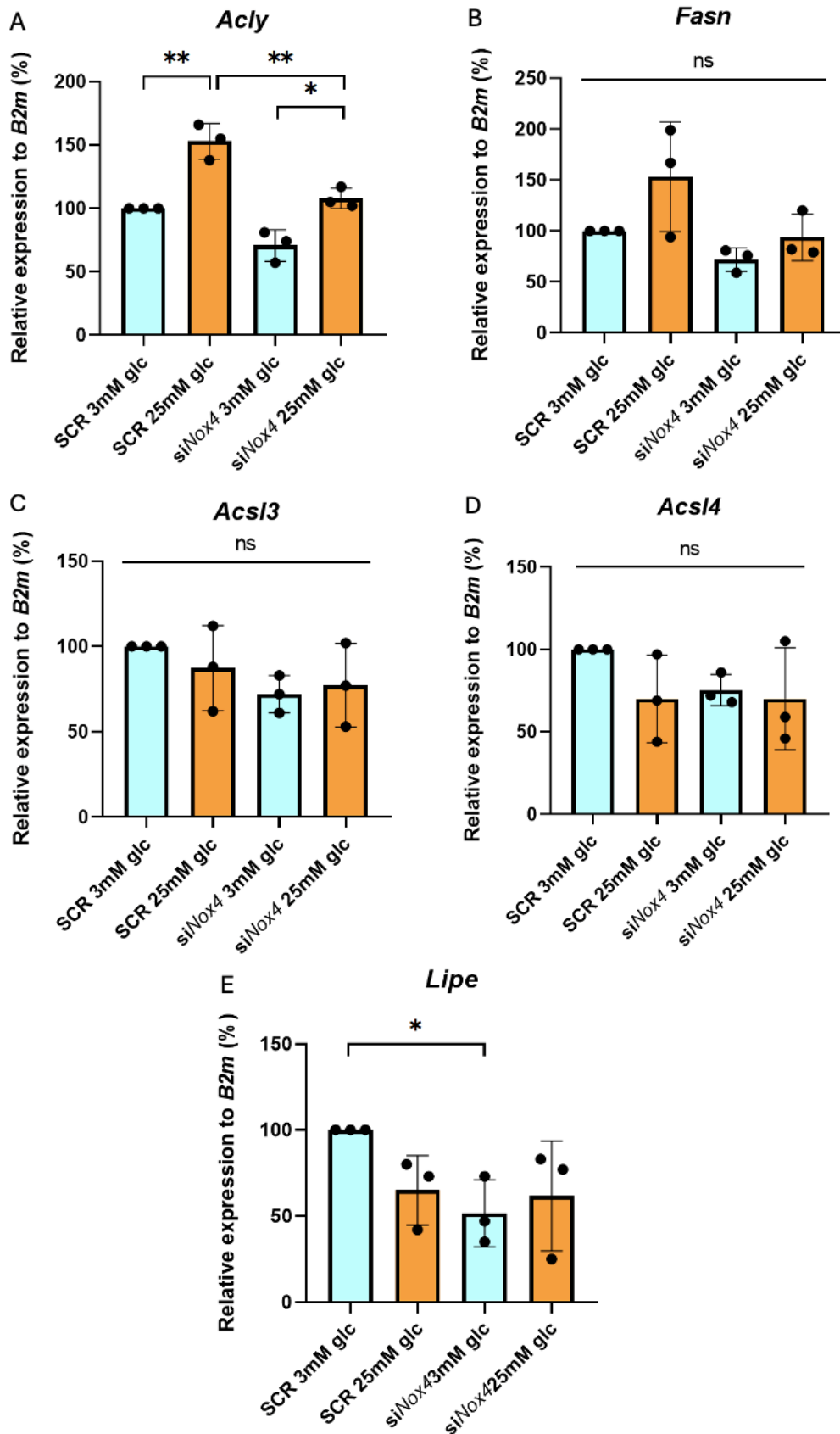
Figure 9: **Expression of genes of lipid metabolism in INS1E cells with the silencing of *Nox4*.** Gene expression of A: *Acsl3* (long-chain acyl-CoA synthetase 3), SD for SCR 3 mM glc = 5%; B: *Acsl4* (long-chain acyl-CoA synthetase 4), SD for SCR 3 mM glc = 5%; C: *Acly* (ATP citrate lyase), SD for SCR 3 mM glc = 13%; D: *Lipe* (hormone sensitive lipase), SD for SCR 3 mM glc = 24%; E: *Fasn* (fatty acid synthase), SD for SCR 3 mM glc = 12%. The cells were exposed to 3 or 25 mM glucose for 24 hours. The gene expression was normalized to the reference gene *B2m* (β-2-microglobulin) expression. The expression of SCR at 3 mM glucose was established as 100%. N = 3-4; * p < 0.05; ** p < 0.01; *** p < 0.0001; **** p < 0.0001. Other compared values were not significant.

5.3. Glucose and reduced redox environment impact on the expression of enzymes involved in lipid metabolism in mouse pancreatic islets

Expression of genes related to lipid metabolism was analysed in isolated mouse pancreatic islets incubated at 5 mM glucose (non-stimulating) or 25 mM glucose (stimulating) for 48 hours. The islets were isolated from WT and β*Nox4*KO (MUT = mutant) mice. The expression was normalised to the expression of the *Hprt* (hypoxanthine phosphoribosyltransferase) gene. The expression of genes in islets isolated from WT mice incubated at 5 mM glucose was established as 100%. Genes representing different pathways involved in lipid metabolism were analysed, including ACLY and ACC from the anaplerotic pathway, FASN for *de novo* FA synthesis, ACSL3 and ACSL4 for FA activation, GPAT4 for lipogenesis, HSL for lipolysis, PLIN2 as a marker of LDs, and PLIN5 for regulating lipolysis. The expression of *Acly* was increased after the stimulating glucose concentration by $63\% \pm 25\%$ in WT, $p = 0.0228$ (Fig. 10A). This effect was augmented in MUT (increase by $118\% \pm 8\%$, $p = 0.0013$). The expression in MUT was significantly ($p = 0.0029$) increased at 25 mM glucose compared to WT (by $93\% \pm 15\%$). At stimulating glucose, *Acc* expression was increased by $131\% \pm 53\%$, $p = 0.0160$ in MUT compared to WT (Fig. 10B). Also, the expression was increased at 25 mM glucose compared to 5 mM glucose both in WT (by $73\% \pm 10\%$) and MUT (by $205\% \pm 48\%$, $p = 0.0011$). Overall, the expression pattern of *Acc* correlated with that of *Acly*, which can be explained by the fact that they are part of the same pathway as the product of ACLY (acetyl-CoA) is a substrate for ACC.

Fasn had an increased expression at 25 mM glucose compared to 5 mM glucose by $81\% \pm 19\%$, $p = 0.0079$ in WT and by $51\% \pm 21\%$ in MUT (Fig. 10C). Both isoforms of ACSL showed significantly increased expression at 25 mM glucose compared to 5 mM glucose (Fig. 10D, E). This effect was observed both in WT and MUT. *Acsl3* in WT was increased by $47\% \pm 12\%$, $p = 0.0460$ and in MUT by $53\% \pm 6\%$ $p = 0.0475$. The expression of *Acsl4* was increased in WT by $54\% \pm 24\%$, $p = 0.0151$ and in MUT by $49\% \pm 7\%$, $p = 0,0260$. The expression of *Gpat4* increased after 25 mM compared to 5 mM glucose, both in WT (by $50\% \pm 16\%$) and in MUT (by $32\% \pm 11\%$) indicating augmented lipogenesis under stimulating glucose condition (Fig. 10F).

Similarly to *Acly, Acc, and Acsl4* the expression of *Lipe* (one of the principal enzymes involved in lipolysis) at 25 mM glucose was augmented in MUT compared to WT (by $40\% \pm 6\%$). *Lipe* showed an increase in the expression at 25 mM glucose compared to 5 mM both in WT (by $25\% \pm 7\%$) and MUT (by $76\% \pm 14\%$, $p = 0.0012$) (Fig. 10G). PLIN2 is a marker of LDs localized on their surface, helping with incorporation of TAGs into the LD core. Its expression was increased at the stimulating glucose by $50\% \pm 26\%$ in WT and by $209\% \pm 29\%$, $p = 0.0012$ in MUT compared to the 5 mM glucose condition (Fig. 10H) indicating the LD accumulation at stimulating glucose concentration. There was a significant difference in the expression at 25 mM glucose between WT and MUT (an increase by $151\% \pm 10\%$, $p = 0.0065$). *Plin5* regulates lipolysis and mediates the interaction of LDs with mitochondria. Its expression was reduced by $57\% \pm 25\%$ at 25 mM glucose compared to 5 mM glucose in WT (Fig. 10I), indicating decreased need of lipolysis at high glucose concentration. However, in MUT the expression increased by $63\% \pm 13\%$. The expression in MUT at 25 mM glucose was significantly

increased by 105% ± 23% compared to WT. Similar to INS1E cells, glucose has a significant impact on the expression of certain genes in mouse pancreatic islets. The impact of glucose is often augmented in MUT, suggesting that the redox environment influences the expression of these genes.
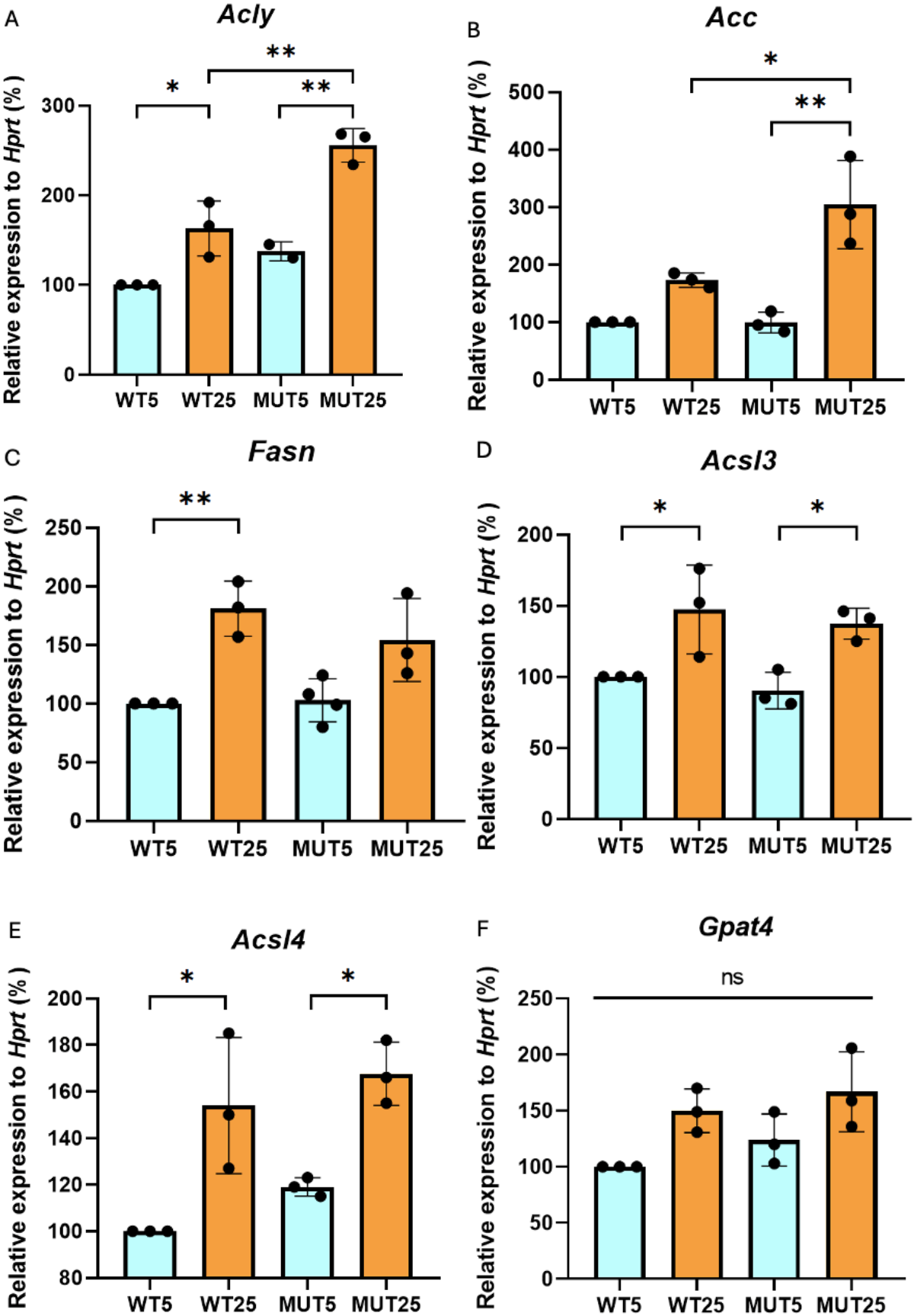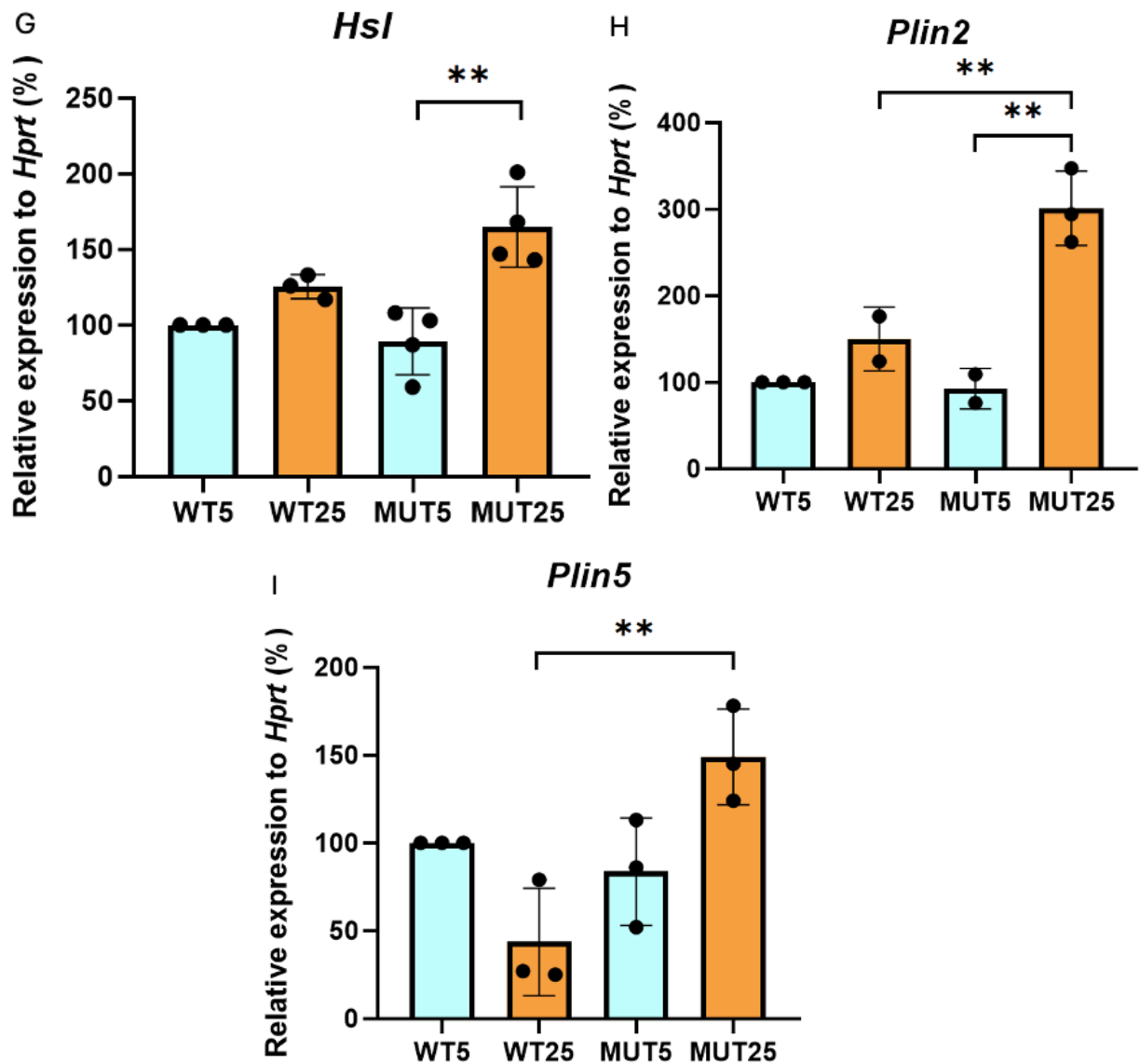
Figure 10: **Expression of genes of lipid metabolism in mouse pancreatic islets.** Gene expression of A: *Acsl3* (long-chain acyl-CoA synthetase 3), SD for WT5 = 9%; B: *Acsl4* (long-chain acyl-CoA synthetase 4), SD for WT5 = 13%; C: *Acly* (ATP citrate lyase), SD for WT5 = 25%; D: *Acc* (acetyl-CoA carboxylase), SD for WT5 = 9%; E: *Plin2* (perilipin 2), SD for WT5 = 9%; F: *Plin5* (perilipin 5), SD for WT5 = 25%; G: *Lipe* (hormone sensitive lipase), SD for WT5 = 18%; H: *Fasn* (fatty acid synthase), SD for WT5 = 14%; I: *Gpat4* (glycerol-3-phosphate acyltransferase), SD for WT5 = 13%. The islets were isolated from WT and β*Nox4*KO mice (MUT) and incubated at 5 or 25 mM glucose for 48 hours. The gene expression was normalized to the reference gene *Hprt* (hypoxanthine phosphoribosyltransferase) expression. The expression of WT at 5 mM glucose was established as 100%. N = 2-4; * $p < 0.05$; ** $p < 0.01$; *** $p < 0.0001$; **** $p < 0.0001$. Other compared values were not significant.

5.4. Lipid droplet analysis in INS1E cells

5.4.1. Lipid droplet analysis by flow cytometry

The content of lipid droplets in INS1E cells was analysed using flow cytometry. As the BODIPY 493/503 stain is known to bind to neutral lipids including triacylglycerols and lipofuscins, a preliminary experiment was conducted to confirm the specificity of BODIPY 493/503 towards LDs. The LDs were stained with the primary antibody against PLIN2 in fixed INS1E cells and a secondary antibody labelled

by Alexa Fluor 555 was used for detection. The PLIN2 signal strongly colocalized with that of BODIPY 493/503 (Fig. 11) confirming the BODIPY staining of LDs.
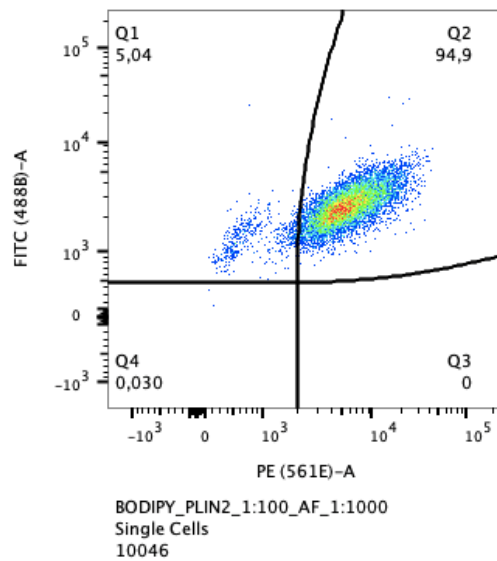

Figure 11: **BODIPY and PLIN2 antibody staining.** INS1E cells were fixed and stained with BODIPY (y axis) and PLIN2 primary antibody with the secondary antibody Alexa Fluor 555 (x axis).

The effect of glucose (3mM/25mM), together with the redox environment (modulated by *Nox4* silencing) on LD number was investigated in live cells (not fixed). Oleate, orlistat (inhibitor of lipolysis) and cerulenin (inhibitor of fatty acid synthesis) were used to assess the range of LD accumulation. The treatment with glucose and oleate was performed for either 24 or 72h to see the maximal LD accumulation, the inhibitors orlistat and cerulenin were added for the last 3 hours of the treatment, as longer treatments caused a major decrease in cell viability. BODIPY was used for the staining of lipid droplets. Hoechst 33258 was used to distinguish between live and dead cells. LD content was measured as a median fluorescence of BODIPY. The condition SCR 3 mM glucose after 24 hours was established as 100%. An example of the gating strategy is demonstrated in Fig. 12. First, a population of cells was chosen based on their size and granularity. Then only single cells were gated with the following exclusion of dead cells. Finally, BODIPY negative and BODIPY positive cells were selected.
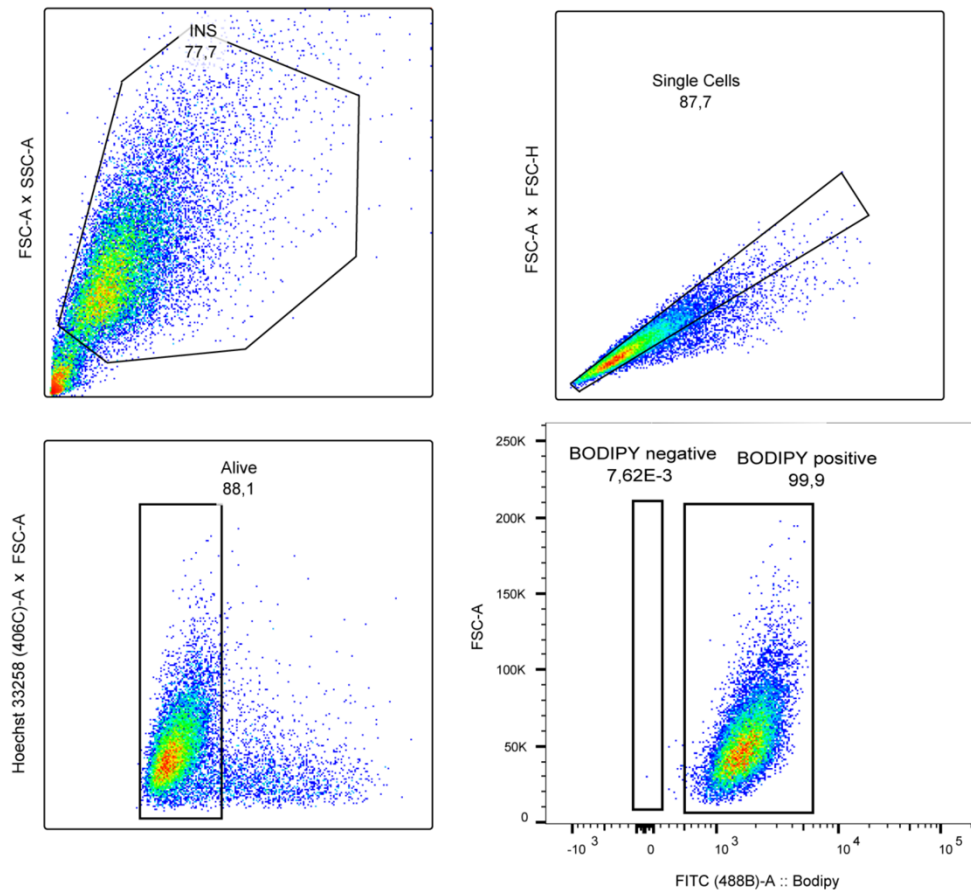
Figure 12: **Gating strategy of the flow cytometry analysis**. SCR 3 mM glucose and SCR 25 mM glucose after 24 hours samples. First, a population of INS1E cells was chosen. Then only single cells were gated with the following exclusion of dead cells. Finally, BODIPY negative and BODIPY positive cells were selected.

At 25 mM glucose, the LD content was increased by 52% ± 9% in SCR and by 56% ± 20% in si*Nox4* after 24h treatment (Fig. 13). After 72h the increase was by 31% ± 14% in SCR and by 69% ± 36% in si*Nox4* (Fig. 14). After the treatment with 25 mM glucose with the addition of oleate there was a significant increase in the LD content by 98% ± 35%, $p < 0,0001$ in SCR and by 115% ± 22%, $p < 0.0001$ in si*Nox4* after 24 hours. This effect was present also after 72 hours (increase by 130% ± 53%, $p = 0.0470$ in SCR and by 154% ± 37%, $p = 0.0059$ in si*Nox4*). LD accumulation was even more pronounced with 25 mM glucose + oleate + orlistat treatment (increase after 24 hours by 148% ± 43%, $p < 0.0001$ in SCR, by 121% ± 15%, $p < 0.0001$ in si*Nox4* and after 72 hours by 279 ± 78%, $p < 0.0001$ in SCR and by 243% ± 28%, $p = 0.0010$ in si*Nox4*). Cerulenin treatment at 3 mM glucose after 24 hours slightly increased LD content by 35% ± 19% in SCR and by 20% ± 10% in si*Nox4* and at 25 mM glucose by 8% ± 26% in SCR and by 27% ± 17% in si*Nox4*) compared to the same glucose concentration without cerulenin. To sum up, glucose and oleate potentiate the formation of LDs. When the lipolysis is blocked by orlistat, triacylglycerols in LDs cannot be hydrolysed and the accumulation is augmented. Cerulenin also increases the content of LD, which is probably due to the fatty acid uptake from the medium when the fatty acid synthesis is blocked as can be seen below.
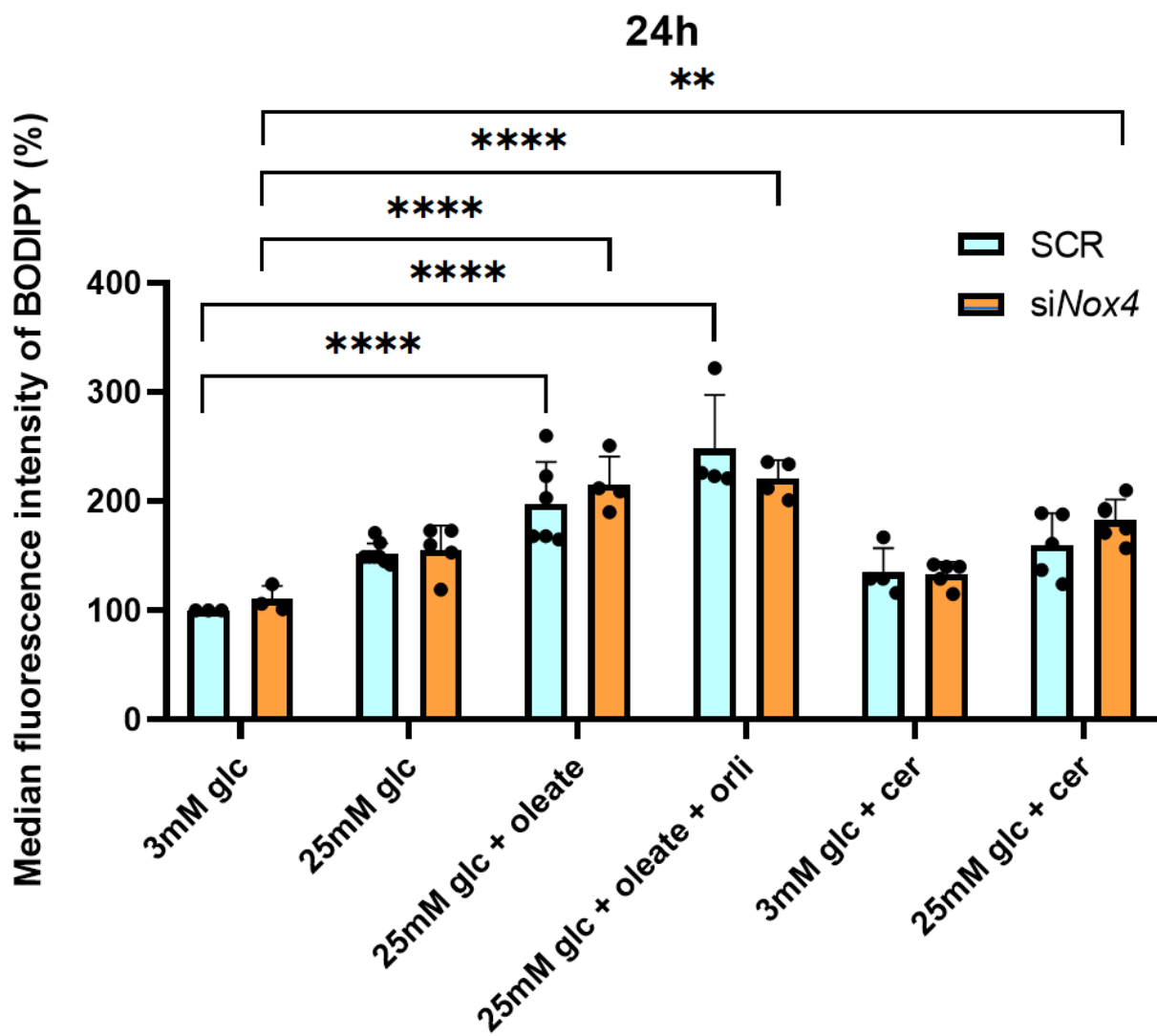
Figure 13: **Lipid droplet analysis using flow cytometry – 24-hour treatment.** INS1E cells were treated with 3 mM or 25 mM glucose and oleate for 24h. The inhibitors (orlistat and cerulenin) were added for the last 3 hours. The sample SCR 3 mM glucose was established as 100%. SD for 3 mM glc = 9%. N = 3-8; * p < 0.05; ** p < 0.01; *** p < 0.0001; **** p < 0.0001. Other compared values were not significant.
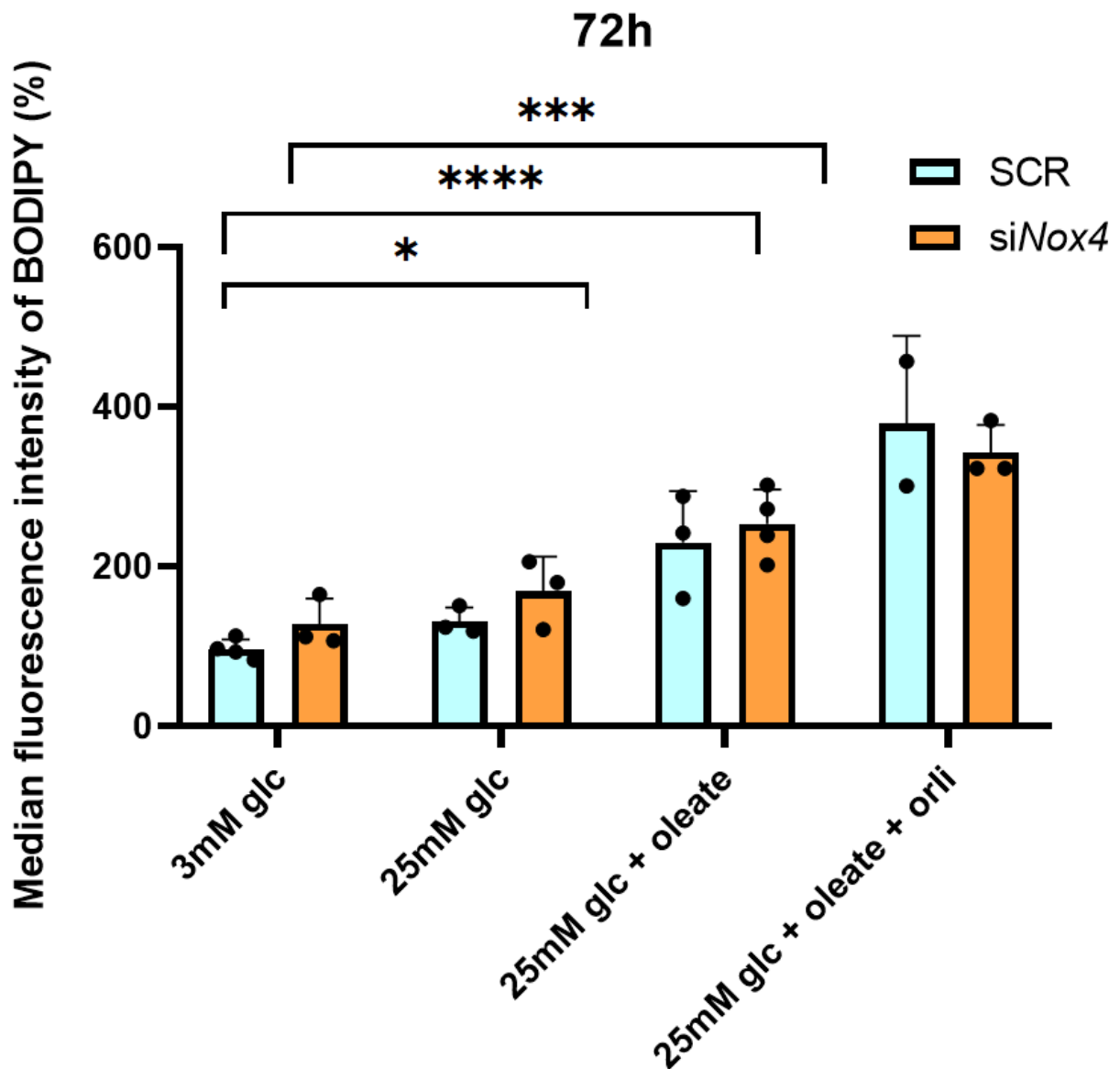
Figure 14: **Lipid droplet analysis using flow cytometry – 72-hour treatment.** INS1E cells were treated with 3 mM or 25 mM glucose and oleate for 72h. The inhibitors (orlistat and cerulenin) were added for the last 3 hours. The sample SCR 3 mM glucose was established as 100%. N = 2-4; * p < 0.05; ** p < 0.01; *** p < 0.0001; **** p < 0.0001. Other compared values were not significant.

To elucidate the importance of the culture medium composition in the experiments while analyzing lipid droplet content, the effect of the medium with FBS (source of fatty acids) commonly used for the INS1E cell culture was compared with serum-free medium (SFM) (the same composition as INS medium only the FBS was omitted). The same samples were prepared culturing in the medium with FBS or SFM. The median fluorescence intensity of BODIPY was compared as a ratio of the SFM and the medium with FBS (Fig. 15). The ratio lower than 1 indicates uptake of fatty acids from the medium. The ratio was lower than 1 in SCR (0.59 ± 0.16) and si*Nox4* (0.74 ± 0.02) at 3 mM glucose, in si*Nox4* at 25 mM glucose (0.8 ± 0.09), in SCR (0.82 ± 0.09) and si*Nox4* (0.91 ± 0.2) at 25 mM glucose + oleate + orlistat, in SCR (0.63 ± 0.001) and si*Nox4* (0.83 ± 0.27) at 3 mM glucose + cerulenin and in si*Nox4* at 25 mM glucose + cerulenin (0.94 ± 0.04). However, none of these data was significant.

This experiment points out that β-cells also uptake fatty acids from the medium and that *de novo* synthesis from glucose is not the only source of fatty acids during certain conditions, particularly at low glucose, during the inhibition of lipolysis by orlistat and the inhibition of fatty acid synthesis by cerulenin at 3 mM glucose. This must be considered when interpreting the data from this kind of experiments.
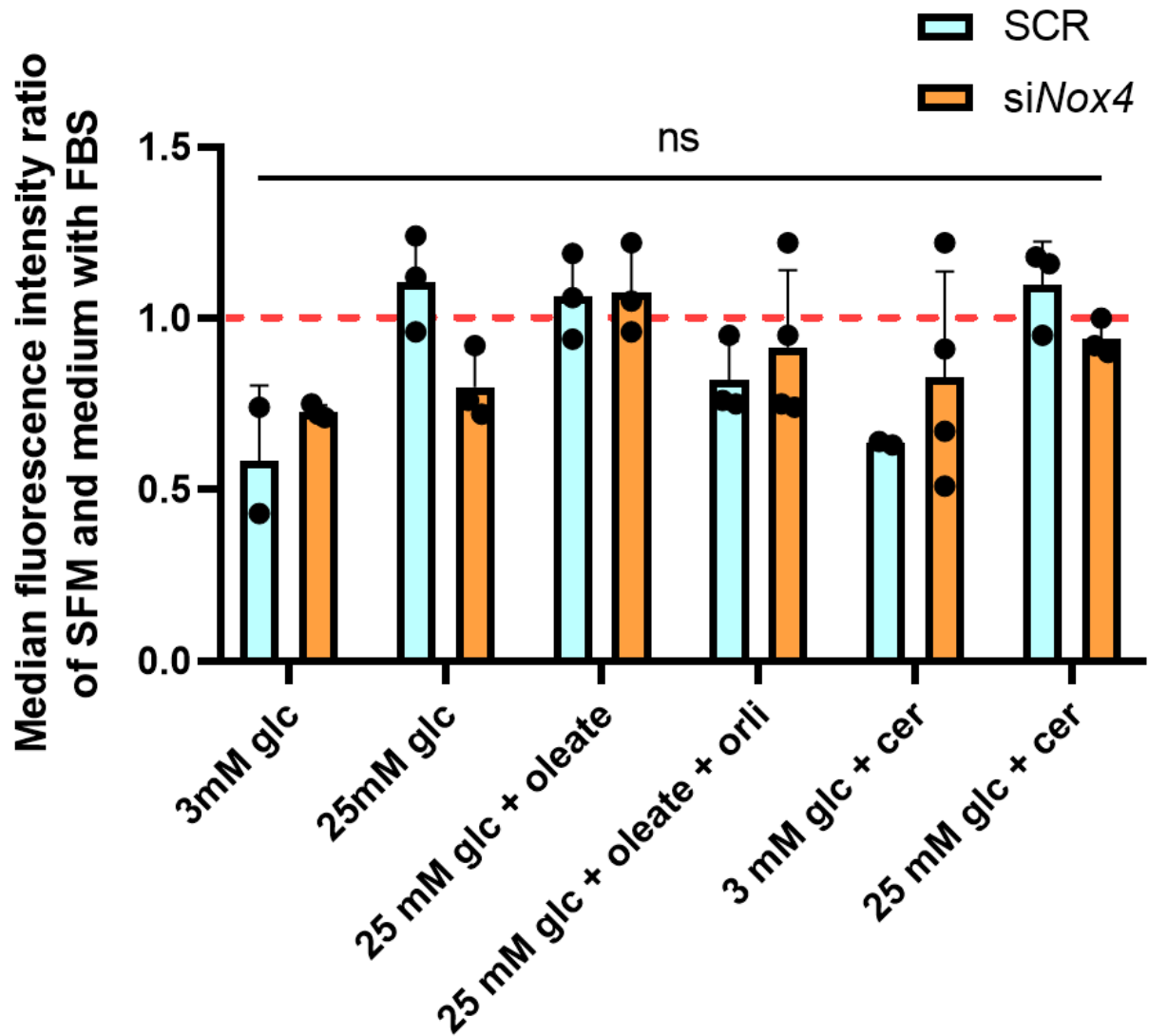

Figure 15: **Comparison of the effects of medium with FBS a serum-free medium (SFM) on the lipid droplet content by flow cytometry.** INS1E cells were incubated in the medium with FBS or SFM for 24 hours and for that period treated with 3 mM or 25 mM glucose and oleate. Orlistat and cerulenin were added for the last 3 hours of the treatment. N = 2-4; * $p < 0.05$; ** $p < 0.01$; *** $p < 0.0001$; **** $p < 0.0001$. The compared values were not significant.

5.4.2. Lipid droplet analysis by confocal microscopy

Lipid droplet content was analysed in variously treated samples of INS1E cells using confocal microscopy. Pre-experiment was conducted to confirm BODIPY 493/503 staining of lipid droplets. BODIPY is used for staining of neutral lipids, in this case, triacylglycerols and sterol esters contained in lipid droplets. Fixed cells were stained with the primary antibody against PLIN2 (a marker of LDs)

and the secondary antibody Alexa Fluor 555 together with BODIPY. Nuclei were stained with Hoechst 33342.

As shown in Fig. 16A, C, E, LDs are represented as bright green dots. In the co-staining experiment, BODIPY and PLIN2 staining (red) are merged and form a yellow signal, representing LDs (Fig. 16B, D, F). The staining quality was confirmed on the samples treated with 3 mM glucose for 24h (Fig. 16A, B), 25 mM glucose for 24h (Fig. 16C, D) and 25 mM glucose + oleate for 24h (Fig. 16E, F).
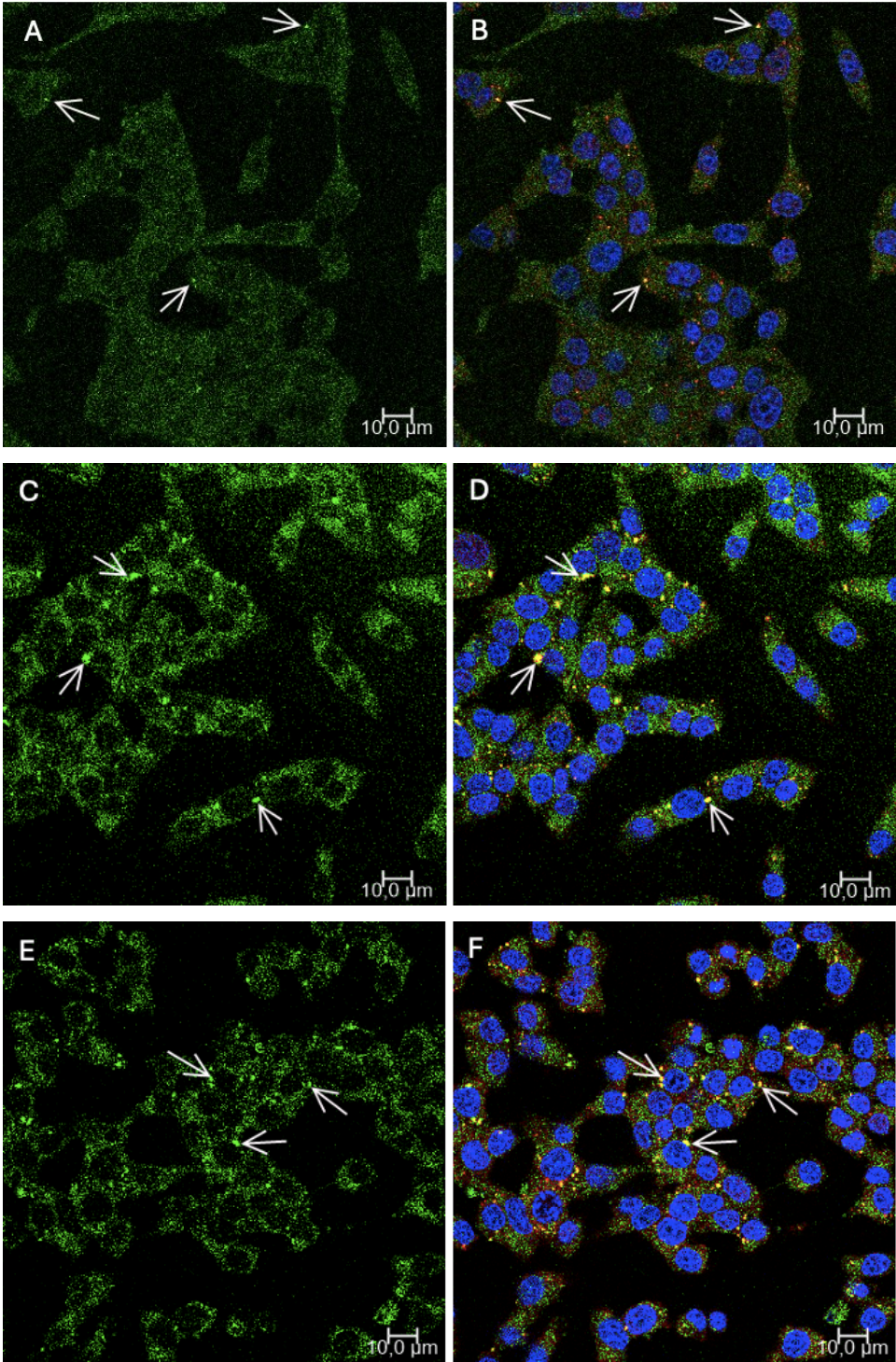
Figure 16: **Lipid droplet analysis by confocal microscopy – the comparison of BODIPY and PLIN2 staining**.
For the experiment, live cells were stained with BODIPY and Hoechst 33342. The treatment included A, B: 3 mM
glucose, C, D: 25 mM glucose, E, F: 25 mM glucose + oleate. The exposure to glucose and oleate lasted 24h.

Lipid droplets were then analysed in live cells with BODIPY staining to see how they change depending on the different conditions induced by non-/stimulating glucose and oleate, redox environment modulated by Nox4 silencing and lipolysis inhibitor orlistat and fatty acid synthesis inhibitor cerulenin. The exposure to glucose and oleate up to 72 h was used. The inhibitors (orlistat and cerulenin) were added for the last 3 hours of the treatment. LDs vary in size and count across the samples, therefore the sum of the area of LDs was measured and normalized for the nuclei number in the image. At 3 mM glucose, the LD area is very small (0.238 ± 0.158 μm^2 in SCR and 2.012 ± 0.372 μm^2 in si*Nox4*) (Fig. 17A, 18A, 19). At 3 mM glucose with cerulenin, the LD area is increased (1.791 ± 0.609 μm^2 in SCR and 3.635 ± 0.318 μm^2 in si*Nox4*) (Fig. 17B, 18B). At 25 mM glucose, LD area increases compared to 3 mM glucose, probably due to *de novo* fatty acid synthesis and their storage in LDs (2.808 ± 0.401 μm^2 in SCR and 2.934 ± 1.432 μm^2 in si*Nox4*) (Fig. 17C, 18C). This effect is even stronger at 25 mM glucose with oleate (8.111 ± 1.272 μm^2 in SCR and 6.327 ± 1.494 μm^2 in si*Nox4*) (Fig. 17E, 18E). Cerulenin again slightly increased the LD area at 25 mM glucose (3.578 ± 0.583 μm^2 in SCR and 6.132 ± 1.101 μm^2 si*Nox4*) (Fig. 17D, 18D) compared to the 25 mM glucose without cerulenin. At 25 mM glucose with oleate and orlistat, the lipolysis is blocked so LDs cannot be degraded, and the storage of LDs is pronounced (11.188 ± 0.885 μm^2 in SCR) (Fig. 17F). Noteworthy, in si*Nox4* samples, the lipid accumulation was more pronounced compared to SCR with a massive accumulation present after treatment by 25 mM glucose, oleate and orlistat reaching probably the maximal storage capacity (13.188 ± 1.628 μm^2) (Fig. 18F). In si*Nox4* samples the LD area was increased compared to SCR samples at 3 mM glucose (by 1.854 ± 0.433 μm^2, p = 0.0034), at 3 mM glucose + cerulenin (by 3.026 ± 0.314 μm^2, p = 0.0192), at 25 mM glucose + cerulenin (by 2.545 ± 0.690 μm^2, p = 0.0442) and at 25 mM glucose + oleate + orlistat (by 8.296 ± 0.537 μm^2, p = 0.0013). Overall, glucose, oleate, orlistat and cerulenin increase LD content (consistent with the data from the flow cytometry) and induce LD accumulation with enhanced effect at more reduced redox environment mediated by *Nox4* silencing.
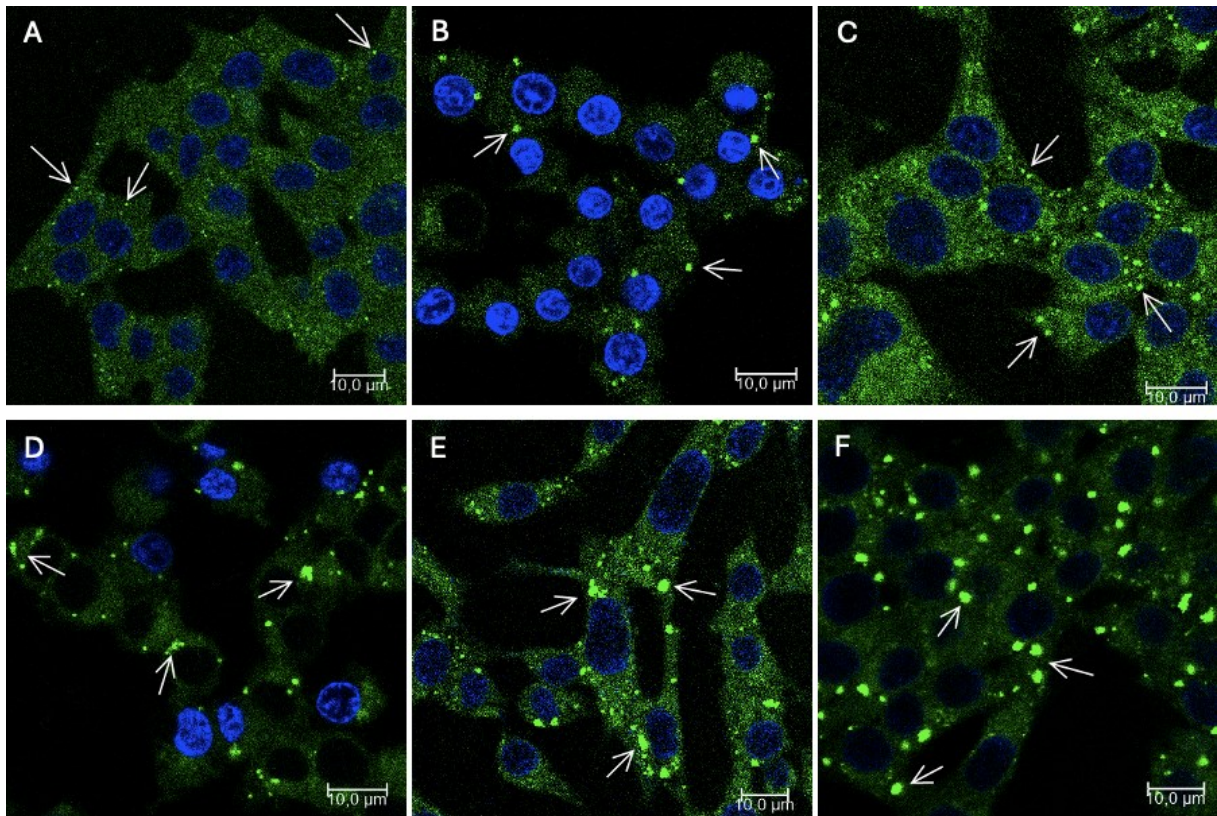
Figure 17: **Lipid droplet analysis by confocal microscopy – scramble (SCR) samples**. A representative image of each sample was chosen. A: 3 mM glucose, B: 3 mM glucose + cerulenin, C: 25 mM glucose, D: 25 mM glucose + cerulenin, E: 25 mM glucose + oleate, F: 25 mM glucose + oleate + orlistat
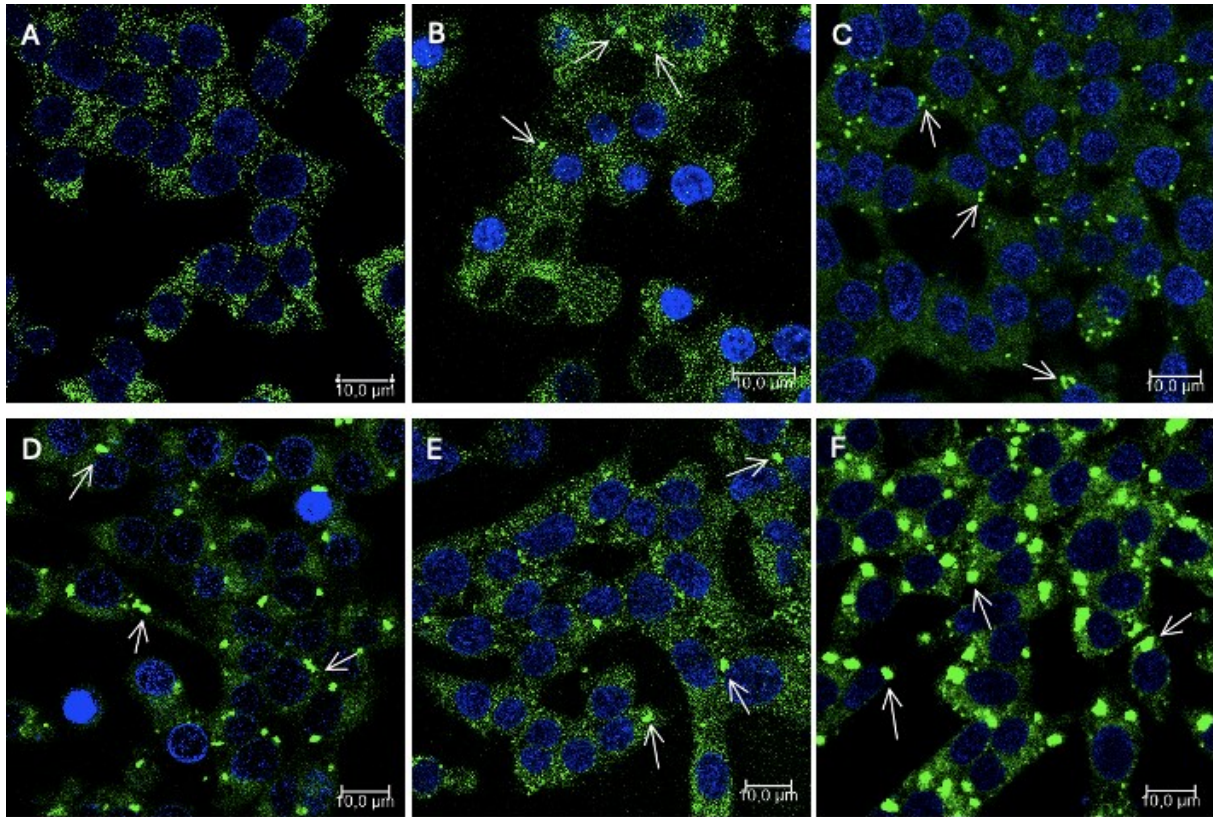
Figure 18: **Lipid droplet analysis by confocal microscopy – si*Nox4* samples**. A representative image of each sample was chosen. A: 3 mM glucose, B: 3 mM glucose + cerulenin, C: 25 mM glucose, D: 25 mM glucose + cerulenin, E: 25 mM glucose + oleate, F: 25 mM glucose + oleate + orlistat
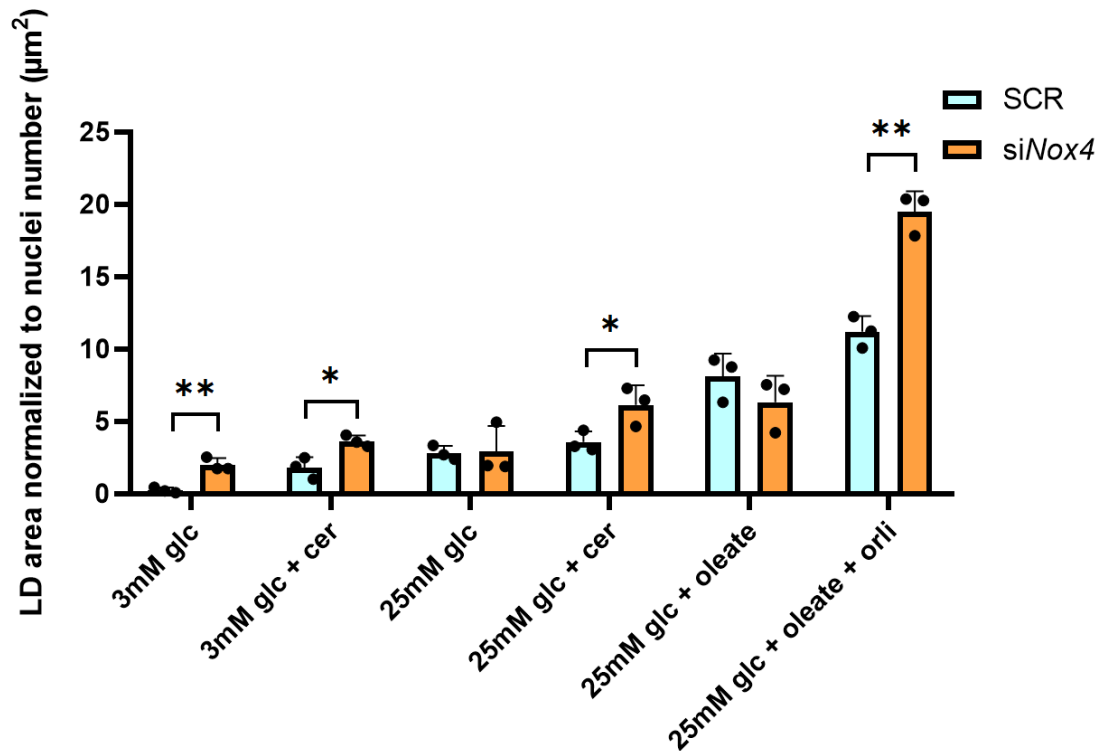
Figure 19: **LD quantification analysed by confocal microscopy**. INS1E cells were incubated for 72 hours in 3 mM or 25 mM glucose and oleate. Orlistat and cerulenin were added for the last 3 hours of the treatment. The area of LDs was analysed in images obtained from confocal microscopy. The LD area was normalized to the nuclei count in the image. N = 3; * $p < 0.05$; ** $p < 0.01$; *** $p < 0.0001$; **** $p < 0.0001$. SCR vs. siNox4 was compared in every condition using, other compared values were not significant.

5.5. The impact of glucose and redox status on NEFA homeostasis

To elucidate the impact of glucose and redox status on NEFA homeostasis, the content of NEFAs was estimated by an enzymatic assay. NEFAs were analysed in the INS1E cell lysates (SCR vs. siNOX4), treated with low/high glucose or glucose + oleate, prepared by sonication. The values were normalized to the amount of protein in the sample. In SCR at 3 mM glucose, there was approximately 10.7 ± 0.9 nmol/mg of NEFA (Fig. 20). In SCR at 25 mM glucose, there was a significant increase of NEFA compared to the low glucose (13.1 ± 0.4 nmol/mg, p = 0.0350). SCR after 25 mM glucose + oleate contained 11.3 ± 0.8 nmol/mg of NEFA. In si*Nox4* samples there was an increase in NEFA amount at 3 mM glucose (12.7 ± 0.6 nmol/mg) and 25 mM glucose + oleate (12.4 ± 0.001 nmol/mg) compared to the same condition in SCR. However, at 25 mM glucose NEFA content in si*Nox4* decreased (11.7 ± 0.2 nmol/mg) compared to SCR at 25 mM glucose. Overall, at 25 mM glucose, the NEFA level is increased; however, this is not the case with the addition of oleate probably because lipid storage is activated otherwise high concentrations of NEFA would be toxic for the cells. Interestingly, *Nox4* silencing leads to different effect on the NEFA content in various nutritional conditions, which is probably connected to a differences in redox environment reflecting the metabolic status of the cells.
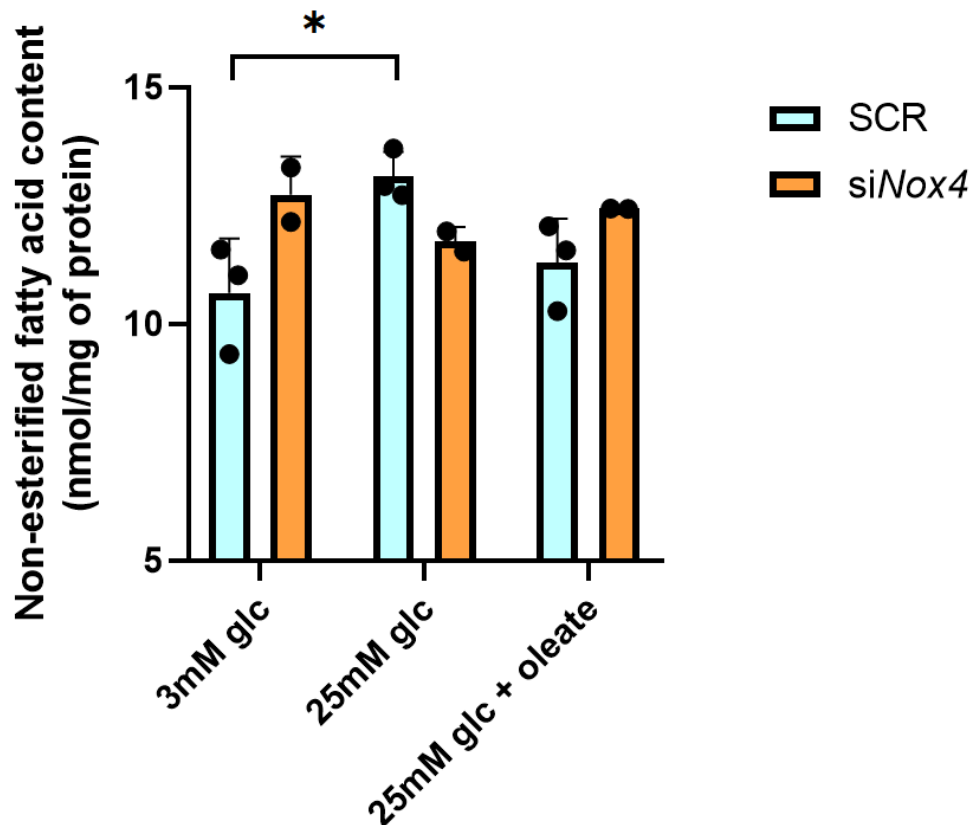

Figure 20: **Non-esterified fatty acid content.** NEFA were quantified in INS1E cell lysates treated with 3 or 25 mM glucose or 25 mM glucose + 15 μM oleate for 72 hours. The cell lysates were prepared by sonication. N = 2-3, * p < 0.05; ** p < 0.01; *** p < 0.0001; **** p < 0.0001. Other compared values were not significant.

5.6. The impact of glucose and redox status on glycerol release

Glycerol, the end product of lipolysis, that was secreted by INS1E cells into the medium was analysed after treatment with low/high glucose and glucose + oleate. Released glycerol was quantified with the fluorometric assay. After low (3 mM) glucose treatment, very small hardly detectable amount of glycerol was detected both in SCR and si*Nox4* samples (0.018 pg/µl in SCR and 0.035 pg/µl in si*Nox4*) (Fig. 21). After exposure to stimulating glucose concentration, glycerol release increased to 1.377 pg/µl in SCR and 1.682 pg/µl in si*Nox4*, respectively, indicating activation of detoxification pathways through G3PP and lipolysis. At 25 mM glucose with the addition of oleate, no significant increase was observed (1.416 pg/µl in SCR and 1.926 pg/µl in si*Nox4*) compared to high glucose condition probably because NEFAs are esterified with the glucose-derived G3P, and more LDs are created as evidenced by confocal microscopy and flow cytometry. Overall, the glycerol secretion was higher in si*Nox4* samples than in SCR samples indicating increased lipid turnover after the *Nox4* silencing.
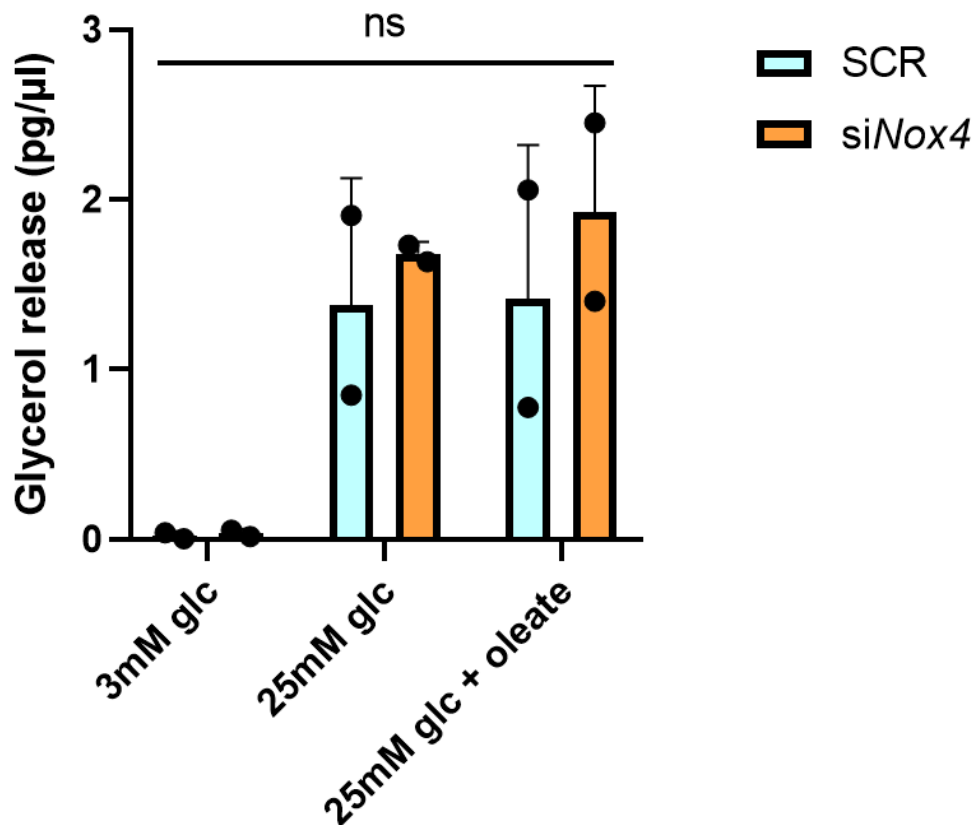

Figure 21: **Glycerol release quantification.** Glycerol secreted from INS1E into the medium was quantified after the treatment with 3 or 25 mM glucose or 25 mM glucose + 15 µM oleate for 24 hours. N = 2, * $p < 0.05$; ** $p < 0.01$; *** $p < 0.0001$; **** $p < 0.0001$. The compared values were not significant.

6. Discussion

Glucose and lipid metabolism are closely intertwined, which is even more relevant for pancreatic β-cells, where maintenance of metabolic homeostasis is crucial for their proper functioning and health, having further impact on keeping the whole-organismal glucose homeostasis. Among others, also redox environment is essential in this respect. From our previous studies with mice lacking the NOX4 enzyme, we uncovered an indispensable role of redox signalling (mediated by NOX4) in insulin secretion from pancreatic β-cells (Plecitá-Hlavatá *et al.,* 2020). Interestingly mice lacking NOX4 specifically in pancreatic β-cells have increased accumulation of ectopic fat in pancreatic islets along with increased weight (Holendová *et al.,* 2024) indicating an imbalance in lipid metabolism caused by a more reductive environment caused by the NOX4 deletion. However, the mechanisms causing this phenotype remain unknown. In light of these findings, the thesis aims to investigate the impact of glucose on lipid metabolism in a physiological redox environment as well as in a more reductive redox environment achieved through *Nox4* knockdown.

The silencing of *Nox4* resulted in a significant augmentation of LD content in INS1E cells across most of the experimental conditions. Notably, the most striking enhancement in LD accumulation was evident following the inhibition of lipolysis through treatment with orlistat, a potent inhibitor of lipases, reaching probably the maximal storage capacity. This effect suggests that the absence of *Nox4* activity leads to an upregulation of lipid storage. Together, these data indicate increased lipid turnover after *Nox4* silencing in β-cells confirming our previous findings on β*Nox4*KO mice (Holendová et al., 2024).

LDs are cellular structures storing lipids. Their composition changes in response to the cellular states and nutrient availability. LD formation, degradation and interaction with other organelles are tightly coupled with the cellular metabolism. LDs also have the ability to buffer lipids; since lipolysis is initiated there and by incorporating fatty acids into triacylglycerols they prevent lipotoxicity. The TAG synthesis occurs within seconds to minutes after the exposure to FAs, whereby they can be incorporated into pre-existing LDs or those newly formed (Kassan *et al.,* 2013). During a chronic nutrient overload, the redox homeostasis is shifted to a more prooxidative deleterious state resulting in the activation of stress pathways. This leads to β-cell dedifferentiation, dysfunction, and insulin resistance and further to the development of T2D (Holendová *et al.,* 2024). The formation of LDs is one of the detoxification mechanisms of how cells can cope with excess fuel. At physiological conditions, lipolysis of triacylglycerols leads to the production of important metabolic coupling factors for insulin secretion and NEFAs in case of the energy demand during starvation. Therefore, a proper LD turnover is important for β-cell function. Recently, LDs have also been linked to the control of the cellular distribution of unsaturated and polyunsaturated fatty acids, crucial for maintaining the correct membrane saturation and redox balance. LDs act as antioxidant structures regulating the trafficking of PUFAs and preventing oxidative stress (Petan, 2023). LDs take part in ferroptosis, a programmed non-apoptotic iron-dependent cell death caused by the accumulation of ROS and lethal levels of oxidized lipids (Dixon & Stockwell,

2019). Interestingly, LDs are also a target of cancer treatment. By restricting the supply of essential lipids or promoting the accumulation of damaging lipids, a decrease in cancer cell proliferation and metastasis is achieved. Preventing cancer cells from forming LDs is also one of the strategies, as it leads to impairment of chemoresistance and immune evasion. (Petan, 2023).

For the quantification of LDs, BODIPY 493/503 staining was used. BODIPY stains neutral lipids, including triacylglycerols and sterol esters stored in LDs, as well as lysosome-derived lipofuscins. However, most of the structures stained by BODIPY colocalized with PLIN2, a marker of LDs, indicating the specificity of BODIPY staining towards LDs. Lipofuscin bodies consist of non-degradable lipids and proteins. They accumulate in postmitotic cells and positively correlate with the cell age in many different cell types (Cnop *et al.,* 2010). However, this is not the case for proliferating insulinoma cells (Skog & Korsgren, 2020). It is possible that LDs contribute to the origin of lipofuscins by delivering lipids to lysosomes through autophagy (Zechner *et al.,* 2017). However, detailed information and mechanisms are lacking.

The analysis of LD content in INS1E cells revealed increased LD storage at 25 mM glucose concentration, which can be explained by the provision of glucose-derived glycerol-3-phosphate backbone for triacylglycerols. This is also the reason why FAs alone would not increase LD accumulation, so for the analysis of LDs oleate was used in combination with glucose (Oberhauser et al., 2022). When cells are provided with the stimulating glucose concentration in combination with the exogenous unsaturated fatty acid oleate, the accumulation is promoted to prevent the toxic concentration of NEFAs. An increase in LD content in INS1E after oleate treatment was observed also by Pinnick *et al.,* 2010. The concentration of oleate used in our experiments was 15 μM, which may seem low compared to other studies (400 μM in Oberhauser *et al.,* 2022 or 500 μM in Ji *et al.,* 2019). However, several concentrations were tested observing the viability of INS1E cells, starting at 200 μM and gradually decreasing the concentration to the final 15 μM, which did not cause significant harm to the cells. The differences between used concentrations may be due to variations in protocols used for the conjugation of oleate with BSA. Factors such as time, temperature, and the ratio of FA:BSA influence the amount of bound and unbound NEFAs in the solution. It is also important to note that albumin should not be heated to 50°C or above during the FA-BSA conjugation process, as this can cause denaturation and the formation of water-insoluble aggregates. In addition, there are differences between pre-complexed and freshly conjugated solutions (Alsabeeh *et al.,* 2018). Complexed solutions of NEFA and BSA are stable and can be stored at -20°C for several years (Oliveira *et al.,* 2015). Furthermore, commercially available FA-free BSA can vary in the amount and type of contaminants present, which can affect NEFA binding (Oliveira *et al.,* 2015; Alsabeeh *et al.,* 2018). Thus, the information and results involving BSA-conjugated NEFAs must be evaluated cautiously.

For the control experiments with LD accumulation, the pan-lipase inhibitor orlistat was used. However, it is not only an inhibitor of lipases, but it also inhibits the thioesterase activity of FAS by forming a covalent adduct in the active site of the thioesterase domain (Hadváry *et al.,* 1991), so this

must be considered when interpreting results. Its primary advantage is that it is a pan-lipase inhibitor, targeting all lipases involved in the GL/NEFA cycle, which was our goal to inhibit. In this respect, orlistat outperforms atglistatin, which specifically inhibits ATGL (Mayer *et al.,* 2013), because TAGs can be also cleaved by HSL. Thus, for the design of future experiments, the best approach would be the use atglistatin in combination with an inhibitor of HSL, for example, NNC0076-0079 (morpholine-4-yl-carbamic acid 4-chlorophenyl ester) (de Jong *et al.,* 2004; Alsted *et al.,* 2009; Schweiger *et al.,* 2006). This would block both lipases capable of cleaving TAGs, while simultaneously allowing *de novo* fatty acid synthesis from glucose to proceed. However, orlistat has been widely used also in other studies for the inhibition of lipolysis (Oberhauser *et al.,* 2022; Mulder *et al.,* 2004; Zhao *et al.,* 2014; Mugabo *et al.,* 2016). The addition of orlistat resulted in a massive accumulation of LDs in INS1E cells, indicating that when the lipases are active, both arms of the GL/NEFA cycle are running. The same observations were made in the study by Oberhauser *et al.,* 2022.

Cerulenin blocks the activity of fatty acid synthase, preventing *de novo* fatty acid synthesis. Consequently, a decrease in the lipid droplet content would be expected. However, an increase in lipid droplet content was observed after cerulenin treatment, which can be attributed to the uptake of fatty acids from the medium when the *de novo* synthesis is inhibited. The cells then incorporate these fatty acids into lipid droplets for storage instead. When free fatty acids and lipid intermediates are needed, the cells mobilize them through lipolysis. Data from the experiment comparing the medium with or without FBS indicate that β-cells uptake fatty acids from the medium when fatty acid synthesis and lipolysis are blocked and in glucose-depleted conditions (starvation). Similarly in cancer cells, when inhibitors of FA synthesis are used, the cells increase the uptake of FAs from the circulation to compensate for the lack of endogenous FA synthesis (Petan, 2023). The uptake of fatty acids from the culture medium by INS1E cells should be verified in future experiments.

LD accumulation was also confirmed by the expression of LD marker PLIN2, which is the most abundant PLIN in non-adipocytes and is located on the surface of LDs (Faleck *et al.,* 2010). It promotes LD formation and prevents lipolysis and lipophagy (Trevino *et al.,* 2015). Through its downregulation, a reduction in LDs is achieved (Tong & Stein, 2021). Therefore, PLIN2 is considered as a marker of lipid droplets. Its expression increases at stimulating glucose concentration in mouse pancreatic islets. This is even more pronounced in β*Nox4*KO, which accumulated significantly more LDs. These data are in accordance with the findings by Oberhauser *et al.,* 2022, where the expression of *Plin2* increased after 3 days at 25 mM glucose, in the presence of palmitate or oleate. Upregulated *Plin2* expression was observed also in T2D patients (Ji *et al.,* 2019). These data clearly indicate the augmented lipid synthesis and their storage in LDs under glucose-stimulating conditions, which is even more pronounced in β*Nox4*KO confirming the role of ROS in these processes.

Together with the confocal microscopy analysis, which is a perfect tool for qualitative analysis, the LDs were also quantified by flow cytometry. The disadvantage of this type of analysis is that it does not reflect any qualitative parameters such as the size of LDs. In addition, the values for fluorescence

intensity are calculated as the median fluorescence intensity of BODIPY, reflecting only the median fluorescence in the sample. Therefore, the results obtained by these two methods can vary. Despite these limitations, we detected increased LD accumulation after nutritional stimulation and after inhibition of lipolysis further confirming LD accumulation in pancreatic β-cells under nutrient-rich conditions and altered redox environment.

To further evaluate the changes in lipid metabolism in pancreatic β-cells, the expression of selected genes was analysed in INS1E cells and isolated pancreatic islets upon different nutritional conditions and redox status. In mouse pancreatic islets, the effect of β*Nox4*KO resulted in an augmented glucose impact on the expression of most of the analysed genes involved in the fatty acid synthesis, their activation, lipogenesis, and lipolysis, including a marker of LDs – PLIN2. Together, these data indicate increased lipid turnover after *Nox4* silencing in β-cells. However, in INS1E there were no significant changes in the expression of the studied genes after *Nox4* silencing between the two glucose concentrations except for the expression of *Acly*, where the glucose effect was preserved. The absence of differences in the expression after the silencing of *Nox4* can be explained by the fact that glucose metabolism and *Nox4* silencing have reverse effects regarding ROS production. Overall, the expression of all quantified genes in INS1E cells was either similar or decreased after silencing compared to SCR samples at the same glucose concentration. The discrepancy between the results from INS1E cells and mouse pancreatic islets can be explained by the fact that pancreatic islets were treated with glucose for a longer period (48 hours) than INS1E (24 hours). The two compared models vary in their complexity and sensitivity. In rat insulinoma cell line INS1E, a basic set of genes involved in lipogenesis and lipolysis was analysed to test the experimental design and conditions. This model was chosen because a cell line is more stable and less sensitive to stress than primary tissue cultures. Subsequently, the entire set of selected genes was analysed in isolated mouse pancreatic islets. Isolation of the islets is a complex procedure, that causes severe mechanical, ischemic, osmotic, and oxidative stress to the islets, altering their expression profile (Kosinová *et al.,* 2016). Commonly used reference genes do not exhibit stable expression immediately after the isolation and the RNA becomes more fragmented. After 48 hours of constant cultivation conditions, the expression stabilizes, and the RNA is nearly intact (Kosinová *et al.,* 2016). Consequently, the islets were cultured with a stimulating concentration of glucose for 48 hours, as opposed to the 24 hours used for INS1E cells. Due to the differences in the characteristics of the two models, the results may vary between each other. Also, mRNA expression does not necessarily need to reflect the enzymatic activity of the analysed proteins, but at least can give us preliminary data that will be confirmed by more functional assays in the future.

As evidenced from our experimental data the expression of genes related to lipid metabolism is enhanced upon nutritional stimulation or altered redox status. Excess of glucose prompts β-cells to produce a greater amount of citrate, which exits mitochondria and is converted to acetyl-CoA by ACLY. Acetyl-CoA is then metabolised to malonyl-CoA by ACC and enters fatty acid synthesis. *De novo* synthesized fatty acids or those already present in the cell in the form of NEFA must be

activated by ACSL3 or ACSL4 to enter further metabolism. Activated fatty acids can then be oxidized in β-oxidation for energy production or enter the lipogenic arm of the GL/NEFA cycle (beginning with GPAT4) for triacylglycerol storage. The pathways of fatty acid synthesis, their activation and lipogenesis of triacylglycerols follow up each other. To prevent glucotoxicity, mitochondrial dysfunction, and to maintain glucose sensing, and subsequent insulin secretion, carbons from glucose must be rapidly diverted to various metabolic pathways (Mugabo *et al.,* 2017). Therefore, lipogenesis is augmented as demonstrated by the increased expression of *Acsl3*, *Acly* and *Fasn* at high glucose concentrations both in INS1E cells and mouse pancreatic islets. In the islets, the expression of *Acc*, *Acsl4*, and *Gpat4* was also increased. These results are consistent with Sandberg et al., 2005, who also observed increased *Acc* and *Fasn* expression in INS1E cells exposed to high glucose. RNA-seq analysis revealed an increase of *Fasn* in human islets even after 3 days of exposure to 25 mM glucose (Oberhauser *et al.,* 2022). In our experiments, the increase in *Fasn* expression was less pronounced than that of *Acly* and *Acc* probably because the created malonyl-CoA does not enter fatty acid synthesis but rather inhibits CPT1 to prevent β-oxidation. To what extent and in which conditions *de novo* fatty acid synthesis is important for β-cells is not very well explored. However, our experiments showed that the inhibition of FAS by cerulenin resulted in the uptake of fatty acids by the INS1E cells from the culture medium, pointing out the importance of NEFAs at their physiological concentrations. It can be assumed that fatty acid synthesis is important for preventing glucotoxicity when the created or uptaken NEFAs can be incorporated into LDs or released from the cell. Another evidence of augmented lipogenesis is increased expression of *Gpat4*; however, according to Oberhauser *et al.,* 2022, the expression of *Gpat4* in INS1E cells is decreased at high glucose after 3 days of treatment. This might be because the cells already have accumulated a high number of LDs, and the increased lipogenesis is no longer favoured. Instead of LD storage, glucose can be metabolized through other pathways, such as conversion to G3P and its dephosphorylation to glycerol, which can be released out of the cell. Overall, the obtained data indicate augmented anaplerotic pathways to fatty acid synthesis, their activation and lipogenesis. When β-cells are exposed to high glucose concentrations, lipogenesis, and detoxification pathways (NEFA and glycerol release) increase to maintain the flux of glucose for its sensing, thus ensuring the maintenance of their major function (Mugabo *et al.,* 2017).

Lipolysis, the hydrolysis of triacylglycerols, produces NEFAs and MCFs for insulin secretion. The demand for these products increases during fasting, when NEFAs are used for energy production in mitochondrial β-oxidation. Due to FA depletion during fasting insulin secretion is impaired (Dobbins *et al.,* 1998). Lipolysis is activated by PKA phosphorylating HSL and PLIN5, which interact with ATGL and its co-activator CGI-58 (Sztalryd *et al.,* 2003; Trevino *et al.,* 2015). ATGL is partly redundant with HSL, which is capable of cleaving both TAG and DAG (Zimmermann *et al.,* 2004). Moreover, HSL can hydrolyse sterol esters stored in LDs (Wei *et al.,* 1997). Therefore, the expression of the *Lipe* gene coding HSL was evaluated. In INS1E cells, the expression of *Lipe* decreases at 25 mM glucose compared to 3 mM glucose, consistent with the increased need for NEFA mobilization

from triacylglycerols during fasting. A similar decrease in *Lipe* expression was observed after 3 days of high glucose in the study by Oberhauser *et al.,* 2022. In mouse pancreatic islets, there was an increase in the expression of *Lipe* after the exposure to high glucose concentration and even more significant in β*Nox4*KO suggesting that both arms of the GL/NEFA cycle are enhanced. The islets accumulate lipids and at the same time, part of them is hydrolysed. According to Oberhauser *et al.,* 2022, lipogenesis and lipolysis turnover in islets are enhanced in animals with obesity and insulin resistance and it becomes impaired in T2D (Prentki & Madiraju, 2012). This is in agreement with our data from β*Nox4*KO animals, which exhibit pre-diabetic phenotype with insulin resistance and enhanced fat accumulation (Holendová *et al.,* 2024; Plecitá-Hlavatá *et al.,* 2020).

Similar to *Lipe,* the expression of *Plin5* also decreases at stimulating glucose concentration in mouse pancreatic islets. *Plin5* is highly expressed in tissues that utilize FA as fuel, such as the heart, type I skeletal muscle, or brown adipose tissue. It facilitates FA transfer from LDs to mitochondria for β-oxidation (Bosma *et al.,* 2012). Overnight incubation with FA or a high-fat diet does not elevate *Plin5* expression (Trevino *et al.,* 2015). However, fasting promotes its expression, enhancing LD formation, and significantly increasing TAGs in fasted versus fed islets. After refeeding the expression of *Plin5* is slowly reduced (Trevino *et al.,* 2015). PLIN5 regulates both LD storage and the hydrolysis of TAGs probably depending on its phosphorylation state. In β-cells, whether lipolysis or lipid storage is performed during fasting probably depends on the nutritional state that preceded it. Pre-existing LDs can be hydrolysed; however, in the absence of such a depot, lipogenesis will be favoured. Cancer cells use neighbouring adipocytes to release FAs into circulation through lipolysis. These fatty acids can then be uptaken by cancer cells to form LDs (Nieman *et al.,* 2011). Similarly, at the organismal level, NEFAs are hydrolysed from adipocytes during fasting or physical activity, and they can provide energy for non-adipose tissues (Haemmerle *et al.,* 2011). This can apply also to fasted pancreatic islets, which increase the uptake of fatty acids and accumulate LDs (Trevino *et al.,* 2015) as confirmed by our experiment with serum-depleted medium lacking FAs for uptake.

When β-cells are chronically exposed to excess nutrients, they accumulate LDs significantly. However, their capacity to store excess fuel is limited (Mugabo *et al.,* 2017), so to prevent nutritional stress and to maintain the flux of glucose for sensing, β-cells release glycerol, a mechanism known as glucolipodetoxification (Mugabo *et al.,* 2017). This release is enabled by the negligible expression of glycerol kinase in β-cells (Noel *et al.,* 1997). Consequently, glycerol generated from lipolysis of TAGs is not phosphorylated and cannot re-enter lipogenesis or other metabolic pathways. As a dead-end product, it exits the cell through aquaglyceroporin 7 (Matsumura *et al.,* 2007). The second source of free glycerol is G3PP, which dephosphorylates G3P. Glycerol release increases linearly at 4 mM, 10 mM, 16 mM, and 25 mM in isolated rat islets (Mugabo *et al.,* 2017). In our experiment at 3 mM glucose, a very low amount of glycerol was released from INS1E cells, which was hardly detectable. However, the amount of released glycerol at 25 mM glucose dramatically increased and was similar to that in the condition of 25 mM glucose in combination with oleate. The data from glycerol release were

conducted in a biological duplicate as they are preliminary. More replicates would be appropriate and will be done in the future using INS1E cells and isolated mouse pancreatic islets. Overall, these data indicate an increased need for a detoxification pathway to divert the carbons from glucose to maintain glucose sensing. After exposure to oleate, glycerol release does not change compared to high glucose because the oleate is probably used for the synthesis of triacylglycerol stored in LDs. *Nox4* silencing increased glycerol release both at high glucose and after the addition of oleate consistent with the increased accumulation of LDs after *Nox4* silencing, which together suggests augmented lipid metabolism (lipid storage and lipolysis).

NEFAs are crucial for β-cell function, influencing energy metabolism and insulin secretion. The majority of NEFAs are long-chained with more than 12 carbons, predominantly 16 (Henderson, 2021). NEFAs are essential for efficient GSIS. When circulating NEFAs were reduced in fasted rats, GSIS was significantly abolished (Stein *et al.,* 1996). However, high concentrations of NEFA can be toxic to cells (Kassan *et al.,* 2013) causing ER stress and ceramide formation, which may result in β-cell death (Oberhauser & Maechler, 2021). To avoid this toxicity, NEFAs are incorporated into lipids, as evidenced by an increase in the number and size of LDs at 25 mM glucose and 25 mM glucose with oleate. Elevated plasma NEFA concentration relates to obesity, insulin resistance and T2D (Henderson, 2021).

Thus, NEFAs in the form of unesterified anions were measured in INS1E cells. The measured NEFA content was approximately 10-13 nmol/mg of protein, consistent with data from isolated rat islets in the study by Mugabo *et al.,* 2017 (about 13 nmol/mg of protein at 25 mM glucose). The NEFA content did not reach higher values, as higher concentrations are probably toxic. This could indicate that β-cells preferentially store them in LDs or release them out of the cells as part of the detoxification mechanism.

It is without any discussion that glucose and lipid metabolism together with redox signalling play an inevitable role in β-cell physiology. The experiments published as part of this diploma thesis represent just the tip of the iceberg of a very complex story, and numerous questions need to be answered before we will be able to shed more light on this topic. In the future among others, I plan to conduct an experiment using a comparative ^{13}C glucose and glutamine tracing to map the ^{13}C incorporation into metabolites. This will help unravel the fate of carbons derived from glucose and run functional assays evaluating the activity of the enzymes of lipid metabolism under different nutritional conditions, mimicking physiological and pathological states. This approach should uncover a wealth of previously unknown information. Another experiment will be an analysis of LDs by flow cytometry in INS1E cells treated with the medium containing lipid-depleted serum to prevent the uptake of fatty acids from the medium to understand the FAs handling by β-cells under changing nutritional conditions. Hopefully, these experiments will provide us with more information and will contribute to a better understanding of the lipid metabolism in β-cells.

7. Conclusions

- In pancreatic β-cells, glucose metabolism is tightly connected with the metabolism of lipids. Exposure of INS1E-cells and mouse pancreatic islets to stimulating glucose concentration leads to an increase in the expression of genes involved in fatty acid synthesis, their activation and lipogenesis to maintain glucose sensing and prevent glucotoxicity. The effect of glucose is augmented in β*Nox4*KO mouse pancreatic islets suggesting dysregulated lipid metabolism consistent with ectopic fat accumulation and enhanced GL/NEFA cycle in β*Nox4*KO mice (Holendová *et al.*, 2024). However, the mechanism of how the NOX4-mediated redox signalling affects lipid metabolism remains unknown.

- INS1E cells accumulate lipid droplets at the stimulating glucose concentration both after acute and chronic exposure. The accumulation is significantly increased in the presence of oleate to prevent toxic concentrations of NEFAs. After the inhibition of lipolysis, the lipid droplet content probably reaches the maximal storage capacity. This was more pronounced in si*Nox4* INS1E cells, indicating a dysregulated lipid metabolism. After the inhibition of *de novo* fatty acid synthesis in INS1E cells, surprisingly instead of the expected decrease in lipid droplet content, more lipid droplets are accumulated because of the enhanced fatty acid uptake from the culture medium. The uptake of fatty acids from the medium was observed also during starvation and when the lipolysis was inhibited.

- Excessive glucose causes an increase in glycerol release as a detoxification pathway as well as increased NEFA content. However, the concentration of NEFAs remains at physiological concentration even after the addition of oleate, which is incorporated into LDs, preventing cytotoxic ceramide formation.

8. References

Ahlgren, U., Jonsson, J., Jonsson, L., Simu, K., & Edlund, H. (1998). beta-cell-specific inactivation of the mouse Ipf1/Pdx1 gene results in loss of the beta-cell phenotype and maturity onset diabetes. *Genes & development*, *12*(12), 1763–1768. https://doi.org/10.1101/gad.12.12.1763

Ahmed Alfar, E., Kirova, D., Konantz, J., Birke, S., Mansfeld, J., & Ninov, N. (2017). Distinct Levels of Reactive Oxygen Species Coordinate Metabolic Activity with Beta-cell Mass Plasticity. *Scientific reports*, *7*(1), 3994. https://doi.org/10.1038/s41598-017-03873-9

Al-Mass, A., Poursharifi, P., Peyot, M. L., Lussier, R., Levens, E. J., Guida, J., Mugabo, Y., Possik, E., Ahmad, R., Al-Mulla, F., Sladek, R., Madiraju, S. R. M., & Prentki, M. (2022). Glycerol-3-phosphate phosphatase operates a glycerol shunt in pancreatic β-cells that controls insulin secretion and metabolic stress. *Molecular metabolism*, *60*, 101471. https://doi.org/10.1016/j.molmet.2022.101471

* Alsabeeh, N., Chausse, B., Kakimoto, P. A., Kowaltowski, A. J., & Shirihai, O. (2018). Cell culture models of fatty acid overload: Problems and solutions. *Biochimica et biophysica acta. Molecular and cell biology of lipids*, *1863*(2), 143–151. https://doi.org/10.1016/j.bbalip.2017.11.006

Alsted, T. J., Nybo, L., Schweiger, M., Fledelius, C., Jacobsen, P., Zimmermann, R., Zechner, R., & Kiens, B. (2009). Adipose triglyceride lipase in human skeletal muscle is upregulated by exercise training. *American journal of physiology. Endocrinology and metabolism*, *296*(3), E445–E453. https://doi.org/10.1152/ajpendo.90912.2008

Ansari, I. H., Longacre, M. J., Stoker, S. W., Kendrick, M. A., O'Neill, L. M., Zitur, L. J., Fernandez, L. A., Ntambi, J. M., & MacDonald, M. J. (2017). Characterization of Acyl-CoA synthetase isoforms in pancreatic beta cells: Gene silencing shows participation of ACSL3 and ACSL4 in insulin secretion. *Archives of biochemistry and biophysics*, *618*, 32–43. https://doi.org/10.1016/j.abb.2017.02.001

Asfari, M., Janjic, D., Meda, P., Li, G., Halban, P. A., & Wollheim, C. B. (1992). Establishment of 2-mercaptoethanol-dependent differentiated insulin-secreting cell lines. *Endocrinology*, *130*(1), 167–178. https://doi.org/10.1210/endo.130.1.1370150

* Ashcroft, F. M., Rohm, M., Clark, A., & Brereton, M. F. (2017). Is Type 2 Diabetes a Glycogen Storage Disease of Pancreatic β Cells?. *Cell metabolism*, *26*(1), 17–23. https://doi.org/10.1016/j.cmet.2017.05.014

Attané, C., Peyot, M. L., Lussier, R., Poursharifi, P., Zhao, S., Zhang, D., Morin, J., Pineda, M., Wang, S., Dumortier, O., Ruderman, N. B., Mitchell, G. A., Simons, B., Madiraju, S. R., Joly, E., & Prentki, M. (2016). A beta cell ATGL-lipolysis/adipose tissue axis controls energy homeostasis and body weight via insulin secretion in mice. *Diabetologia*, *59*(12), 2654–2663. https://doi.org/10.1007/s00125-016-4105-2

Barsby, T., & Otonkoski, T. (2022). Maturation of beta cells: lessons from in vivo and in vitro models. *Diabetologia*, *65*(6), 917–930. https://doi.org/10.1007/s00125-022-05672-y

Bartholomew, S. R., Bell, E. H., Summerfield, T., Newman, L. C., Miller, E. L., Patterson, B., Niday, Z. P., Ackerman, W. E., 4th, & Tansey, J. T. (2012). Distinct cellular pools of perilipin 5 point to roles in lipid trafficking. *Biochimica et biophysica acta*, *1821*(2), 268–278. https://doi.org/10.1016/j.bbalip.2011.10.017

Bartz, R., Zehmer, J. K., Zhu, M., Chen, Y., Serrero, G., Zhao, Y., & Liu, P. (2007). Dynamic activity of lipid droplets: protein phosphorylation and GTP-mediated protein translocation. *Journal of proteome research*, *6*(8), 3256–3265. https://doi.org/10.1021/pr070158j

* Berger, C., & Zdzieblo, D. (2020). Glucose transporters in pancreatic islets. *Pflugers Archiv : European journal of physiology*, *472*(9), 1249–1272. https://doi.org/10.1007/s00424-020-02383-4

Best, L., Brown, P. D., Yates, A. P., Perret, J., Virreira, M., Beauwens, R., Malaisse, W. J., Sener, A., & Delporte, C. (2009). Contrasting effects of glycerol and urea transport on rat pancreatic beta-cell function. *Cellular physiology and biochemistry : international journal of experimental cellular physiology, biochemistry, and pharmacology*, *23*(4-6), 255–264. https://doi.org/10.1159/000218172

* Bienert, G. P., Schjoerring, J. K., & Jahn, T. P. (2006). Membrane transport of hydrogen peroxide. *Biochimica et biophysica acta*, *1758*(8), 994–1003. https://doi.org/10.1016/j.bbamem.2006.02.015

Blankman, J. L., Simon, G. M., & Cravatt, B. F. (2007). A comprehensive profile of brain enzymes that hydrolyze the endocannabinoid 2-arachidonoylglycerol. *Chemistry & biology*, *14*(12), 1347–1356. https://doi.org/10.1016/j.chembiol.2007.11.006

Bliss, C. R., & Sharp, G. W. (1992). Glucose-induced insulin release in islets of young rats: time-dependent potentiation and effects of 2-bromostearate. *The American journal of physiology*, *263*(5 Pt 1), E890–E896. https://doi-org.d360prx.biomed.cas.cz/10.1152/ajpendo.1992.263.5.E890

* Bonner-Weir, S., Aguayo-Mazzucato, C., & Weir, G. C. (2016). Dynamic development of the pancreas from birth to adulthood. *Upsala journal of medical sciences*, *121*(2), 155–158. https://doi.org/10.3109/03009734.2016.1154906

Borgström B. (1988). Mode of action of tetrahydrolipstatin: a derivative of the naturally occurring lipase inhibitor lipstatin. *Biochimica et biophysica acta*, *962*(3), 308–316. https://doi.org/10.1016/0005-2760(88)90260-3

Bosma, M., Minnaard, R., Sparks, L. M., Schaart, G., Losen, M., de Baets, M. H., Duimel, H., Kersten, S., Bickel, P. E., Schrauwen, P., & Hesselink, M. K. (2012). The lipid droplet coat protein perilipin 5 also localizes to muscle mitochondria. *Histochemistry and cell biology*, *137*(2), 205–216. https://doi.org/10.1007/s00418-011-0888-x

Briscoe, C. P., Tadayyon, M., Andrews, J. L., Benson, W. G., Chambers, J. K., Eilert, M. M., Ellis, C., Elshourbagy, N. A., Goetz, A. S., Minnick, D. T., Murdock, P. R., Sauls, H. R., Jr, Shabon, U., Spinage, L. D., Strum, J. C., Szekeres, P. G., Tan, K. B., Way, J. M., Ignar, D. M., Wilson, S., … Muir, A. I. (2003). The orphan G protein-coupled receptor GPR40 is activated by medium and long chain fatty acids. *The Journal of biological chemistry*, *278*(13), 11303–11311. https://doi.org/10.1074/jbc.M211495200

Brun, T., Assimacopoulos-Jeannet, F., Corkey, B. E., & Prentki, M. (1997). Long-chain fatty acids inhibit acetyl-CoA carboxylase gene expression in the pancreatic beta-cell line INS-1. *Diabetes*, *46*(3), 393–400. https://doi.org/10.2337/diab.46.3.393

Brun, T., Roche, E., Assimacopoulos-Jeannet, F., Corkey, B. E., Kim, K. H., & Prentki, M. (1996). Evidence for an anaplerotic/malonyl-CoA pathway in pancreatic beta-cell nutrient signaling. *Diabetes*, *45*(2), 190–198. https://doi.org/10.2337/diab.45.2.190

Busch, A. K., Cordery, D., Denyer, G. S., & Biden, T. J. (2002). Expression profiling of palmitate- and oleate-regulated genes provides novel insights into the effects of chronic lipid exposure on pancreatic beta-cell function. *Diabetes*, *51*(4), 977–987. https://doi.org/10.2337/diabetes.51.4.977

Cantley, J., Davenport, A., Vetterli, L., Nemes, N. J., Whitworth, P. T., Boslem, E., Thai, L. M., Mellett, N., Meikle, P. J., Hoehn, K. L., James, D. E., & Biden, T. J. (2019). Disruption of beta cell acetyl-CoA carboxylase-1 in mice impairs insulin secretion and beta cell mass. *Diabetologia*, *62*(1), 99–111. https://doi.org/10.1007/s00125-018-4743-7

Chen, J. S., Greenberg, A. S., & Wang, S. M. (2002). Oleic acid-induced PKC isozyme translocation in RAW 264.7 macrophages. *Journal of cellular biochemistry*, *86*(4), 784–791. https://doi.org/10.1002/jcb.10266

Chen, S., Ogawa, A., Ohneda, M., Unger, R. H., Foster, D. W., & McGarry, J. D. (1994). More direct evidence for a malonyl-CoA-carnitine palmitoyltransferase I interaction as a key event in pancreatic beta-cell signaling. *Diabetes*, *43*(7), 878–883. https://doi.org/10.2337/diab.43.7.878

Cinti, F., Bouchi, R., Kim-Muller, J. Y., Ohmura, Y., Sandoval, P. R., Masini, M., Marselli, L., Suleiman, M., Ratner, L. E., Marchetti, P., & Accili, D. (2016). Evidence of β-Cell Dedifferentiation in Human Type 2 Diabetes. *The Journal of clinical endocrinology and metabolism*, *101*(3), 1044–1054. https://doi.org/10.1210/jc.2015-2860

Cnop, M., Hughes, S. J., Igoillo-Esteve, M., Hoppa, M. B., Sayyed, F., van de Laar, L., Gunter, J. H., de Koning, E. J., Walls, G. V., Gray, D. W., Johnson, P. R., Hansen, B. C., Morris, J. F., Pipeleers-Marichal, M., Cnop, I., & Clark, A. (2010). The long lifespan and low turnover of human islet beta cells estimated by mathematical modelling of lipofuscin accumulation. *Diabetologia*, *53*(2), 321–330. https://doi.org/10.1007/s00125-009-1562-x

* Dixon, S. J., & Stockwell, B. R. (2019). The hallmarks of ferroptosis. *Annual Review of Cancer Biology*, *3*, 35-54.

Dobbins, R. L., Chester, M. W., Daniels, M. B., McGarry, J. D., & Stein, D. T. (1998). Circulating fatty acids are essential for efficient glucose-stimulated insulin secretion after prolonged fasting in humans. *Diabetes*, *47*(10), 1613–1618. https://doi.org/10.2337/diabetes.47.10.1613

* Dolenšek, J., Rupnik, M. S., & Stožer, A. (2015). Structural similarities and differences between the human and the mouse pancreas. *Islets*, *7*(1), e1024405.

de Jong, J. C., Sørensen, L. G., Tornqvist, H., & Jacobsen, P. (2004). Carbazates as potent inhibitors of hormone-sensitive lipase. *Bioorganic & medicinal chemistry letters*, *14*(7), 1741–1744. https://doi.org/10.1016/j.bmcl.2004.01.038https://doi.org/10.1080/19382014.2015.1024405

Dor, Y., Brown, J., Martinez, O. I., & Melton, D. A. (2004). Adult pancreatic beta-cells are formed by self-duplication rather than stem-cell differentiation. *Nature*, *429*(6987), 41–46. https://doi.org/10.1038/nature02520

 * Efrat S. (1997). Making sense of glucose sensing. *Nature genetics*, *17*(3), 249–250. https://doi.org/10.1038/ng1197-249

Eichmann, T. O., Kumari, M., Haas, J. T., Farese, R. V., Jr, Zimmermann, R., Lass, A., & Zechner, R. (2012). Studies on the substrate and stereo/regioselectivity of adipose triglyceride lipase, hormone-sensitive lipase, and diacylglycerol-O-acyltransferases. *The Journal of biological chemistry*, *287*(49), 41446–41457. https://doi.org/10.1074/jbc.M112.400416

Eitel, K., Staiger, H., Rieger, J., Mischak, H., Brandhorst, H., Brendel, M. D., Bretzel, R. G., Häring, H. U., & Kellerer, M. (2003). Protein kinase C delta activation and translocation to the nucleus are required for fatty acid-induced apoptosis of insulin-secreting cells. *Diabetes*, *52*(4), 991–997. https://doi.org/10.2337/diabetes.52.4.991

Eizirik, D. L., Pipeleers, D. G., Ling, Z., Welsh, N., Hellerström, C., & Andersson, A. (1994). Major species differences between humans and rodents in the susceptibility to pancreatic beta-cell injury. *Proceedings of the National Academy of Sciences of the United States of America*, *91*(20), 9253–9256. https://doi.org/10.1073/pnas.91.20.9253

El Azzouny, M., Longacre, M. J., Ansari, I. H., Kennedy, R. T., Burant, C. F., & MacDonald, M. J. (2016). Knockdown of ATP citrate lyase in pancreatic beta cells does not inhibit insulin secretion or glucose flux and implicates the acetoacetate pathway in insulin secretion. *Molecular metabolism*, *5*(10), 980–987. https://doi.org/10.1016/j.molmet.2016.07.011

El-Assaad, W., Buteau, J., Peyot, M. L., Nolan, C., Roduit, R., Hardy, S., Joly, E., Dbaibo, G., Rosenberg, L., & Prentki, M. (2003). Saturated fatty acids synergize with elevated glucose to cause pancreatic beta-cell death. *Endocrinology*, *144*(9), 4154–4163. https://doi.org/10.1210/en.2003-0410

El-Gohary, Y., Wiersch, J., Tulachan, S., Xiao, X., Guo, P., Rymer, C., Fischbach, S., Prasadan, K., Shiota, C., Gaffar, I., Song, Z., Galambos, C., Esni, F., & Gittes, G. K. (2016). Intraislet Pancreatic Ducts Can Give Rise to Insulin-Positive Cells. *Endocrinology*, *157*(1), 166–175. https://doi.org/10.1210/en.2015-1175

Elsner, M., Gehrmann, W., & Lenzen, S. (2011). Peroxisome-generated hydrogen peroxide as important mediator of lipotoxicity in insulin-producing cells. *Diabetes*, *60*(1), 200–208. https://doi.org/10.2337/db09-1401

Faleck, D. M., Ali, K., Roat, R., Graham, M. J., Crooke, R. M., Battisti, R., Garcia, E., Ahima, R. S., & Imai, Y. (2010). Adipose differentiation-related protein regulates lipids and insulin in pancreatic islets. *American journal of physiology. Endocrinology and metabolism*, *299*(2), E249–E257. https://doi.org/10.1152/ajpendo.00646.2009

Farfari, S., Schulz, V., Corkey, B., & Prentki, M. (2000). Glucose-regulated anaplerosis and cataplerosis in pancreatic beta-cells: possible implication of a pyruvate/citrate shuttle in insulin secretion. *Diabetes*, *49*(5), 718–726. https://doi.org/10.2337/diabetes.49.5.718

Ferreira, G. C., & McKenna, M. C. (2017). L-Carnitine and Acetyl-L-carnitine Roles and Neuroprotection in Developing Brain. *Neurochemical research*, *42*(6), 1661–1675. https://doi.org/10.1007/s11064-017-2288-7

Ferreri, C., & Chatgilialoglu, C. (2009). Membrane lipidomics and the geometry of unsaturated fatty acids from biomimetic models to biological consequences. *Methods in molecular biology (Clifton, N.J.)*, *579*, 391–411. https://doi.org/10.1007/978-1-60761-322-0_20

Flamez, D., Berger, V., Kruhøffer, M., Orntoft, T., Pipeleers, D., & Schuit, F. C. (2002). Critical role for cataplerosis via citrate in glucose-regulated insulin release. *Diabetes*, *51*(7), 2018–2024. https://doi-org.d360prx.biomed.cas.cz/10.2337/diabetes.51.7.2018

Fu, J., Cui, Q., Yang, B., Hou, Y., Wang, H., Xu, Y., Wang, D., Zhang, Q., & Pi, J. (2017). The impairment of glucose-stimulated insulin secretion in pancreatic β-cells caused by prolonged glucotoxicity and lipotoxicity is associated with elevated adaptive antioxidant response. *Food and chemical toxicology : an international journal published for the British Industrial Biological Research Association*, *100*, 161–167. https://doi.org/10.1016/j.fct.2016.12.016

* Gehrmann, W., Elsner, M., & Lenzen, S. (2010). Role of metabolically generated reactive oxygen species for lipotoxicity in pancreatic β-cells. *Diabetes, obesity & metabolism*, *12 Suppl 2*, 149–158. https://doi.org/10.1111/j.1463-1326.2010.01265.x

Gheni, G., Ogura, M., Iwasaki, M., Yokoi, N., Minami, K., Nakayama, Y., Harada, K., Hastoy, B., Wu, X., Takahashi, H., Kimura, K., Matsubara, T., Hoshikawa, R., Hatano, N., Sugawara, K., Shibasaki, T., Inagaki, N., Bamba, T., Mizoguchi, A., Fukusaki, E., … Seino, S. (2014). Glutamate acts as a key signal linking glucose metabolism to incretin/cAMP action to amplify insulin secretion. *Cell reports*, *9*(2), 661–673. https://doi.org/10.1016/j.celrep.2014.09.030

* Gluchowski, N. L., Becuwe, M., Walther, T. C., & Farese, R. V., Jr (2017). Lipid droplets and liver disease: from basic biology to clinical implications. *Nature reviews. Gastroenterology & hepatology*, *14*(6), 343–355. https://doi.org/10.1038/nrgastro.2017.32

Gorovits, N., & Charron, M. J. (2003). What we know about facilitative glucose transporters: Lessons from cultured cells, animal models, and human studies. *Biochemistry and Molecular Biology Education*, *31*(3), 163-172.

Guay, C., Madiraju, S. R., Aumais, A., Joly, E., & Prentki, M. (2007). A role for ATP-citrate lyase, malic enzyme, and pyruvate/citrate cycling in glucose-induced insulin secretion. *The Journal of biological chemistry*, *282*(49), 35657–35665. https://doi-org.d360prx.biomed.cas.cz/10.1074/jbc.M707294200

Hadváry, P., Sidler, W., Meister, W., Vetter, W., & Wolfer, H. (1991). The lipase inhibitor tetrahydrolipstatin binds covalently to the putative active site serine of pancreatic lipase. *The Journal of biological chemistry*, *266*(4), 2021–2027.

Haeiwa, H., Fujita, T., Saitoh, Y., & Miwa, N. (2014). Oleic acid promotes adaptability against oxidative stress in 3T3-L1 cells through lipohormesis. *Molecular and cellular biochemistry*, *386*(1-2), 73–83. https://doi-org.d360prx.biomed.cas.cz/10.1007/s11010-013-1846-9

Haemmerle, G., Moustafa, T., Woelkart, G., Büttner, S., Schmidt, A., van de Weijer, T., Hesselink, M., Jaeger, D., Kienesberger, P. C., Zierler, K., Schreiber, R., Eichmann, T., Kolb, D., Kotzbeck, P., Schweiger, M., Kumari, M., Eder, S., Schoiswohl, G., Wongsiriroj, N., Pollak, N. M., … Zechner, R. (2011). ATGL-mediated fat catabolism regulates cardiac mitochondrial function via PPAR-α and PGC-1. *Nature medicine*, *17*(9), 1076–1085. https://doi.org/10.1038/nm.2439

Hasan, N. M., Longacre, M. J., Seed Ahmed, M., Kendrick, M. A., Gu, H., Ostenson, C. G., Fukao, T., & MacDonald, M. J. (2010). Lower succinyl-CoA:3-ketoacid-CoA transferase (SCOT) and ATP citrate lyase in pancreatic islets of a rat model of type 2 diabetes: knockdown of SCOT inhibits insulin release in rat insulinoma cells. *Archives of biochemistry and biophysics*, *499*(1-2), 62–68. https://doi.org/10.1016/j.abb.2010.05.007

Helman, A., Cangelosi, A. L., Davis, J. C., Pham, Q., Rothman, A., Faust, A. L., Straubhaar, J. R., Sabatini, D. M., & Melton, D. A. (2020). A Nutrient-Sensing Transition at Birth Triggers Glucose-Responsive Insulin Secretion. *Cell metabolism*, *31*(5), 1004–1016.e5. https://doi.org/10.1016/j.cmet.2020.04.004

* Henderson G. C. (2021). Plasma Free Fatty Acid Concentration as a Modifiable Risk Factor for Metabolic Disease. *Nutrients*, *13*(8), 2590. https://doi.org/10.3390/nu13082590

* Henquin J. C. (2000). Triggering and amplifying pathways of regulation of insulin secretion by glucose. *Diabetes*, *49*(11), 1751–1760. https://doi.org/10.2337/diabetes.49.11.1751

Henquin, J. C., Dufrane, D., & Nenquin, M. (2006). Nutrient control of insulin secretion in isolated normal human islets. *Diabetes*, *55*(12), 3470–3477. https://doi.org/10.2337/db06-0868

Hirasawa, A., Tsumaya, K., Awaji, T., Katsuma, S., Adachi, T., Yamada, M., Sugimoto, Y., Miyazaki, S., & Tsujimoto, G. (2005). Free fatty acids regulate gut incretin glucagon-like peptide-1 secretion through GPR120. *Nature medicine*, *11*(1), 90–94. https://doi.org/10.1038/nm1168

Holendova, B., & Plecita-Hlavata, L. (2023). Cysteine residues in signal transduction and its relevance in pancreatic beta cells. *Frontiers in endocrinology*, *14*, 1221520. https://doi.org/10.3389/fendo.2023.1221520

Holendová, B., Benáková, Š., Křivonosková, M., Pavluch, V., Tauber, J., Gabrielová, E., Ježek, P., & Plecitá-Hlavatá, L. (2024). NADPH oxidase 4 in mouse β cells participates in inflammation on chronic nutrient overload. *Obesity (Silver Spring, Md.)*, *32*(2), 339–351. https://doi.org/10.1002/oby.23956

Igoillo-Esteve, M., Marselli, L., Cunha, D. A., Ladrière, L., Ortis, F., Grieco, F. A., Dotta, F., Weir, G. C., Marchetti, P., Eizirik, D. L., & Cnop, M. (2010). Palmitate induces a pro-inflammatory response in human pancreatic islets that mimics CCL2 expression by beta cells in type 2 diabetes. *Diabetologia*, *53*(7), 1395–1405. https://doi.org/10.1007/s00125-010-1707-y

* Imai, Y., Cousins, R. S., Liu, S., Phelps, B. M., & Promes, J. A. (2020). Connecting pancreatic islet lipid metabolism with insulin secretion and the development of type 2 diabetes. *Annals of the New York Academy of Sciences*, *1461*(1), 53–72. https://doi.org/10.1111/nyas.14037

Itoh, Y., Kawamata, Y., Harada, M., Kobayashi, M., Fujii, R., Fukusumi, S., Ogi, K., Hosoya, M., Tanaka, Y., Uejima, H., Tanaka, H., Maruyama, M., Satoh, R., Okubo, S., Kizawa, H., Komatsu, H., Matsumura, F., Noguchi, Y., Shinohara, T., Hinuma, S., … Fujino, M. (2003). Free fatty acids regulate insulin secretion from pancreatic beta cells through GPR40. *Nature*, *422*(6928), 173–176. https://doi.org/10.1038/nature01478

Jacqueminet, S., Briaud, I., Rouault, C., Reach, G., & Poitout, V. (2000). Inhibition of insulin gene expression by long-term exposure of pancreatic beta cells to palmitate is dependent on the presence of a stimulatory glucose concentration. *Metabolism: clinical and experimental*, *49*(4), 532–536. https://doi-org.d360prx.biomed.cas.cz/10.1016/s0026-0495(00)80021-9

Ji, J., Petropavlovskaia, M., Khatchadourian, A., Patapas, J., Makhlin, J., Rosenberg, L., & Maysinger, D. (2019). Type 2 diabetes is associated with suppression of autophagy and lipid accumulation in β-cells. *Journal of cellular and molecular medicine*, *23*(4), 2890–2900. https://doi.org/10.1111/jcmm.14172

Kassan, A., Herms, A., Fernández-Vidal, A., Bosch, M., Schieber, N. L., Reddy, B. J., Fajardo, A., Gelabert-Baldrich, M., Tebar, F., Enrich, C., Gross, S. P., Parton, R. G., & Pol, A. (2013). Acyl-CoA synthetase 3 promotes lipid droplet biogenesis in ER microdomains. *The Journal of cell biology*, *203*(6), 985–1001. https://doi.org/10.1083/jcb.201305142

Khan, A., Ling, Z. C., & Landau, B. R. (1996). Quantifying the carboxylation of pyruvate in pancreatic islets. *The Journal of biological chemistry*, *271*(5), 2539–2542. https://doi.org/10.1074/jbc.271.5.2539

* Koh, A., De Vadder, F., Kovatcheva-Datchary, P., & Bäckhed, F. (2016). From Dietary Fiber to Host Physiology: Short-Chain Fatty Acids as Key Bacterial Metabolites. *Cell*, *165*(6), 1332–1345. https://doi.org/10.1016/j.cell.2016.05.041

Kosinová, L., Cahová, M., Fábryová, E., Týcová, I., Koblas, T., Leontovyč, I., Saudek, F., & Kříž, J. (2016). Unstable Expression of Commonly Used Reference Genes in Rat Pancreatic Islets Early after Isolation Affects Results of Gene Expression Studies. *PloS one*, *11*(4), e0152664. https://doi.org/10.1371/journal.pone.0152664

Kridel, S. J., Axelrod, F., Rozenkrantz, N., & Smith, J. W. (2004). Orlistat is a novel inhibitor of fatty acid synthase with antitumor activity. *Cancer research*, *64*(6), 2070–2075. https://doi.org/10.1158/0008-5472.can-03-3645

Kurohane Kaneko, Y., Kobayashi, Y., Motoki, K., Nakata, K., Miyagawa, S., Yamamoto, M., Hayashi, D., Shirai, Y., Sakane, F., & Ishikawa, T. (2013). Depression of type I diacylglycerol kinases in pancreatic β-cells from male mice results in impaired insulin secretion. *Endocrinology*, *154*(11), 4089–4098. https://doi.org/10.1210/en.2013-1356

* Labar, G., Wouters, J., & Lambert, D. M. (2010). A review on the monoacylglycerol lipase: at the interface between fat and endocannabinoid signalling. *Current medicinal chemistry*, *17*(24), 2588–2607. https://doi.org/10.2174/092986710791859414

Lee, Y. K., Sohn, J. H., Han, J. S., Park, Y. J., Jeon, Y. G., Ji, Y., Dalen, K. T., Sztalryd, C., Kimmel, A. R., & Kim, J. B. (2018). *Perilipin 3* Deficiency Stimulates Thermogenic Beige Adipocytes Through *PPARα* Activation. *Diabetes*, *67*(5), 791–804. https://doi.org/10.2337/db17-0983

* Lenzen S. (2017). Chemistry and biology of reactive species with special reference to the antioxidative defence status in pancreatic β-cells. *Biochimica et biophysica acta. General subjects*, *1861*(8), 1929–1942. https://doi.org/10.1016/j.bbagen.2017.05.013

Lenzen, S., Drinkgern, J., & Tiedge, M. (1996). Low antioxidant enzyme gene expression in pancreatic islets compared with various other mouse tissues. *Free radical biology & medicine*, *20*(3), 463–466. https://doi-org.d360prx.biomed.cas.cz/10.1016/0891-5849(96)02051-5

* Levetan, C. S., & Pierce, S. M. (2013). Distinctions between the islets of mice and men: implications for new therapies for type 1 and 2 diabetes. *Endocrine practice : official journal of the American College of Endocrinology and the American Association of Clinical Endocrinologists*, *19*(2), 301–312. https://doi.org/10.4158/EP12138.RA

Liu, P., Ying, Y., Zhao, Y., Mundy, D. I., Zhu, M., & Anderson, R. G. (2004). Chinese hamster ovary K2 cell lipid droplets appear to be metabolic organelles involved in membrane traffic. *The Journal of biological chemistry*, *279*(5), 3787–3792. https://doi.org/10.1074/jbc.M311945200

MacDonald, M. J., Dobrzyn, A., Ntambi, J., & Stoker, S. W. (2008). The role of rapid lipogenesis in insulin secretion: Insulin secretagogues acutely alter lipid composition of INS-1 832/13 cells. *Archives of biochemistry and biophysics*, *470*(2), 153–162. https://doi.org/10.1016/j.abb.2007.11.017

MacDonald, M. J., Hasan, N. M., Dobrzyn, A., Stoker, S. W., Ntambi, J. M., Liu, X., & Sampath, H. (2013a). Knockdown of pyruvate carboxylase or fatty acid synthase lowers numerous lipids and glucose-stimulated insulin release in insulinoma cells. *Archives of biochemistry and biophysics*, *532*(1), 23–31. https://doi.org/10.1016/j.abb.2013.01.002

MacDonald, M. J., Longacre, M. J., Stoker, S. W., Kendrick, M., Thonpho, A., Brown, L. J., Hasan, N. M., Jitrapakdee, S., Fukao, T., Hanson, M. S., Fernandez, L. A., & Odorico, J. (2011). Differences between human and rodent pancreatic islets: low pyruvate carboxylase, atp citrate lyase, and pyruvate carboxylation and high glucose-stimulated acetoacetate in human pancreatic islets. *The Journal of biological chemistry*, *286*(21), 18383–18396. https://doi.org/10.1074/jbc.M111.241182

MacDonald, M. J., Longacre, M. J., Warner, T. F., & Thonpho, A. (2013b). High level of ATP citrate lyase expression in human and rat pancreatic islets. *Hormone and metabolic research = Hormon- und Stoffwechselforschung = Hormones et metabolisme*, *45*(5), 391–393. https://doi.org/10.1055/s-0032-1329987

MacDonald, M. J., Smith, A. D., 3rd, Hasan, N. M., Sabat, G., & Fahien, L. A. (2007). Feasibility of pathways for transfer of acyl groups from mitochondria to the cytosol to form short chain acyl-CoAs in the pancreatic beta cell. *The Journal of biological chemistry*, *282*(42), 30596–30606. https://doi.org/10.1074/jbc.M702732200

Malaisse, W. J., Best, L., Kawazu, S., Malaisse-Lagae, F., & Sener, A. (1983). The stimulus-secretion coupling of glucose-induced insulin release: fuel metabolism in islets deprived of exogenous nutrient. *Archives of biochemistry and biophysics*, *224*(1), 102–110. https://doi-org.d360prx.biomed.cas.cz/10.1016/0003-9861(83)90193-5

Manukyan, L., Ubhayasekera, S. J., Bergquist, J., Sargsyan, E., & Bergsten, P. (2015). Palmitate-induced impairments of β-cell function are linked with generation of specific ceramide species via acylation of sphingosine. *Endocrinology*, *156*(3), 802–812. https://doi.org/10.1210/en.2014-1467

Martinez-Sanchez, A., Pullen, T. J., Chabosseau, P., Zhang, Q., Haythorne, E., Cane, M. C., Nguyen-Tu, M. S., Sayers, S. R., & Rutter, G. A. (2016). Disallowance of Acot7 in β-Cells Is Required for Normal Glucose Tolerance and Insulin Secretion. *Diabetes*, *65*(5), 1268–1282. https://doi.org/10.2337/db15-1240

Martins, E. F., Miyasaka, C. K., Newsholme, P., Curi, R., & Carpinelli, A. R. (2004). Changes of fatty acid composition in incubated rat pancreatic islets. *Diabetes & metabolism*, *30*(1), 21–27. https://doi-org.d360prx.biomed.cas.cz/10.1016/s1262-3636(07)70085-x

Matsumura, K., Chang, B. H., Fujimiya, M., Chen, W., Kulkarni, R. N., Eguchi, Y., Kimura, H., Kojima, H., & Chan, L. (2007). Aquaporin 7 is a beta-cell protein and regulator of intraislet glycerol content and glycerol kinase activity, beta-cell mass, and insulin production and secretion. *Molecular and cellular biology*, *27*(17), 6026–6037. https://doi-org.d360prx.biomed.cas.cz/10.1128/MCB.00384-07

* Maulucci, G., Daniel, B., Cohen, O., Avrahami, Y., & Sasson, S. (2016). Hormetic and regulatory effects of lipid peroxidation mediators in pancreatic beta cells. *Molecular aspects of medicine*, *49*, 49–77. https://doi-org.d360prx.biomed.cas.cz/10.1016/j.mam.2016.03.001

Mayer, N., Schweiger, M., Romauch, M., Grabner, G. F., Eichmann, T. O., Fuchs, E., Ivkovic, J., Heier, C., Mrak, I., Lass, A., Höfler, G., Fledelius, C., Zechner, R., Zimmermann, R., & Breinbauer, R. (2013). Development of small-molecule inhibitors targeting adipose triglyceride lipase. *Nature chemical biology*, *9*(12), 785–787. https://doi.org/10.1038/nchembio.1359

McCulloch, L. J., van de Bunt, M., Braun, M., Frayn, K. N., Clark, A., & Gloyn, A. L. (2011). GLUT2 (SLC2A2) is not the principal glucose transporter in human pancreatic beta cells: implications for understanding genetic association signals at this locus. *Molecular genetics and metabolism*, *104*(4), 648–653. https://doi.org/10.1016/j.ymgme.2011.08.026

Mehmeti, I., Lortz, S., Elsner, M., & Lenzen, S. (2014). Peroxiredoxin 4 improves insulin biosynthesis and glucose-induced insulin secretion in insulin-secreting INS-1E cells. *The Journal of biological chemistry*, *289*(39), 26904–26913. https://doi.org/10.1074/jbc.M114.568329

Miwa, I., Ichimura, N., Sugiura, M., Hamada, Y., & Taniguchi, S. (2000). Inhibition of glucose-induced insulin secretion by 4-hydroxy-2-nonenal and other lipid peroxidation products. *Endocrinology*, *141*(8), 2767–2772. https://doi.org/10.1210/endo.141.8.7614

* Mráček, T., Drahota, Z., & Houštěk, J. (2013). The function and the role of the mitochondrial glycerol-3-phosphate dehydrogenase in mammalian tissues. *Biochimica et biophysica acta*, *1827*(3), 401–410. https://doi.org/10.1016/j.bbabio.2012.11.014

Moffitt, J. H., Fielding, B. A., Evershed, R., Berstan, R., Currie, J. M., & Clark, A. (2005). Adverse physicochemical properties of tripalmitin in beta cells lead to morphological changes and lipotoxicity in vitro. *Diabetologia*, *48*(9), 1819–1829. https://doi.org/10.1007/s00125-005-1861-9

Mugabo, Y., Zhao, S., Lamontagne, J., Al-Mass, A., Peyot, M. L., Corkey, B. E., Joly, E., Madiraju, S. R. M., & Prentki, M. (2017). Metabolic fate of glucose and candidate signaling and excess-fuel detoxification pathways in pancreatic β-cells. *The Journal of biological chemistry*, *292*(18), 7407–7422. https://doi.org/10.1074/jbc.M116.763060

Mugabo, Y., Zhao, S., Seifried, A., Gezzar, S., Al-Mass, A., Zhang, D., Lamontagne, J., Attane, C., Poursharifi, P., Iglesias, J., Joly, E., Peyot, M. L., Gohla, A., Madiraju, S. R., & Prentki, M. (2016). Identification of a mammalian glycerol-3-phosphate phosphatase: Role in metabolism and signaling in pancreatic β-cells and hepatocytes. *Proceedings of the National Academy of Sciences of the United States of America*, *113*(4), E430–E439. https://doi.org/10.1073/pnas.1514375113

Mulder, H., Holst, L. S., Svensson, H., Degerman, E., Sundler, F., Ahrén, B., Rorsman, P., & Holm, C. (1999). Hormone-sensitive lipase, the rate-limiting enzyme in triglyceride hydrolysis, is expressed and active in beta-cells. *Diabetes*, *48*(1), 228–232. https://doi.org/10.2337/diabetes.48.1.228

Mulder, H., Yang, S., Winzell, M. S., Holm, C., & Ahrén, B. (2004). Inhibition of lipase activity and lipolysis in rat islets reduces insulin secretion. *Diabetes*, *53*(1), 122–128. https://doi.org/10.2337/diabetes.53.1.122

* Murphy D. J. (2012). The dynamic roles of intracellular lipid droplets: from archaea to mammals. *Protoplasma*, *249*(3), 541–585. https://doi.org/10.1007/s00709-011-0329-7

Nagasumi, K., Esaki, R., Iwachidow, K., Yasuhara, Y., Ogi, K., Tanaka, H., Nakata, M., Yano, T., Shimakawa, K., Taketomi, S., Takeuchi, K., Odaka, H., & Kaisho, Y. (2009). Overexpression of GPR40 in pancreatic beta-cells augments glucose-stimulated insulin secretion and improves glucose tolerance in normal and diabetic mice. *Diabetes*, *58*(5), 1067–1076. https://doi.org/10.2337/db08-1233

Nieman, K. M., Kenny, H. A., Penicka, C. V., Ladanyi, A., Buell-Gutbrod, R., Zillhardt, M. R., Romero, I. L., Carey, M. S., Mills, G. B., Hotamisligil, G. S., Yamada, S. D., Peter, M. E., Gwin, K., & Lengyel, E. (2011). Adipocytes promote ovarian cancer metastasis and provide energy for rapid tumor growth. *Nature medicine*, *17*(11), 1498–1503. https://doi.org/10.1038/nm.2492

Noel, R. J., Antinozzi, P. A., McGarry, J. D., & Newgard, C. B. (1997). Engineering of glycerol-stimulated insulin secretion in islet beta cells. Differential metabolic fates of glucose and glycerol provide insight into mechanisms of stimulus-secretion coupling. *The Journal of biological chemistry*, *272*(30), 18621–18627. https://doi.org/10.1074/jbc.272.30.18621

* Nolan, C. J., Madiraju, M. S., Delghingaro-Augusto, V., Peyot, M. L., & Prentki, M. (2006). Fatty acid signaling in the beta-cell and insulin secretion. *Diabetes*, *55 Suppl 2*, S16–S23. https://doi.org/10.2337/db06-s003

Noushmehr, H., D'Amico, E., Farilla, L., Hui, H., Wawrowsky, K. A., Mlynarski, W., Doria, A., Abumrad, N. A., & Perfetti, R. (2005). Fatty acid translocase (FAT/CD36) is localized on insulin-containing granules in human pancreatic beta-cells and mediates fatty acid effects on insulin secretion. *Diabetes*, *54*(2), 472–481. https://doi.org/10.2337/diabetes.54.2.472

Oberhauser, L., Jiménez-Sánchez, C., Madsen, J. G. S., Duhamel, D., Mandrup, S., Brun, T., & Maechler, P. (2022). Glucolipotoxicity promotes the capacity of the glycerolipid/NEFA cycle supporting the secretory response of pancreatic beta cells. *Diabetologia*, *65*(4), 705–720. https://doi.org/10.1007/s00125-021-05633-x

* Oberhauser, L., & Maechler, P. (2021). Lipid-Induced Adaptations of the Pancreatic Beta-Cell to Glucotoxic Conditions Sustain Insulin Secretion. *International journal of molecular sciences*, *23*(1), 324. https://doi.org/10.3390/ijms23010324

Ohno, T., Kesado, T., Awaya, J., & Omura, S. (1974). Target of inhibition by the anti-lipogenic antibiotic cerulenin of sterol synthesis in yeast. *Biochemical and biophysical research communications*, *57*(4), 1119–1124. https://doi-org.d360prx.biomed.cas.cz/10.1016/0006-291x(74)90812-2

Oliveira, A. F., Cunha, D. A., Ladriere, L., Igoillo-Esteve, M., Bugliani, M., Marchetti, P., & Cnop, M. (2015). In vitro use of free fatty acids bound to albumin: A comparison of protocols. *BioTechniques*, *58*(5), 228–233. https://doi.org/10.2144/000114285

Oliveira, H. R., Verlengia, R., Carvalho, C. R., Britto, L. R., Curi, R., & Carpinelli, A. R. (2003). Pancreatic beta-cells express phagocyte-like NAD(P)H oxidase. *Diabetes*, *52*(6), 1457–1463. https://doi.org/10.2337/diabetes.52.6.1457

Pancreas - Normal Histology. Medicine.nus.edu.sg. (n.d.). Retrieved February 9, 2024 from https://medicine.nus.edu.sg/pathweb/normal-histology/pancreas/

Pandolfi, P. P., Sonati, F., Rivi, R., Mason, P., Grosveld, F., & Luzzatto, L. (1995). Targeted disruption of the housekeeping gene encoding glucose 6-phosphate dehydrogenase (G6PD): G6PD is dispensable for pentose synthesis but essential for defense against oxidative stress. *The EMBO journal*, *14*(21), 5209–5215. https://doi.org/10.1002/j.1460-2075.1995.tb00205.x

Panse, M., Gerst, F., Kaiser, G., Teutsch, C. A., Dölker, R., Wagner, R., Häring, H. U., & Ullrich, S. (2015). Activation of extracellular signal-regulated protein kinases 1 and 2 (ERK1/2) by free fatty acid receptor 1 (FFAR1/GPR40) protects from palmitate-induced beta cell death, but plays no role in insulin secretion. *Cellular physiology and biochemistry : international journal of experimental cellular physiology, biochemistry, and pharmacology*, *35*(4), 1537–1545. https://doi.org/10.1159/000373969

Pappan, K. L., Pan, Z., Kwon, G., Marshall, C. A., Coleman, T., Goldberg, I. J., McDaniel, M. L., & Semenkovich, C. F. (2005). Pancreatic beta-cell lipoprotein lipase independently regulates islet glucose metabolism and normal insulin secretion. *The Journal of biological chemistry*, *280*(10), 9023–9029. https://doi.org/10.1074/jbc.M409706200

* Pekala, J., Patkowska-Sokoła, B., Bodkowski, R., Jamroz, D., Nowakowski, P., Lochyński, S., & Librowski, T. (2011). L-carnitine--metabolic functions and meaning in humans life. *Current drug metabolism*, *12*(7), 667–678. https://doi.org/10.2174/138920011796504536

* Petan T. (2023). Lipid Droplets in Cancer. *Reviews of physiology, biochemistry and pharmacology*, *185*, 53–86. https://doi.org/10.1007/112_2020_51

Peyot, M. L., Guay, C., Latour, M. G., Lamontagne, J., Lussier, R., Pineda, M., Ruderman, N. B., Haemmerle, G., Zechner, R., Joly, É., Madiraju, S. R. M., Poitout, V., & Prentki, M. (2009). Adipose triglyceride lipase is implicated in fuel- and non-fuel-stimulated insulin secretion. *The Journal of biological chemistry*, *284*(25), 16848–16859. https://doi.org/10.1074/jbc.M109.006650

Pi, J., Bai, Y., Zhang, Q., Wong, V., Floering, L. M., Daniel, K., Reece, J. M., Deeney, J. T., Andersen, M. E., Corkey, B. E., & Collins, S. (2007). Reactive oxygen species as a signal in glucose-stimulated insulin secretion. *Diabetes*, *56*(7), 1783–1791. https://doi.org/10.2337/db06-1601

Pinnick, K., Neville, M., Clark, A., & Fielding, B. (2010). Reversibility of metabolic and morphological changes associated with chronic exposure of pancreatic islet beta-cells to fatty acids. *Journal of cellular biochemistry*, *109*(4), 683–692. https://doi.org/10.1002/jcb.22445

Plecitá-Hlavatá, L., Jabůrek, M., Holendová, B., Tauber, J., Pavluch, V., Berková, Z., Cahová, M., Schröder, K., Brandes, R. P., Siemen, D., & Ježek, P. (2020). Glucose-Stimulated Insulin Secretion Fundamentally Requires H_2O_2 Signaling by NADPH Oxidase 4. *Diabetes*, *69*(7), 1341–1354. https://doi.org/10.2337/db19-1130

* Possik, E., Al-Mass, A., Peyot, M. L., Ahmad, R., Al-Mulla, F., Madiraju, S. R. M., & Prentki, M. (2021). New Mammalian Glycerol-3-Phosphate Phosphatase: Role in β-Cell, Liver and Adipocyte Metabolism. *Frontiers in endocrinology*, *12*, 706607. https://doi.org/10.3389/fendo.2021.706607

* Prentki, M., & Madiraju, S. R. (2008). Glycerolipid metabolism and signaling in health and disease. *Endocrine reviews*, *29*(6), 647–676. https://doi.org/10.1210/er.2008-0007

* Prentki, M., & Madiraju, S. R. (2012). Glycerolipid/free fatty acid cycle and islet β-cell function in health, obesity and diabetes. *Molecular and cellular endocrinology*, *353*(1-2), 88–100. https://doi.org/10.1016/j.mce.2011.11.004

* Prentki, M., Corkey, B. E., & Madiraju, S. R. M. (2020). Lipid-associated metabolic signalling networks in pancreatic beta cell function. *Diabetologia*, *63*(1), 10–20. https://doi.org/10.1007/s00125-019-04976-w

* Quan, J., Bode, A. M., & Luo, X. (2021). ACSL family: The regulatory mechanisms and therapeutic implications in cancer. *European journal of pharmacology*, *909*, 174397. https://doi.org/10.1016/j.ejphar.2021.174397

Rahier, J., Goebbels, R. M., & Henquin, J. C. (1983). Cellular composition of the human diabetic pancreas. *Diabetologia*, *24*(5), 366–371. https://doi.org/10.1007/BF00251826

Rahier, J., Wallon, J., & Henquin, J. C. (1981). Cell populations in the endocrine pancreas of human neonates and infants. *Diabetologia*, *20*(5), 540–546. https://doi.org/10.1007/BF00252762

Rando, R. R., & Young, N. (1984). The stereospecific activation of protein kinase C. *Biochemical and biophysical research communications*, *122*(2), 818–823. https://doi-org.d360prx.biomed.cas.cz/10.1016/s0006-291x(84)80107-2

Rhee, J. S., Betz, A., Pyott, S., Reim, K., Varoqueaux, F., Augustin, I., Hesse, D., Südhof, T. C., Takahashi, M., Rosenmund, C., & Brose, N. (2002). Beta phorbol ester- and diacylglycerol-induced augmentation of transmitter release is mediated by Munc13s and not by PKCs. *Cell*, *108*(1), 121–133. https://doi.org/10.1016/s0092-8674(01)00635-3

* Risé, P., Eligini, S., Ghezzi, S., Colli, S., & Galli, C. (2007). Fatty acid composition of plasma, blood cells and whole blood: relevance for the assessment of the fatty acid status in humans. *Prostaglandins, leukotrienes, and essential fatty acids*, *76*(6), 363–369. https://doi.org/10.1016/j.plefa.2007.05.003

Rodriguez, J. A., Ben Ali, Y., Abdelkafi, S., Mendoza, L. D., Leclaire, J., Fotiadu, F., Buono, G., Carrière, F., & Abousalham, A. (2010). In vitro stereoselective hydrolysis of diacylglycerols by hormone-sensitive lipase. *Biochimica et biophysica acta*, *1801*(1), 77–83. https://doi-org.d360prx.biomed.cas.cz/10.1016/j.bbalip.2009.09.020

Roduit, R., Nolan, C., Alarcon, C., Moore, P., Barbeau, A., Delghingaro-Augusto, V., Przybykowski, E., Morin, J., Massé, F., Massie, B., Ruderman, N., Rhodes, C., Poitout, V., & Prentki, M. (2004). A role for the malonyl-CoA/long-chain acyl-CoA pathway of lipid signaling in the regulation of insulin secretion in response to both fuel and nonfuel stimuli. *Diabetes*, *53*(4), 1007–1019. https://doi-org.d360prx.biomed.cas.cz/10.2337/diabetes.53.4.1007

Rose Z. B. (1981). Phosphoglycolate phosphatase from human red blood cells. *Archives of biochemistry and biophysics, 208*(2), 602–609. https://doi-org.d360prx.biomed.cas.cz/10.1016/0003-9861(81)90549-x

Rubí, B., Antinozzi, P. A., Herrero, L., Ishihara, H., Asins, G., Serra, D., Wollheim, C. B., Maechler, P., & Hegardt, F. G. (2002). Adenovirus-mediated overexpression of liver carnitine palmitoyltransferase I in INS1E cells: effects on cell metabolism and insulin secretion. *The Biochemical journal*, *364*(Pt 1), 219–226. https://doi.org/10.1042/bj3640219

Saisho, Y., Butler, A. E., Meier, J. J., Monchamp, T., Allen-Auerbach, M., Rizza, R. A., & Butler, P. C. (2007). Pancreas volumes in humans from birth to age one hundred taking into account sex, obesity, and presence of type-2 diabetes. *Clinical anatomy (New York, N.Y.)*, *20*(8), 933–942. https://doi.org/10.1002/ca.20543

Sakai, K., Matsumoto, K., Nishikawa, T., Suefuji, M., Nakamaru, K., Hirashima, Y., Kawashima, J., Shirotani, T., Ichinose, K., Brownlee, M., & Araki, E. (2003). Mitochondrial reactive oxygen species reduce insulin secretion by pancreatic beta-cells. *Biochemical and biophysical research communications*, *300*(1), 216–222. https://doi-org.d360prx.biomed.cas.cz/10.1016/s0006-291x(02)02832-2

Salvadó, L., Coll, T., Gómez-Foix, A. M., Salmerón, E., Barroso, E., Palomer, X., & Vázquez-Carrera, M. (2013). Oleate prevents saturated-fatty-acid-induced ER stress, inflammation and insulin resistance in skeletal muscle cells through an AMPK-dependent mechanism. *Diabetologia*, *56*(6), 1372–1382. https://doi.org/10.1007/s00125-013-2867-3

Sandberg, M. B., Fridriksson, J., Madsen, L., Rishi, V., Vinson, C., Holmsen, H., Berge, R. K., & Mandrup, S. (2005). Glucose-induced lipogenesis in pancreatic beta-cells is dependent on SREBP-1. *Molecular and cellular endocrinology*, *240*(1-2), 94–106. https://doi.org/10.1016/j.mce.2005.05.005

Sargsyan, E., Artemenko, K., Manukyan, L., Bergquist, J., & Bergsten, P. (2016). Oleate protects beta-cells from the toxic effect of palmitate by activating pro-survival pathways of the ER stress response. *Biochimica et biophysica acta*, *1861*(9 Pt A), 1151–1160. https://doi-org.d360prx.biomed.cas.cz/10.1016/j.bbalip.2016.06.012

* Sasson S. (2017). Nutrient overload, lipid peroxidation and pancreatic beta cell function. *Free radical biology & medicine*, *111*, 102–109. https://doi.org/10.1016/j.freeradbiomed.2016.09.003

Sawatani, T., Kaneko, Y. K., & Ishikawa, T. (2019). Dual effect of reduced type I diacylglycerol kinase activity on insulin secretion from MIN6 β-cells. *Journal of pharmacological sciences*, *140*(2), 178–186. https://doi.org/10.1016/j.jphs.2019.06.001

Schindelin, J., Arganda-Carreras, I., Frise, E., Kaynig, V., Longair, M., Pietzsch, T., Preibisch, S., Rueden, C., Saalfeld, S., Schmid, B., Tinevez, J. Y., White, D. J., Hartenstein, V., Eliceiri, K., Tomancak, P., & Cardona, A. (2012). Fiji: an open-source platform for biological-image analysis. *Nature methods*, *9*(7), 676–682. https://doi.org/10.1038/nmeth.2019

Schnell, S., Schaefer, M., & Schöfl, C. (2007). Free fatty acids increase cytosolic free calcium and stimulate insulin secretion from beta-cells through activation of GPR40. *Molecular and cellular endocrinology*, *263*(1-2), 173–180. https://doi-org.d360prx.biomed.cas.cz/10.1016/j.mce.2006.09.013

Schuit, F., De Vos, A., Farfari, S., Moens, K., Pipeleers, D., Brun, T., & Prentki, M. (1997). Metabolic fate of glucose in purified islet cells. Glucose-regulated anaplerosis in beta cells. *The Journal of biological chemistry*, *272*(30), 18572–18579. https://doi.org/10.1074/jbc.272.30.18572

* Schuit, F., Van Lommel, L., Granvik, M., Goyvaerts, L., de Faudeur, G., Schraenen, A., & Lemaire, K. (2012). β-cell-specific gene repression: a mechanism to protect against inappropriate or maladjusted insulin secretion?. *Diabetes*, *61*(5), 969–975. https://doi.org/10.2337/db11-1564

Schweiger, M., Schreiber, R., Haemmerle, G., Lass, A., Fledelius, C., Jacobsen, P., Tornqvist, H., Zechner, R., & Zimmermann, R. (2006). Adipose triglyceride lipase and hormone-sensitive lipase are the major enzymes in adipose tissue triacylglycerol catabolism. *The Journal of biological chemistry*, *281*(52), 40236–40241. https://doi.org/10.1074/jbc.M608048200

Sekine, N., Cirulli, V., Regazzi, R., Brown, L. J., Gine, E., Tamarit-Rodriguez, J., Girotti, M., Marie, S., MacDonald, M. J., & Wollheim, C. B. (1994). Low lactate dehydrogenase and high mitochondrial glycerol phosphate dehydrogenase in pancreatic beta-cells. Potential role in nutrient sensing. *The Journal of biological chemistry*, *269*(7), 4895–4902.

Sheu, L., Pasyk, E. A., Ji, J., Huang, X., Gao, X., Varoqueaux, F., Brose, N., & Gaisano, H. Y. (2003). Regulation of insulin exocytosis by Munc13-1. *The Journal of biological chemistry*, *278*(30), 27556–27563. https://doi.org/10.1074/jbc.M303203200

Skinner, J. R., Shew, T. M., Schwartz, D. M., Tzekov, A., Lepus, C. M., Abumrad, N. A., & Wolins, N. E. (2009). Diacylglycerol enrichment of endoplasmic reticulum or lipid droplets recruits perilipin 3/TIP47 during lipid storage and mobilization. *The Journal of biological chemistry*, *284*(45), 30941–30948. https://doi.org/10.1074/jbc.M109.013995

* Skog, O., & Korsgren, O. (2020). On the dynamics of the human endocrine pancreas and potential consequences for the development of type 1 diabetes. *Acta diabetologica*, *57*(4), 503–511. https://doi.org/10.1007/s00592-019-01420-8

Soga, T., Ohishi, T., Matsui, T., Saito, T., Matsumoto, M., Takasaki, J., Matsumoto, S., Kamohara, M., Hiyama, H., Yoshida, S., Momose, K., Ueda, Y., Matsushime, H., Kobori, M., & Furuichi, K. (2005). Lysophosphatidylcholine enhances glucose-dependent insulin secretion via an orphan G-protein-coupled receptor. *Biochemical and biophysical research communications*, *326*(4), 744–751. https://doi-org.d360prx.biomed.cas.cz/10.1016/j.bbrc.2004.11.120

Soni, M. S., Rabaglia, M. E., Bhatnagar, S., Shang, J., Ilkayeva, O., Mynatt, R., Zhou, Y. P., Schadt, E. E., Thornberry, N. A., Muoio, D. M., Keller, M. P., & Attie, A. D. (2014). Downregulation of carnitine acyl-carnitine translocase by miRNAs 132 and 212 amplifies glucose-stimulated insulin secretion. *Diabetes*, *63*(11), 3805–3814. https://doi-org.d360prx.biomed.cas.cz/10.2337/db13-1677

Spector, A. A., & Hoak, J. C. (1975). Letter: Fatty acids, platelets, and microcirculatory obstruction. *Science (New York, N.Y.)*, *190*(4213), 490–492. https://doi-org.d360prx.biomed.cas.cz/10.1126/science.1166323

Spégel, P., Sharoyko, V. V., Goehring, I., Danielsson, A. P., Malmgren, S., Nagorny, C. L., Andersson, L. E., Koeck, T., Sharp, G. W., Straub, S. G., Wollheim, C. B., & Mulder, H. (2013). Time-resolved metabolomics analysis of β-cells implicates the pentose phosphate pathway in the control of insulin release. *The Biochemical journal*, *450*(3), 595–605. https://doi.org/10.1042/BJ20121349

Stancill, J. S., Broniowska, K. A., Oleson, B. J., Naatz, A., & Corbett, J. A. (2019). Pancreatic β-cells detoxify H_2O_2 through the peroxiredoxin/thioredoxin antioxidant system. *The Journal of biological chemistry*, *294*(13), 4843–4853. https://doi.org/10.1074/jbc.RA118.006219

Stanley, C. A., Hale, D. E., Berry, G. T., Deleeuw, S., Boxer, J., & Bonnefont, J. P. (1992). Brief report: a deficiency of carnitine-acylcarnitine translocase in the inner mitochondrial membrane. *The New England journal of medicine*, *327*(1), 19–23. https://doi.org/10.1056/NEJM199207023270104

Stein, D. T., Esser, V., Stevenson, B. E., Lane, K. E., Whiteside, J. H., Daniels, M. B., Chen, S., & McGarry, J. D. (1996). Essentiality of circulating fatty acids for glucose-stimulated insulin secretion in

the fasted rat. *The Journal of clinical investigation*, *97*(12), 2728–2735. https://doi.org/10.1172/JCI118727

Stöcker, S., Maurer, M., Ruppert, T., & Dick, T. P. (2018). A role for 2-Cys peroxiredoxins in facilitating cytosolic protein thiol oxidation. *Nature chemical biology*, *14*(2), 148–155. https://doi.org/10.1038/nchembio.2536

Sztalryd, C., Xu, G., Dorward, H., Tansey, J. T., Contreras, J. A., Kimmel, A. R., & Londos, C. (2003). Perilipin A is essential for the translocation of hormone-sensitive lipase during lipolytic activation. *The Journal of cell biology*, *161*(6), 1093–1103. https://doi.org/10.1083/jcb.200210169

Tamarit-Rodriguez, J., Vara, E., & Tamarit, J. (1984). Starvation-induced secretory changes of insulin, somatostatin, and glucagon and their modification by 2-bromostearate. *Hormone and metabolic research = Hormon- und Stoffwechselforschung = Hormones et metabolisme*, *16*(3), 115–119. https://doi-org.d360prx.biomed.cas.cz/10.1055/s-2007-1014715

Thorens, B., Sarkar, H. K., Kaback, H. R., & Lodish, H. F. (1988). Cloning and functional expression in bacteria of a novel glucose transporter present in liver, intestine, kidney, and beta-pancreatic islet cells. *Cell*, *55*(2), 281–290. https://doi.org/10.1016/0092-8674(88)90051-7

Tiedge, M., Lortz, S., Drinkgern, J., & Lenzen, S. (1997). Relation between antioxidant enzyme gene expression and antioxidative defense status of insulin-producing cells. *Diabetes*, *46*(11), 1733–1742. https://doi.org/10.2337/diab.46.11.1733

Tong, X., & Stein, R. (2021). Lipid Droplets Protect Human β-Cells From Lipotoxicity-Induced Stress and Cell Identity Changes. *Diabetes*, *70*(11), 2595–2607. https://doi.org/10.2337/db21-0261

Tornqvist, H., & Belfrage, P. (1976). Purification and some properties of a monoacylglycerol-hydrolyzing enzyme of rat adipose tissue. *The Journal of biological chemistry*, *251*(3), 813–819.

Toyokuni, S., Yamada, S., Kashima, M., Ihara, Y., Yamada, Y., Tanaka, T., Hiai, H., Seino, Y., & Uchida, K. (2000). Serum 4-hydroxy-2-nonenal-modified albumin is elevated in patients with type 2 diabetes mellitus. *Antioxidants & redox signaling*, *2*(4), 681–685. https://doi-org.d360prx.biomed.cas.cz/10.1089/ars.2000.2.4-681

Trevino, M. B., Machida, Y., Hallinger, D. R., Garcia, E., Christensen, A., Dutta, S., Peake, D. A., Ikeda, Y., & Imai, Y. (2015). Perilipin 5 regulates islet lipid metabolism and insulin secretion in a cAMP-dependent manner: implication of its role in the postprandial insulin secretion. *Diabetes*, *64*(4), 1299–1310. https://doi.org/10.2337/db14-0559

Uchizono, Y., Takeya, R., Iwase, M., Sasaki, N., Oku, M., Imoto, H., Iida, M., & Sumimoto, H. (2006). Expression of isoforms of NADPH oxidase components in rat pancreatic islets. *Life sciences*, *80*(2), 133–139. https://doi-org.d360prx.biomed.cas.cz/10.1016/j.lfs.2006.08.031

Vance, D., Goldberg, I., Mitsuhashi, O., & Bloch, K. (1972). Inhibition of fatty acid synthetases by the antibiotic cerulenin. *Biochemical and biophysical research communications*, *48*(3), 649–656. https://doi-org.d360prx.biomed.cas.cz/10.1016/0006-291x(72)90397-x

* Virreira, M., Perret, J., & Delporte, C. (2011). Pancreatic beta-cells: Role of glycerol and aquaglyceroporin 7. *The international journal of biochemistry & cell biology*, *43*(1), 10–13. https://doi.org/10.1016/j.biocel.2010.10.018

Wang, Z., & Gleichmann, H. (1998). GLUT2 in pancreatic islets: crucial target molecule in diabetes induced with multiple low doses of streptozotocin in mice. *Diabetes*, *47*(1), 50–56. https://doi.org/10.2337/diab.47.1.50

Wang, H., Bell, M., Sreenivasan, U., Sreenevasan, U., Hu, H., Liu, J., Dalen, K., Londos, C., Yamaguchi, T., Rizzo, M. A., Coleman, R., Gong, D., Brasaemle, D., & Sztalryd, C. (2011). Unique regulation of adipose triglyceride lipase (ATGL) by perilipin 5, a lipid droplet-associated protein. *The Journal of biological chemistry*, *286*(18), 15707–15715. https://doi.org/10.1074/jbc.M110.207779

Wei, S., Lai, K., Patel, S., Piantedosi, R., Shen, H., Colantuoni, V., Kraemer, F. B., & Blaner, W. S. (1997). Retinyl ester hydrolysis and retinol efflux from BFC-1beta adipocytes. *The Journal of biological chemistry*, *272*(22), 14159–14165. https://doi.org/10.1074/jbc.272.22.14159

* Welte, M. A., & Gould, A. P. (2017). Lipid droplet functions beyond energy storage. *Biochimica et biophysica acta. Molecular and cell biology of lipids*, *1862*(10 Pt B), 1260–1272. https://doi.org/10.1016/j.bbalip.2017.07.006

Wilfling, F., Wang, H., Haas, J. T., Krahmer, N., Gould, T. J., Uchida, A., Cheng, J. X., Graham, M., Christiano, R., Fröhlich, F., Liu, X., Buhman, K. K., Coleman, R. A., Bewersdorf, J., Farese, R. V., Jr, & Walther, T. C. (2013). Triacylglycerol synthesis enzymes mediate lipid droplet growth by relocalizing from the ER to lipid droplets. *Developmental cell*, *24*(4), 384–399. https://doi.org/10.1016/j.devcel.2013.01.013

* Xu, S., Zhang, X., & Liu, P. (2018). Lipid droplet proteins and metabolic diseases. *Biochimica et biophysica acta. Molecular basis of disease*, *1864*(5 Pt B), 1968–1983. https://doi.org/10.1016/j.bbadis.2017.07.019

Yu, W., Bozza, P. T., Tzizik, D. M., Gray, J. P., Cassara, J., Dvorak, A. M., & Weller, P. F. (1998). Co-compartmentalization of MAP kinases and cytosolic phospholipase A2 at cytoplasmic arachidonate-rich lipid bodies. *The American journal of pathology*, *152*(3), 759–769.

Yu, W., Cassara, J., & Weller, P. F. (2000). Phosphatidylinositide 3-kinase localizes to cytoplasmic lipid bodies in human polymorphonuclear leukocytes and other myeloid-derived cells. *Blood*, *95*(3), 1078–1085.

* Zechner, R., Madeo, F., & Kratky, D. (2017). Cytosolic lipolysis and lipophagy: two sides of the same coin. *Nature reviews. Molecular cell biology*, *18*(11), 671–684. https://doi-org.d360prx.biomed.cas.cz/10.1038/nrm.2017.76

Zhang, S., & Kim, K. H. (1998). Essential role of acetyl-CoA carboxylase in the glucose-induced insulin secretion in a pancreatic beta-cell line. *Cellular signalling*, *10*(1), 35–42. https://doi-org.d360prx.biomed.cas.cz/10.1016/s0898-6568(97)00070-3

Zhang, Z., Liew, C. W., Handy, D. E., Zhang, Y., Leopold, J. A., Hu, J., Guo, L., Kulkarni, R. N., Loscalzo, J., & Stanton, R. C. (2010). High glucose inhibits glucose-6-phosphate dehydrogenase, leading to increased oxidative stress and beta-cell apoptosis. *FASEB journal : official publication of the Federation of American Societies for Experimental Biology*, *24*(5), 1497–1505. https://doi-org.d360prx.biomed.cas.cz/10.1096/fj.09-136572

Zhao, S., Mugabo, Y., Iglesias, J., Xie, L., Delghingaro-Augusto, V., Lussier, R., Peyot, M. L., Joly, E., Taïb, B., Davis, M. A., Brown, J. M., Abousalham, A., Gaisano, H., Madiraju, S. R., & Prentki, M. (2014). α/β-Hydrolase domain-6-accessible monoacylglycerol controls glucose-stimulated insulin secretion. *Cell metabolism*, *19*(6), 993–1007. https://doi.org/10.1016/j.cmet.2014.04.003

Zhou, Y. P., Berggren, P. O., & Grill, V. (1996). A fatty acid-induced decrease in pyruvate dehydrogenase activity is an important determinant of beta-cell dysfunction in the obese diabetic db/db mouse. *Diabetes*, *45*(5), 580–586. https://doi.org/10.2337/diab.45.5.580

Zimmermann, R., Strauss, J. G., Haemmerle, G., Schoiswohl, G., Birner-Gruenberger, R., Riederer, M., Lass, A., Neuberger, G., Eisenhaber, F., Hermetter, A., & Zechner, R. (2004). Fat mobilization in adipose tissue is promoted by adipose triglyceride lipase. *Science (New York, N.Y.)*, *306*(5700), 1383–1386. https://doi.org/10.1126/science.1100747

* Review